LATERAL-TORSIONAL BUCKLING OF A ROLLED WIDE FLANGE BEAM WITH CHANNEL CAP

By

DUNG MYAU LUE

A DISSERTATION PRESENTED TO THE GRADUATE SCHOOL
OF THE UNIVERSITY OF FLORIDA IN PARTIAL FULFILLMENT
OF THE REQUIREMENTS FOR THE DEGREE OF
DOCTOR OF PHILOSOPHY

UNIVERSITY OF FLORIDA

1993

ACKNOWLEDGEMENTS

The author is grateful to the people and companies who helped and supported him in this endeavor. Special thanks go to members of my supervisory committee, especially the chairman, Dr. Duane S. Ellifritt, and cochairman, Dr. Ronald A. Cook. Their professional guidance and uninhibited access granted for frequent consultations during the past three years have been invaluable.

Thanks are also due to Professors Ibrahim K. Ebcioglu, Mang Tia, and Myron Chang for having served on the author's committee and having instructed the author in their classes.

The author would also extend gratitude to the following companies for their donations of test specimen and related devices. The Morrison Molded Fiber Glass Company of Bristol, Virginia, for providing fiberglass specimen; the Owen Steel Company of Jacksonville, Florida, for providing the steel specimen; the Balfour-Beatty Company of Jacksonville, Florida, for providing the lifter; the Whitley Steel Company of Baldwin, Florida, for providing small pieces of steel angles, plates, and bars; and the Allstate Steel Company of Jacksonville, Florida, for providing and making the simulators. Without their kind contributions, the test would not been completed.

Financial support in the form of teaching assistantship provided, in the face of restricted resources, by Professor Paul Y. Thompson, Chairman, Department of Civil Engineering, was a critical factor in the accomplishment of this graduate work.

The assistance of Ed Dobson, Hubert Martin, Danny Richardson, and Bill Studstill, engineers and technicians in the Civil Engineering Structures and Materials Laboratory at the University of Florida, is gratefully acknowledged. Without their assistance in conducting the tests, the laboratory testing reported in this dissertation would not have been completed. Thanks are also due to all the other professors not mentioned above and fellow graduate students, William Mbwambo, Ming-Gin Lee, Chui-Te Chiu, and Gary Consolazio.

Words are insufficient to express the author's gratitude to his mother and younger sister, to whom this work is dedicated, for their continuous support during all his education. The acknowledgment will not be complete without a mention of the author's wife, Hsiu-Fang, for her continued patience and encouragement, without which this work would not have been possible.

TABLE OF CONTENTS

NOMENCLATURE

a = distance from the shear center of the compression flange to the shear center of the section

b = distance from the shear center of the tension flange to the shear center of the section

b_1 = width of compression, tension flange

b_2 = width of compression, tension flange

C_b = bending coefficient dependent upon moment gradient

C_w = section warping constant of wide flange

C_{wc} = section warping constant of wide flange with channel

d' = distance between the centers of areas of the two flanges

E = modulus of elasticity of steel (29,000 ksi)

G = elastic shear modulus of steel (11,200 ksi)

h = clear distance between flanges less the fillet or corner radius for rolled shapes

h_L = distance from the shear center of the compression flange to the shear center of the tension flange, a lipped section

h_U = distance from the shear center of the compression flange to the shear center of the tension flange, an unlipped section

I_x = moment of inertia of the combined section about X axis

I_y = moment of inertia of the combined section about Y axis

I_{wx} = warping product of inertia about X axis

I_{yc} = moment of inertia of the compression flange about the axis parallel to web

I_{wy} = warping product of inertia about Y axis

J = section torsional constant

r = distance from any section element to center of twist

r^2 = coefficient of determination in statistics

K = effective length factor for prismatic member

L = length of plate element

L_b = laterally unbraced length

LVDT = linear variable differential transformer

M_n = maximum moment which the section can resist when the elastic lateral-torsional buckling occurs

t = thickness of plate element

t_1 = thickness of compression, tension flange

t_2 = thickness of compression, tension flange

X_c = centroid of section (X coordinate)

X_s = shear center of section (X coordinate)

Y_c = centroid of section (Y coordinate)

Y_s = shear center of section (Y coordinate)

Y_o = distance between the shear center and the centroid of the section (positive if the shear center lies between the centroid and compressive flange, otherwise negative)

W = unit warping with respect to the centroid

W_o = unit warping with respect to the shear center

W_n = normalized unit warping

S_w = warping statical moment

X_o = coordinates of the shear center

Y_o = coordinates of the shear center

X = coordinates of any point on the section

Y = coordinates of any point on the section

β_x = coefficient of monosymmetry

ρ = perpendicular distance between a point on the cross section and the centroid

ρ_o = perpendicular distance between a point the cross section and the shear center

Abstract of Dissertation Presented to the Graduate School of the University of Florida in Partial Fulfillment of the Requirements for the Degree of Doctor of Philosophy

LATERAL-TORSIONAL BUCKLING OF A ROLLED WIDE FLANGE BEAM WITH CHANNEL CAP

By

DUNG MYAU LUE

December 1993

Chairman: Duane S. Ellifritt
Major Department: Civil Engineering

Design against lateral-torsional buckling is an important aspect of the beam design process because of the sudden and possibly catastrophic nature of failure. Lateral-torsional buckling is a complex problem. Although substantial research has been done on I-shaped beams, doubly and singly symmetric, there is a shortage of research information in wide flange beams with channel caps, which are common in crane runway beams. Because of the lack of this information, the current Load and Resistance Factor Design (LRFD) code provides no specific provision for the design of beams with this type of section. However, the code does provide formulas to meet design needs. These formulas are derived from the research on singly symmetric I-shaped beams. When these formulas are applied to wide flange beams with channel caps, it can be shown that the results could be as much as 23% conservative

compared with results from the exact formulas. To avoid such a conservative design, a designer can employ the exact formulas. However, the evaluations of some section properties are not straight forward and the effort required is prohibitive in routine design.

In this study, the exact coefficients of monosymmetry parameter (β_x), warping section constant (C_w), and torsional section constant (J) were derived and evaluated based on numerical procedures. Simple and rational models for determining β_x, C_w, and J are proposed. The procedure for developing the models involved computer modeling, statistical techniques, and derivations based on structural mechanics.

When the models are applied to the forty-five sections listed in the current American Institute of Steel Construction (AISC) manual, the prediction of the elastic nominal moment (M_n) results in a maximum error of ± 2%.

Eighteen steel beams were tested as part of the study. Theoretical buckling loads, computed by the computer program developed by the author, are compared with experimental results. Based on the limited beam tests, revised bending coefficients (C_b) are proposed.

CHAPTER 1
INTRODUCTION

1.1 Background and Research Needs

Beams are usually considered to be members subjected to transverse loads. A typical rolled wide-flange shape beam, which is the doubly symmetric I-shaped beam, is shown in Figure 1-1a. A beam is a combination of a compression element, a tension element, and a web which is a brace element. A compression element can be either the top flange or bottom flange depending on the applied loading and the location of the section. This is also true for a tension element. Because a tension element is a tensile member, there is no lateral stability problem under normal transverse loads. A compression element, however, is a compressive member whose strength is affected by the distance between lateral braces. Unless a compressive member is properly braced against lateral deflection and twisting, it is subjected to failure by lateral-torsional buckling (LTB) prior to reaching its full capacity. The overall capacity of a beam is, therefore, limited by the LTB of the compression element.

The current legal criteria which regulate beam design originate with, or are influenced by, the Structural Stability Research Council (SSRC). The methods and formulas, in the

current provisions (footnote b on page 6-96) of the American Institute of Steel Construction (AISC) manual [1986], applied to doubly symmetric I-shaped beams provide results with reasonable accuracy.

Although many steel beams used in practice are doubly symmetric I-shaped beams, there are a great number of beams whose sections are not doubly symmetric. The sections, as shown in Figures 1-1b, 1-1c, and 1-1d, are widely used in monosymmetric beams. The two most common types of monosymmetric beams employed in industry practice are shown in Figures 1-1b and 1-1c. For a crane runway beam, it is common practice that a channel cap is placed over a wide flange beam, as shown in Figure 1-1c. The purpose of placing a channel over a wide flange is to increase the runway beam's lateral stability.

The current design code provides the provisions (footnote c on page 6-96 of the AISC manual [1986]) for monosymmetric beams. The formulas adopted by the code were based on the research of monosymmetric I-shaped beams as shown in Figure 1-1b. In current practice, if a designer is assigned to design a wide flange beam with a channel cap, the code provides no specific formulas to apply. A designer, of course, can apply the code formulas to obtain an approximate and conservative design (as much as 23%). A designer who needs a more rational design can employ the exact formulas as given by Eqs. 1.1 to 1.1d. Although the exact method could provide a good design,

the procedure is rather tedious and the computations of some section properties (such as Y_c, Y_o, C_{wc} and β_x) are never easy. In routine design, the warping section constant (C_{wc}) and the coefficient of monosymmetry (β_x) are not obtainable without the help of a computer program. However, the program may not be available to every designer.

1.2 Objectives of This Research

The elastic nominal moment (M_n) of a monosymmetric beam, including the case of this study, is given by the following formulas whose derivations are included in Chapter 3.

$$M_n = \frac{\pi C_b}{KL} \left\{ \sqrt{EI_y GJ} \left(B_1 + \sqrt{1 + B_2 + B_1^2} \right) \right\} \tag{1.1}$$

where

$$B_1 = \frac{\pi \beta_x}{2KL}\sqrt{\frac{EI_y}{GJ}} , \qquad B_2 = \frac{\pi^2 EC_{wc}}{(KL)^2 GJ} \tag{1.1a}$$

$$\beta_x = \frac{1}{I_x}\int_A y(x^2 + y^2)\,dA - 2(Y_s - Y_c) \tag{1.1b}$$

$$C_{wc} = \int_o^L W_n^2 t\,ds , \qquad J = \int_A r^2\,dA \tag{1.1c}$$

$$W_n = \frac{1}{A}\int_o^L W_o t\,ds - W_o , \qquad W_o = \int_o^s \rho_o\,ds \tag{1.1d}$$

To evaluate the elastic nominal moment (M_n), a designer has to determine the centroid (X_c,Y_c), the shear center (X_s,Y_s), the monosymmetry coefficient (β_x), the warping

section constant (C_{wc}), and the torsional section constant (J). The evaluation of these is not straightforward and the effort required is not recommended as a day-to-day structural design course.

Approximate design methods by Kitipornchai and Trahair [1980] and the AISC [1986] have been developed, which either avoid these computations, or replace them by gross simplifications. However, none of these approximate design methods considered the section of wide flange with channel cap, which is the subject of this research.

The objective of this study is to develop numerical procedures to evaluate the exact C_{wc}, β_x, and J, and to develop simple and rational models for C_{wc}, β_x, and J. The models for computing C_{wc}, β_x, and J are expressed in terms of known section properties, which are listed in the AISC manual. The calculations of the elastic nominal moments of beams are, therefore, simplified by using the proposed models of C_{wc}, β_x, and J.

The elastic nominal moment based on the proposed models is compared with the one obtained by the exact solution. Laboratory tests, including eighteen beam tests, were conducted as part of the research. More accurate bending coefficients (C_b) are proposed based on the conducted tests.

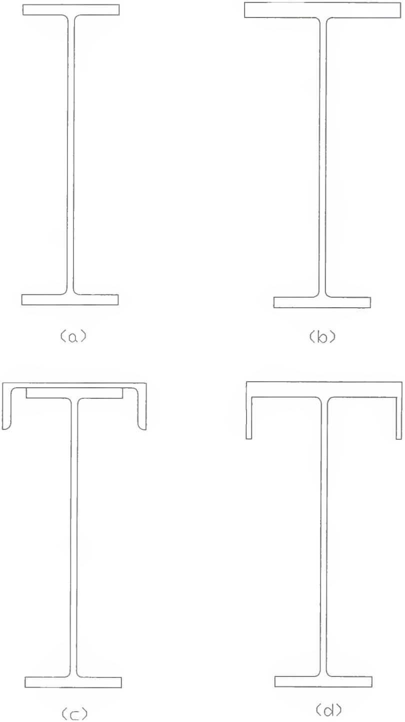

Figure 1-1. Beam cross-section.
a) Doubly symmetric I-shaped section; b) Singly symmetric I-shaped section; c) W-section with channel cap; d) I-section with lipped flange.

CHAPTER 2
LITERATURE REVIEW

Previous research on the subject of lateral-torsional buckling has been extensive. Theory and design applications are covered in many books and published papers. In the following discussions, the previous studies on lateral-torsional buckling are briefly summarized.

2.1 Elastic Lateral-Torsional Buckling

The analytical solutions of elastic lateral-torsional buckling are quite complex, and closed-form solutions exist only for a few simple cases. One of the simple cases which lead to a closed-form solution is a simply supported prismatic beam under uniform bending.

There are many variables affecting the lateral-torsional buckling strength and the principal variable is the unbraced length. Some other variables include the magnitude and distribution of the residual stresses, the type and position of the loads, the type of cross sections, the material properties, and the initial imperfections of geometry.

For the analysis of elastic lateral-torsional buckling, energy methods were presented by Bleich [1952], Salvadori [1955], Timoshenko and Gere [1961], Vlasov [1961], and Pi, Trahair, and Rajasekaran [1992]; finite-difference methods by

Galambos [1968] and Vinnakota [1977]; finite element methods by Barsoum and Gallagher [1970], Powell and Klingner [1970]. The lateral stability of doubly symmetric I-shaped beams was investigated by Clark and Hill [1960], Hechtman, Hattup, and Tiedemann [1955], Hartman [1967], Trahair [1969], Powell and Klingner [1970], Hancock [1978], Kubo and Fukumoto [1988], and Pi and Trahair [1992]. There have also been a number of investigations which have considered the lateral stability of singly symmetric I-shaped beams by Winter [1941], Hill [1942], O'Connor [1964], Anderson and Trahair [1972], and Kitipornchai and Trahair [1980].

A review of the early research in elastic lateral-torsional buckling was given by Lee [1960] and Johnson [1976], while Trahair [1977] , Nethercot [1983], and Galambos [1988] provided reviews of the recent development.

When a beam is subjected to a nonuniform bending, numerical or approximate solutions are required to obtain the buckling load. Because of the complications associated with numerical or approximate solutions, the practical professions had looked for a simple modifier or equivalent uniform moment factor to account the effect of moment gradient. Researchers including Nethercot and Rockey [1971] , Kirby and Nethercot [1979], and Chen and Lui [1988] have done some work on this topic.

The above-mentioned investigators, as well as many other contributors, made efforts to study elastic lateral-torsional

buckling of beams. However, the work was limited to beams with either doubly or singly symmetric I-shaped sections as shown in Figure 1-1a and 1-1b, respectively.

A wide flange beam with a channel cap, as shown in Figure 1-1c which is the case of this research, has been used as a crane runway beam in industrial buildings. No research, either analytical or experimental, dealing specifically with this case has been undertaken.

A section which is somewhat related to the case of this research, as shown in Figure 1-1d, has been investigated and published by Kitipornchai and Trahair [1980]. Their study proposed approximate models to calculate the difficult section properties which included the warping constant (C_{wc}) and monosymmetry coefficient (β_x) . Although the proposed models are simplified, the evaluations of C_{wc} and β_x require the location of the shear center of the section and the shear center of compression flanges which are not easy tasks for most design engineers. When the approximate models are applied to predict the C_{wc} and β_x for the case of this research, the maximum estimated errors, as given in Chapter 6, are 19% and 12%, respectively.

2.2 Inelastic Lateral-Torsional Buckling

As mentioned in the previous section, the unbraced length is the principal variable affecting the lateral-torsional buckling strength. A beam buckles elastically only when its unbraced length is long and buckles inelastically when its

unbraced length is intermediate. In practical terms, the elastic lateral-torsional buckling is useful when considering the strength of beams during the construction stage. Most of beams in service are designed to buckle in the inelastic range. Because the extent of yielding varies from section to section in a beam under nonuniform bending, the stiffness of the section is not constant along the length of the beam and the inelastic is performed by a numerical method. The analysis of inelastic lateral-torsional buckling has been based on the tangent-modulus theory which provides a theoretically lower bound to the buckling load. However, due to the unavoidable initial geometric imperfections, the tangent-modulus approach is shown as a satisfactory model.

Analytical and experimental studies on inelastic lateral-torsional buckling have been performed extensively in the past. The first to consider the problem of inelastic lateral-torsional buckling was Neal [1950] and the residual stress effect was first presented by Galambos [1963]. Later Trahair and Kitipornchai [1972] and Vinnakota [1979] also published papers in this field. A review in inelastic lateral-torsional buckling has been given by Trahair [1983]. The review provided a detailed description of the theory, the methods of analysis, the assumptions, tabulated and graphical results, and experimental verifications. All test results published in the past have been analyzed statistically by Fukumoto and Itoh [1981].

Other researchers and contributors have also made efforts to study the inelastic lateral-torsional buckling of beams. However, all the work done was confined to beams with either doubly or singly symmetric I-shaped sections as shown in Figures 1-1a and 1-1b, respectively. No study, either analytical or experimental, dealing specifically with the wide flange beam with channel cap has been undertaken to date.

CHAPTER 3
ANALYTICAL SOLUTIONS OF LATERAL-TORSIONAL BUCKLING

3.1 Introduction

If a beam is loaded in the plane of its weak axis and is not adequately braced laterally, the beam will deflect and rotate laterally when the load has reached a critical value, which is called the buckling load. This phenomenon is known as lateral-torsional buckling. The lateral-torsional buckling of a beam is possible only when the cross section has different bending stiffness in its two principal axes and the applied load act in the plane of the weak axis. Therefore, lateral-torsional buckling will never occur in square box sections or circular cross sections in which all thin plates in the section have the same thicknesses.

The analysis of lateral-torsional buckling behavior of beams are rather complex. For a geometrically perfect elastic beam, we can use the concept of neutral equilibrium to obtain the critical load. In this approach, a slightly deformed state of the beam corresponding to its buckled position is first drawn and equilibrium equations are then written with respect to this deformed configuration. The eigenvalue solution to the characteristic equation of the resulting equilibrium equation gives the critical load of the beam. Depending on the

type and nature of the loading condition, the resulting linear differential equations may have constant or variable coefficients. For the case of variable coefficients, it is often necessary to be solved by numerical techniques.

3.2 Elastic Lateral-Torsional Buckling

This section is intended to provide the derivation of elastic nominal moment (M_n), which the section can resist when the elastic lateral-torsional buckling occurs.

Consider a beam AB of span L, as shown in Figure 3-1, loaded in the plane of the web by transverse loads. For the convenience of the derivation, assume that the section of beam is 3-plate elements as shown in Figure 3-1. The coordinates of the shear center are X_s and Y_s, but because of the symmetry about the Y-axis we have $X_s = 0$; u and v, as shown in Figure 3-2, are the components of the displacement of the shear center parallel to the axes X and Y. The derivation is based upon the following assumptions:

1. The beam is a prismatic beam.
2. The lines of action of the applied loads pass through the shear center and the centroid, and the shear center lies on a principal axis through the centroid.
3. The deformation of the beam when bent and twisted is such that its cross section does not change its shape.

4. The fiber stresses due to the applied load do not exceed the proportional limit when the beam buckles.
5. The applied loads remain parallel to their original direction when the points of application of these loads are displaced.

Consider the beam in its deflected state under compression just prior to buckling and shall then determine an expression for the change of potential energy associated with the lateral displacement and twisting which occur at the instant of buckling. The total potential energy V consists of the internal strain energy of the deformed beam and of potential energy of the applied loads P(z). According to Clark and Hill [1960], the total potential energy V is given by the following equation.

$$V = \frac{1}{2}\int_{o}^{L} \left[EI_y(u'')^2+EC_w(\beta'')^2+GJ(\beta')^2+2M\beta u''+2jM(\beta')^2+Pg\beta^2\right]dz \qquad (3.1)$$

where u is the displacement parallel to initial position of the X-axis and β is the rotation of the cross section, E is the modulus of elasticity, I_y is the moment of inertia about Y-axis, C_w is the warping section constant, G is the elastic shear modulus, J is the torsional constant for the section, M is the section moment along the beam, P(z) is the applied load along the beam, and is a function of z, g refers to the distance from shear center to point of application of transverse load (positive when load is below shear center and negative otherwise). The monosymmetry parameter is j. The j

term had been given various conflicting expressions by Bleich [1952], O'Connor [1964], and Galambos [1968]. Trahair and Anderson's [1972] tests verified that the appropriate expression should take the form as given by the following equation.

$$j = \frac{1}{2I_x} \int_A Y(X^2+Y^2)\, dA - (Y_s - Y_c) \tag{3.2}$$

where $(Y_s - Y_c)$ is the distance from centroid to shear center (positive if the shear center lies between the centroid and compression flange, otherwise negative), I_x is the moment of inertia about X-axis, and X and Y are the coordinates of any point on the section. To satisfy the equilibrium considerations, it is required that

$$EI_y u'' = - M\, \beta \tag{3.3}$$

The applied load P(z) can be written in terms of the moment,

$$P = - M'' \tag{3.4}$$

Substitute Eqs. 3.3 and 3.4 into Eq. 3.1 to eliminate u" and P. Also, make the following substitutions in Eq. 3.1: Z = z/L and M = m x M_n, where m is a function of z and M_n is the maximum moment in the beam. To obtain the buckling moment (M_n), let V = 0, thus Eq. 3.1 becomes:

$$\frac{M_n^2}{EI_y}\int_o^L m^2\beta^2 dZ - \frac{M_n}{L^2}\left(g\int_o^L \frac{d^2m}{dZ^2}\beta^2 dZ + 2j\int_o^L m(\frac{d\beta}{dZ})^2 dZ\right)$$

$$-\left(\frac{GJ}{L^2}\int_o^L (\frac{d\beta}{dZ})^2 dZ + \frac{EC_w}{L^4}\int_o^L (\frac{d^2\beta}{dZ^2})^2 dZ\right) = 0 \qquad (3.5)$$

According to Clark and Hill [1960], the following equation (Eq. 3.6) can be obtained by solving Eq. 3.5 for M_n.

$$M_n = A_1\frac{\pi^2 EI_y}{(KL)^2}\left\{A_2 g + A_3 j + \sqrt{(A_2 g + A_3 j)^2 + \frac{C_w}{I_y}\left(1 + \frac{GJ(KL)^2}{\pi^2 EC_w}\right)}\right\} \qquad (3.6)$$

where

$$A_1 = \frac{\int_o^L (\frac{d\beta}{dZ})^2 dZ}{\int_o^L m^2\beta^2 dZ \quad \int_o^L (\frac{d^2\beta}{dZ^2})^2 dZ} \qquad (3.7a)$$

$$A_2 = -\frac{1}{2}\,\frac{\int_o^L \frac{d^2m}{dZ^2}\beta^2 dZ}{\int_o^L m^2\beta^2 dZ \quad \int_o^L (\frac{d^2\beta}{dZ^2})^2 dZ} \qquad (3.7b)$$

$$A_3 = \frac{\int_o^L m(\frac{d\beta}{dZ})^2 dZ}{\int_o^L m^2\beta^2 dZ \quad \int_o^L (\frac{d^2\beta}{dZ^2})^2 dZ} \qquad (3.7c)$$

$$K^2 = \pi^2 \frac{\int_o^L (\frac{d\beta}{dZ})^2 dZ}{\int_o^L (\frac{d^2\beta}{dZ^2})^2 dZ} \tag{3.7d}$$

Eq. 3.6 is a general formula, which as clark and Hill [1960] have shown, gives accurate solutions for either doubly or singly symmetric beams under a wide variety of load and end conditions. The values of A_1, A_2, A_3, and K depend on the loading and on the boundary conditions.

According to T. V. Galambos [1968], Eq. 3.6 can also be expressed by the following equation:

$$M_n = C_b \frac{\pi^2 E I_y}{(KL)^2} \left\{ 1 + \sqrt{1 + \frac{4}{\beta_x^2} \left(\frac{C_w}{I_y} + \frac{GJ(KL)^2}{\pi^2 E I_y} \right)} \right\} \tag{3.8}$$

In which C_b is the equivalent uniform moment factor, K is the effective length factor, and β_x is the coefficient of monosymmetry. The general expression for β_x is given by the following equation.

$$\beta_x = \frac{1}{I_x} \int_A Y(X^2+Y^2)\, dA - 2(Y_s - Y_c) = 2j \tag{3.9}$$

Eq. 3.8 can be further simplified in terms of B_1 and B_2 as given in Eq. 3.11, and the derivation is given below:

$$M_n = C_b \frac{\pi^2 E I_y \beta_x}{2(KL)^2} \left\{ 1 + \sqrt{1 + \frac{4}{\beta_x^2}\left(\frac{C_w}{I_y} + \frac{GJ(KL)^2}{\pi^2 E I_y} \right)} \right\}$$

$$= \frac{C_b \pi^2 E I_y \beta_x}{2(KL)^2} + \frac{C_b \pi^2 E I_y \beta_x}{2(KL)^2} \sqrt{1 + \frac{4}{\beta_x^2}\left(\frac{C_w}{I_y} + \frac{GJ(KL)^2}{\pi^2 E I_y} \right)}$$

$$= \frac{C_b \pi^2 E I_y \beta_x}{2(KL)^2} + \frac{C_b \pi^2 E I_y \beta_x}{2(KL)^2} \sqrt{1 + \frac{4C_w}{\beta_x^2 I_y} + \frac{4GJ(KL)^2}{\beta_x^2 \pi^2 E I_y}}$$

$$= \frac{C_b \pi^2 E I_y \beta_x}{2(KL)^2} + \frac{C_b \pi}{KL} \frac{\pi \beta_x E I_y}{2(KL)} \sqrt{1 + \frac{4C_w}{\beta_x^2 I_y} + \frac{4GJ(KL)^2}{\beta_x^2 \pi^2 E I_y}}$$

$$= \frac{C_b \pi^2 E I_y \beta_x}{2(KL)^2} + \frac{C_b \pi}{KL} \sqrt{\frac{(\pi \beta_x E I_y)^2}{(2KL)^2} + \frac{\pi^2 E^2 I_y C_w}{(KL)^2} + E I_y G J}$$

$$= \frac{C_b \pi}{(KL)} \left\{ \frac{\pi \beta_x E I_y}{2(KL)} + \sqrt{1 + \frac{\pi^2 E C_w}{(KL)^2 GJ} + \frac{\pi^2 \beta_x^2 E I_y}{(2KL)^2 GJ}} \right\}$$

$$= \frac{C_b \pi}{(KL)} \left\{ \frac{\pi \beta_x E I_y}{2(KL)} + \sqrt{E I_y G J} \sqrt{1 + \frac{\pi^2 E C_w}{(KL)^2 GJ} + \frac{\pi^2 \beta_x^2 E I_y}{(2KL)^2 GJ}} \right\}$$

$$= \frac{C_b \pi}{(KL)} \left\{ \frac{\pi \beta_x}{2(KL)} \sqrt{\frac{E I_y}{GJ}} \sqrt{E I_y G J} + \sqrt{E I_y G J} \sqrt{1 + \frac{\pi^2 E C_w}{(KL)^2 GJ} + \frac{\pi^2 \beta_x^2 E I_y}{(2KL)^2 GJ}} \right\}$$

$$= \frac{C_b \pi}{(KL)} \sqrt{E I_y G J} \left\{ \frac{\pi \beta_x}{2(KL)} \sqrt{\frac{E I_y}{GJ}} + \sqrt{1 + \frac{\pi^2 E C_w}{(KL)^2 GJ} + \frac{\pi^2 \beta_x^2 E I_y}{(2KL)^2 GJ}} \right\}$$

$$= \frac{C_b \pi}{KL} \sqrt{E I_y G J} \left\{ \frac{\pi \beta_x}{2KL} \sqrt{\frac{E I_y}{GJ}} + \sqrt{1 + \frac{\pi^2 E C_w}{(KL)^2 GJ} + \left(\frac{\pi \beta_x}{2KL} \sqrt{\frac{E I_y}{GJ}} \right)^2} \right\}$$

$$\therefore\ M_n = \frac{C_b \pi}{KL}\sqrt{EI_y GJ}\left\{\frac{\pi\beta_x}{2KL}\sqrt{\frac{EI_y}{GJ}} + \sqrt{1+\frac{\pi^2 EC_w}{(KL)^2 GJ}+\left(\frac{\pi\beta_x}{2KL}\sqrt{\frac{EI_y}{GJ}}\right)^2}\right\}$$

$$Let \qquad B_1 = \frac{\pi\beta_x}{2KL}\sqrt{\frac{EI_y}{GJ}} \qquad\qquad B_2 = \frac{\pi^2 EC_w}{(KL)^2 GJ} \tag{3.11}$$

The elastic nominal Moment (M_n) can then be expressed by the following equation.

$$M_n = \frac{C_b \pi}{KL}\sqrt{EI_y GJ}\left\{ B_1 + \sqrt{1 + B_2 + B_1^2}\right\} \tag{3.12}$$

Eq. 3.12 is the general formula for the elastic nominal moment (M_n) of monosymmetric beams.

The parameter B_1 is a function of β_x, as given by Eq. 3.11, arises from the bending compressive and tensile stresses that may form a resultant torque when the beam twists during buckling. For doubly symmetric beams, the torque component due to the compressive stresses exactly balances that due to the tensile stresses, and β_x is zero. According to Eq. 3.11, B_1 is therefore equal to zero. Since B_1 is zero, Eq. 3.12 can be simplified as given by the following equations.

$$M_n = \frac{C_b \pi}{KL}\sqrt{EI_y GJ}\sqrt{1 + B_2} \tag{3.13}$$

$$= \frac{C_b \pi}{KL}\sqrt{EI_y GJ + \frac{\pi^2 E^2 I_y C_w}{(KL)^2}} \tag{3.14}$$

Eq. 3.13 is the general formula for the elastic nominal moment (M_n) of doubly symmetric beams.

3.3 Inelastic Lateral-Torsional Buckling

Although lateral-torsional buckling is a complex problem, there are two undebatable facts: A beam with a small unbraced length should be able to develop its full plastic moment (M_p), and a beam with a large unbraced length should develop its elastic moment (M_n). For a beam with an intermediate unbraced length, the critical moment should fall between the plastic moment and the elastic moment.

Many research attempts on inelastic lateral-torsional buckling of beams has been performed in the past to obtain the smooth transition curve between the plastic moment and the elastic moment. For most specifications used today, the choice of this transition moment is rather empirical. For example, in the LRFD method, a straight line is used for this transition range; in the Allowable Stress Design (ASD) method, a parabola is used to represent this transition range.

A typical M_n versus L_b curve of a beam in LRFD is shown in Figure 3-3. The M_n is the nominal moment, M_p the plastic moment, and M_r the limiting lateral-torsional buckling moment. The limiting lateral-torsional buckling (M_r) is the elastic lateral-torsional buckling when $\lambda = \lambda_r$ and $C_b = 1.0$, and λ is the slenderness parameter, λ_r the largest value of λ for which buckling is inelastic. The L_b is the unbraced length, L_p the limiting unbraced length for full plastic bending capacity, and L_r the limiting unbraced length for inelastic lateral-torsional buckling.

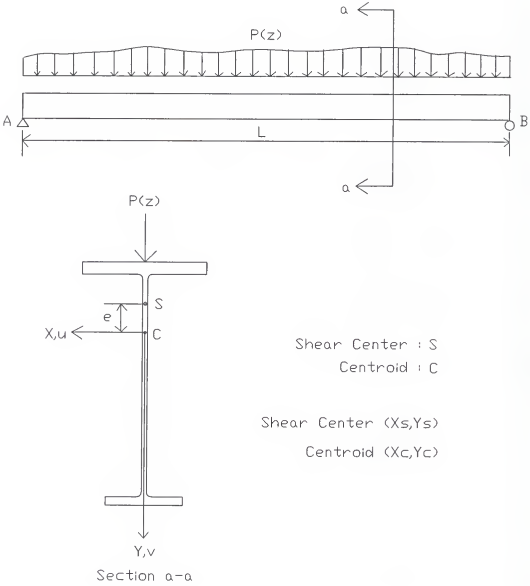

Figure 3-1. Beam general loading and cross-section.

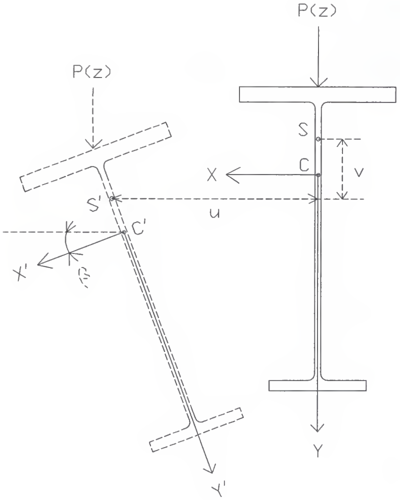

Figure 3-2. Section rotation.

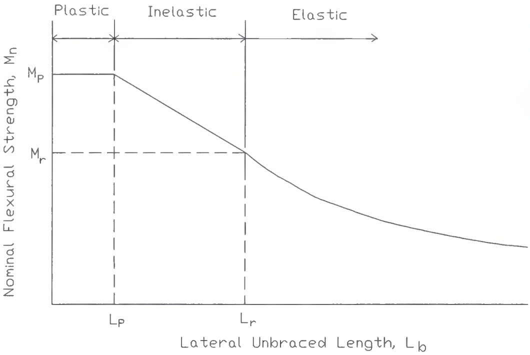

Figure 3-3. Schematic plot of M_n versus L_b in LRFD.

CHAPTER 4
LATERAL-TORSIONAL BUCKLING OF A ROLLED WIDE FLANGE BEAM WITH CHANNEL CAP

4.1 Introduction

It is common practice in crane runway beams to place a channel, open-side down, over the top of a wide flange, as shown in Figure 4-1, to increase its lateral stability. This is done because it is not always convenient to brace the compression flange between columns. The resulting beam has a singly symmetric or monosymmetric section. In this chapter, the elastic nominal moment (M_n) of this type of beam will be determined by using the formulas provided in chapter 3.

4.2 Elastic Lateral-Torsional Buckling

From chapter 3, the elastic nominal moment (M_n) of the monosymmetric beam can be obtained by the following equations.

$$M_n = \frac{C_b \pi}{KL} \sqrt{EI_y GJ} \left\{ B_1 + \sqrt{1 + B_2 + B_1^2} \right\} \tag{4.1}$$

where

$$B_1 = \frac{\pi \beta_x}{2KL} \sqrt{\frac{EI_y}{GJ}} , \qquad B_2 = \frac{\pi^2 EC_{wc}}{(KL)^2 GJ} \tag{4.2}$$

The difficulties associated with the computation of the elastic nominal moment (M_n) are in the determinations of the monosymmetry coefficient (β_x) and the section warping constant

(C_{wc}). The evaluations of β_x and C_{wc} are not straightforward. A step-by-step method is presented in the next section to evaluate β_x, C_{wc}, and other related section properties.

4.2.1 Section Properties

A typical section for a wide flange beam with a channel cap is shown in Figure 4-1. The section coordinate system, the shear center, and the centroid are also specified in the same figure. Because of the symmetry about the Y-axis, both X_c and X_s equal zero. There are five parameters (Y_c, Y_s, β_x, C_{wc}, J) which are essential to the computation of the elastic nominal moment (M_n). The Y_c is the location of centroid, Y_s is the location of shear center, β_x is the coefficient of monosymmetry, C_{wc} is the warping section constant, and J is the torsional section constant. Figures 4-3 and 4-4 show all the necessary notations used in the following equations below.

The centroid (X_c,Y_c). It is necessary to locate the centroid of section since all the computations of section properties are referred to it. The centroid of a general open thin-walled cross section is given by

$$X_c = \frac{\int_A X\,dA}{\int_A dA}\,, \qquad Y_c = \frac{\int_A Y\,dA}{\int_A dA} \tag{4.3}$$

The shear center (X_s,Y_s). The shear center is defined as the point in the plane of the cross section through which the shear force must act if no twisting of the section is to take place. According to Galambos [1968], the shear center of a

general open thin-walled cross section is given by the following equations:

$$X_s = -\frac{1}{I_x}\int_o^L\int_o^s yt\ ds\ dw = \frac{I_{wy}}{I_x} \tag{4.4}$$

$$Y_s = \frac{1}{I_y}\int_o^L\int_o^s xt\ ds\ dw = -\frac{I_{wx}}{I_y} \tag{4.5}$$

L and s are defined in Figure 4-3, t is the thickness of the plate, and W is expressed by

$$W = 2A_o = \int_o^s \rho ds \tag{4.6}$$

It is not an easy task to integrate directly the expressions given in Eqs. 4.4 to 4.6. However, the section is composed of thin, flat elements which lend themselves to a numerical procedure. The equivalent numerical procedure for a typical flat element and its related notations, as shown in Figure 4-4, is given by the following equations according to Heins [1975].

$$X_s = \frac{I_{wy}}{I_x}\ , \qquad Y_s = -\frac{I_{wy}}{I_y} \tag{4.7}$$

where

$$I_x = \frac{1}{3}\sum_o^n\ (Y_i^2 + Y_iY_j + Y_j^2)\,t_{ij}L_{ij} \tag{4.8}$$

$$I_y = \frac{1}{3} \sum_{o}^{n} (X_i^2 + X_i X_j + X_j^2)\, t_{ij} L_{ij} \tag{4.9}$$

$$I_{wx} = \frac{1}{3} \sum_{o}^{n} (W_i X_i + W_j X_j)\, t_{ij} L_{ij} + \frac{1}{6} \sum_{o}^{n} (W_i X_j + W_j X_i)\, t_{ij} L_{ij} \tag{4.10}$$

$$I_{wy} = \frac{1}{3} \sum_{o}^{n} (W_i Y_i + W_j Y_j)\, t_{ij} L_{ij} + \frac{1}{6} \sum_{o}^{n} (W_i Y_j + W_j Y_i)\, t_{ij} L_{ij} \tag{4.11}$$

$$W = W_i + \frac{(W_j - W_i)(x - x_i)}{(x_j - x_i)}, \qquad W_j = W_i + \rho_{ij} L_{ij} \tag{4.12}$$

Although the numerical procedure greatly simplifies the computation, it is still rather laborious for use in routine design. A better way to deal with these calculations is to use a computer. The description of the computer program to do the above calculations is discussed in Section 4.3.

The coefficient of monosymmetry (β_x). The coefficient of monosymmetry (β_x) is an important section property. According to Galambos [1968], the exact β_x is given by:

$$\beta_x = \frac{1}{I_x} \int_A Y(X^2 + Y^2)\, dA - 2(Y_s - Y_c) \tag{4.13}$$

To obtain β_x, one has to find the centroid of the section first and then the shear center of the section. Once this has been done, the distance between the centroid and the shear center, $(Y_s - Y_o)$, is determined. The β_x can then be evaluated by performing the integration over the section. The integration over the section is not difficult but tedious.

<u>The warping section constant (C_{wc})</u>. The warping section constant (C_{wc}) is the most difficult section property to be obtained. According to Galambos [1968], the C_{wc} for a general open thin-walled cross section can be computed by following equations.

$$C_{wc} = \int_{o}^{s} W_n^2 t ds \tag{4.14}$$

where

$$W_n = \frac{1}{A} \int_{o}^{L} W_o t ds - W_o \; , \qquad W_o = \int_{o}^{s} \rho_o \, ds \tag{4.15}$$

The ρ_o and s are defined in Figure 4-3 and t is the thickness of the plate. It can be seen from Eqs. 4.14 to 4.15 that the computation of C_{wc} includes the use of the integral forms, which is not favored by the design profession. However, since the cross section is made of thin, flat plate elements , the computation of C_{wc} can be greatly simplified by the fact that between points of intersection the unit warping properties W_o and W_n vary linearly, as shown in Figure 4-4. The determination of the warping torsional properties W_o and W_n can be obtained by considering the section to be composed of a series of interconnected plate elements. By numerical procedure, the warping section constant, therefore, can be evaluated. According to Heins [1975], the formulas which were used in the numerical procedure can be summarized by the following equations.

$$C_{wc} = \frac{1}{3} \sum_{o}^{n} (W_{ni}^2 + W_{nj}W_{ni} + W_{nj}^2)\, t_{ij}L_{ij} \tag{4.16}$$

where

$$W_n = W_{ni} + \left[(W_{nj} - W_n)/L_{ij}\right]s \tag{4.17}$$

$$W_o = \sum_{o}^{n} \rho_o L\ , \qquad W_{ni} = \frac{1}{2A} \sum_{o}^{n} (\ W_{oi} + W_{oj}\ )\, t_{ij}L_{ij} - W_{oi} \tag{4.18}$$

Again the numerical procedure greatly simplifies the computations, but they are laborious for use in the design profession.

The torsional section constant (J). The computation of J is much easier than β_x or C_{wc}. Figure 4-2 gives details of the section modeled into torsional plate elements with sides b_i and t_i. The b_i and t_i are the length and thickness of the plate element, respectively. The torsional section constant is then evaluated by the following equation.

$$J = \int_A r^2 dA = \frac{1}{3} \sum_{o}^{n} b_i\ t_i^3 \tag{4.19}$$

where n is the number of plate elements.

All section properties now can be calculated by using Eqs. 4.4 to 4.19 and the elastic nominal moment (M_n) are computed according to Eq. 4.1.

4.3 Inelastic Lateral-Torsional Buckling

As discussed in chapter 3, inelastic lateral-torsional designs in most specifications used today are based on

empirical results. For example, in the LRFD method, a straight line is used for the transition between M_p and M_r. M_p and M_r are the plastic moment and the limiting nominal moment, respectively.

4.4 Section Properties by Computer

From the preceding sections, it can be seen that the evaluations of some section properties (such as Y_c, Y_s, β_x, C_{wc}, J) are laborious tasks. Therefore, it would be very useful to develop a computer program to do the job.

The author has enhanced a computer program (LTBMN), which was originally written in BASIC language by Professor T. V. Galambos of the University of Minnesota and converted to FORTRAN language by Dr. Thomas Sputo, a consulting engineer in Gainesville, to compute the exact value of C_{wc}. The program was written based on the numerical procedure provided in section 4.2. The original program was written to calculate the warping section constant (C_{wc}) only. The author has expanded the program to evaluate the values of β_x, Z_x and some other important section properties. Once these section properties are obtained, the exact nominal moment (M_n) can be easily determined by using Eqs. 4.1 and 4.2. The user's manual and the listing of the LTBMN program are included in Appendices A and B, respectively.

The forty-five combined sections listed in the current AISC manual, with their exact β_x, C_{wc}, and J as computed by the program described above, are given in Tables 4-1 and 4-2.

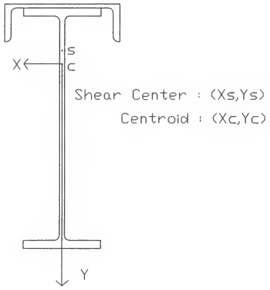

Figure 4-1. Section coordinate system.

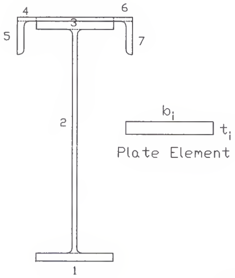

Figure 4-2. Torsional plate elements.

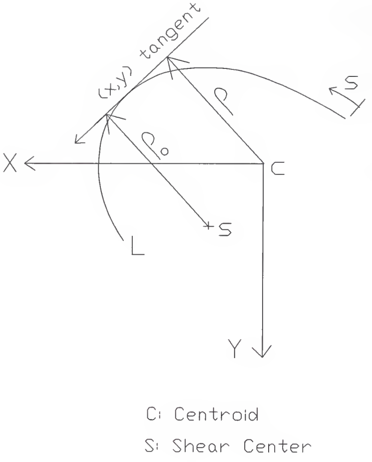

Figure 4-3. Coordinates and tangential distances in an open thin-walled section.

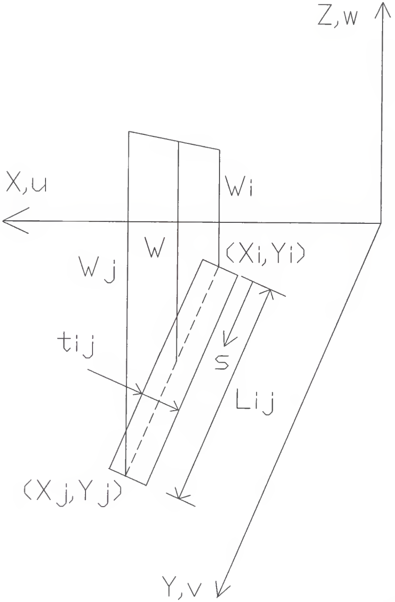

Figure 4-4. Distribution of W on a plane element.

Table 4-1. Section properties of W-Sections with channels listed in the ASD manual.

W		C	A_c/A_w	β_x	C_{wc}	J
36X194	*	18x42.7	0.221	20.60	195,616	34.328
30x173	*	18x42.7	0.248	13.86	201,928	26.854
36x170	*	18x42.7	0.252	21.81	170,231	24.738
30x132		15x33.9	0.256	17.83	72,261	16.115
33x152	*	18x42.7	0.282	21.45	128,022	21.238
27x146	*	18x42.7	0.294	14.52	129,011	20.460
27x114		15x33.9	0.297	17.42	49,422	12.914
24x62		12X20.7	0.335	18.31	9,052	2.923
24x104	*	18x42.7	0.412	15.85	65,510	10.864
21x101	*	18x42.7	0.423	14.27	49,820	11.726
18x76		15X33.9	0.447	11.99	22,137	6.900
14x43		12x20.7	0.483	10.15	3,999	2.210
16x67		15x33.9	0.506	11.61	14,635	6.124
24x62		15x33.9	0.547	20.69	10,077	4.120
14x61		15X33.9	0.556	10.12	9,934	5.611
18x76	*	18x42.7	0.565	13.86	24,702	7.717
16x67	*	18x42.7	0.640	13.01	16,388	6.882

<u>Note</u>:
W - Wide flange; C - Channel; * MC - Misc. channel
A_c - Area of channel; A_w - Area of wide flange
β_x - Coefficient of monosymmetry (in)
C_{wc} - Warping section constant (in^6)
J - Torsional section constant (in^4)

Table 4-2. Section properties of W-Sections with channels listed in the LRFD manual.

W		C	A_c/A_w	β_x	C_{wc}	J
36X150		15X33.9	0.225	18.28	13,2114	16.414
33X141		15X33.9	0.239	17.76	105,605	16.122
24X84		12X20.7	0.247	13.49	21,634	5.939
36X150	*	18X42.7	0.285	23.02	146,167	17.665
33X118		15X33.9	0.287	19.68	83,080	9.660
30X116		15X33.9	0.291	18.91	61,752	11.414
33X141	*	18X42.7	0.303	22.08	116,761	17.368
24X68		12X20.7	0.303	14.98	16,733	3.354
21X68		12X20.7	0.305	13.78	12,301	4.183
21X62		12X20.7	0.333	14.27	11,064	3.318
30X99		15X33.9	0.342	20.27	49,336	7.352
27X94		15X33.9	0.360	18.66	39,606	8.089
33X118	*	18X42.7	0.363	23.57	91,024	10.578
30X116	*	18X42.7	0.368	22.28	67,602	12.416
27X84		15X33.9	0.402	19.35	34,221	6.137
24X84		15X33.9	0.403	18.00	25,162	7.702
18X50		12X20.7	0.414	13.62	6,066	2.534
30X99	*	18X42.7	0.433	23.18	53,558	8.127
24X68		15X33.9	0.496	18.87	19,164	4.711
21X68		15X33.9	0.498	17.09	14,140	5.670
14X30		10X15.3	0.507	10.81	1,826	0.915
21X62		15X33.9	0.544	17.33	12,647	4.666
16X36		12X20.7	0.575	13.32	3,162	1.427
12X26		10X15.3	0.587	9.90	1,306	0.834
18X50		15X33.9	0.678	15.62	6,931	3.738
14X30		12X20.7	0.688	12.06	2,042	1.153
12X26		12X20.7	0.796	10.88	1,476	1.067
16X36		15X33.9	0.940	14.36	3,654	2.393

Note:
W - Wide flange; C - Channel; * MC - Misc. channel
A_c - Area of channel; A_w - Area of wide flange
β_x - Coefficient of monosymmetry (in)
C_{wc} - Warping section constant (in^6)
J - Torsional section constant (in^4)

CHAPTER 5
LATERAL-TORSIONAL BUCKLING BY LRFD APPROACH

5.1 Introduction

In this chapter, the nominal moment (M_n) of a wide flange beam with a channel cap will be determined by using the current LRFD formulas. The LRFD is based on the concept of limit states. For a beam, there are three possible types of failure modes: (1) plastic yielding, (2) lateral instability, and (3) local buckling. In this research, the attention will be limited to the first two failure modes, plastic yielding and lateral instability. The subject of local buckling is beyond the scope of this research. All sections used are considered to be compact sections.

5.2 LRFD Approach

The schematic plot of M_n versus L_b of a beam in LRFD is shown in Figure 5-1. The M_n is the nominal moment, M_p the plastic moment, and M_r the limiting lateral-torsional buckling moment. The M_r is the elastic lateral-torsional buckling when $\lambda = \lambda_r$ and $C_b = 1.0$, and λ is the slenderness parameter, λ_r the largest value of λ for which buckling is inelastic. The L_b is the unbraced length, L_p the limiting unbraced length for full plastic bending capacity, and L_r the limiting unbraced length for inelastic lateral-torsional buckling.

Plastic yielding. If L_b is less than or equal to L_p, the nominal moment is given by

$$M_n = M_p \tag{5.1}$$

Inelastic lateral-torsional buckling. If L_b is larger than L_p and less than L_r, the nominal moment is given by

$$M_n = C_b\left[M_p-(M_p-M_r)\left(\frac{L_b-L_p}{L_r-L_p}\right)\right] \leq M_p \tag{5.2}$$

Elastic lateral-torsional buckling. When L_b is larger than L_r, the beam will buckle elastically and the elastic lateral-torsional buckling formulas should be applied. From chapter 4, it is known that the difficulties associated with the calculations of the elastic critical moment are the section properties (β_x and C_{wc}). The LRFD code [1986] avoids these section properties and provides simplified but conservative formulas to compute the elastic lateral-torsional buckling of all monosymmetric beams, including the case of this research. No calculations of section properties (β_x and C_{wc}) are required in these LRFD formulas.

According to the current LRFD code [1986], the following formulas are used for the computation of the elastic nominal moment of a monosymmetric beam.

$$M_n = \frac{57000C_b}{L_b}\sqrt{I_yJ}\left[\,B_1 + \sqrt{1 + B_2 + B_1^2}\,\right] \leq M_p \tag{5.3}$$

where

$$B_1 = 2.25\left(\frac{2\ I_{yc}}{I_y} - 1\right)\left(\frac{h}{L_b}\right)\sqrt{\frac{I_y}{J}} \tag{5.4}$$

$$B_2 = 25\left(1 - \frac{I_{yc}}{I_y}\right)\left(\frac{I_{yc}}{J}\right)\left(\frac{h}{L_b}\right)^2 \tag{5.5}$$

Although these formulas are provided for the use of all monosymmetric beams including the case of this research, they were actually based on the research of a monosymmetric I-shaped beam, shown in Figure 5-2. The derivation of these formulas is given below.

According to Kitipornchai and Trahair [1980] and Galambos [1988], the following equations are used for the computation of the elastic lateral-torsional buckling of a monosymmetric I-shaped beam. The details of the section and its related notations used in the equations are also shown in Figure 5-2.

$$M_n = \frac{\pi C_b}{KL}\left\{\sqrt{EI_yGJ}\left[\ B_1 + \sqrt{1 + B_2 + B_1^{\ 2}}\ \right]\right\} \tag{5.6}$$

where

$$B_1 = \frac{\pi\beta_x}{2KL}\sqrt{\frac{EI_y}{GJ}}\ , \qquad B_2 = \frac{\pi^2 EC_{wc}}{(KL)^2 GJ} \tag{5.7}$$

$$\beta_x \approx 0.9h\left(\frac{2I_{yc}}{I_y} - 1\right)\left\{1 - \left(\frac{I_y}{I_x}\right)^2\right\} \tag{5.8}$$

$$C_{wc} = \frac{h^2 b_1^3 t_1 \alpha}{12}, \qquad \alpha = \frac{1}{1+(b_1/b_2)^3(t_1/t_2)} \tag{5.9}$$

$$I_y = \frac{t_1 b_1^3}{12} + \frac{t_2 b_2^3}{12} \qquad I_{yc} = \frac{t_1 b_1^3}{12} \tag{5.10}$$

With E = 29000 ksi, G = 11200 ksi, KL = L_b, and β_x given in Eq. 5.8, B_1 from Eq. 5.7 becomes:

$$B_1 = \frac{\pi \beta_x}{2KL}\sqrt{\frac{EI_y}{GJ}} = \frac{\pi \beta_x}{2L_b}\sqrt{\frac{29000 I_y}{11200 J}} = \frac{2.528}{L_b}\sqrt{\frac{I_y}{J}}\,\beta_x$$

$$\approx \frac{2.528}{L_b}\sqrt{\left(\frac{I_y}{J}\right)}\,(0.9)(h)\left(\frac{2I_{yc}}{I_y} - 1\right)\left(1 - (\frac{I_y}{I_x})^2\right)$$

$$\approx \frac{2.528}{L_b}\sqrt{\left(\frac{I_y}{J}\right)}\,(0.9)(h)\left(\frac{2I_{yc}}{I_y} - 1\right), \quad since \left(1-(\frac{I_y}{I_x})^2\right) \approx 1.0$$

$$\approx 2.25\left(\frac{2I_{yc}}{I_y} - 1\right)\left(\frac{h}{L_b}\right)\sqrt{\frac{I_y}{J}} \tag{5.11}$$

$$\therefore \; B_1 \approx 2.25\left(\frac{2I_{yc}}{I_y} - 1\right)\left(\frac{h}{L_b}\right)\sqrt{\frac{I_y}{J}} \tag{5.12}$$

With E = 29,000 ksi, G = 11,200 ksi, KL = L_b, I_y and I_{yc} given in Eq. 5.10, and C_{wc} given in Eq. 5.9, B_2 from Eq. 5.7 becomes:

$$B_2 = \frac{\pi^2 E C_{wc}}{(KL)^2 GJ} = \frac{\pi^2 E C_{wc}}{L_b^2 GJ} = \frac{\pi^2 E}{L_b^2 GJ}\,\frac{h^2 b_1^3 t_1 \alpha}{12}$$

$$= \frac{\pi^2 E}{L_b^2 GJ}\frac{h^2 b_1^3 t_1}{12}\frac{1}{1+(b_1/b_2)^3(t_1/t_2)} = \frac{\pi^2 E}{L_b^2 GJ}\frac{h^2 b_1^3 t_1}{12}\frac{b_2^3 t_2}{b_1^3 t_1 + b_2^3 t_2}$$

$$= \frac{\pi^2 E h^2}{L_b^2 GJ}\left(\frac{b_1^3 t_1}{12}\right)\left(\frac{b_2^3 t_2}{b_1^3 t_1 + b_2^3 t_2}\right) = \frac{25.56 h^2}{L_b^2 J}\left(\frac{b_1^3 t_1}{12}\right)\left(\frac{b_1^3 t_1 + b_2^3 t_2 - b_1^3 t_1}{b_1^3 t_1 + b_2^3 t_2}\right)$$

$$= \frac{25.56}{J}\left(\frac{h}{L_b}\right)^2 (I_{yc})\left(1 - \frac{I_{yc}}{I_y}\right) = 25.56\left(\frac{h}{L_b}\right)^2\left(\frac{I_{yc}}{J}\right)\left(1 - \frac{I_{yc}}{I_y}\right)$$

$$= 25.56\left(1 - \frac{I_{yc}}{I_y}\right)\left(\frac{I_{yc}}{J}\right)\left(\frac{h}{L_b}\right)^2$$

$$\approx 25\left(1 - \frac{I_{yc}}{I_y}\right)\left(\frac{I_{yc}}{J}\right)\left(\frac{h}{L_b}\right)^2 \tag{5.13}$$

$$\therefore B_2 \approx 25\left(1 - \frac{I_{yc}}{I_y}\right)\left(\frac{I_{yc}}{J}\right)\left(\frac{h}{L_b}\right)^2 \tag{5.14}$$

$$\frac{\pi C_b}{(KL)}\sqrt{EI_y GJ} = \frac{56618 C_b}{L_b}\sqrt{I_y J} \approx \frac{57000 C_b}{L_b}\sqrt{I_y J} \tag{5.15}$$

With Eqs. 5.12, 5.14, and 5.15, Eqs. 5.6 and 5.7 can be approximated by the following equations.

$$M_n = \frac{\pi C_b}{KL}\left\{\sqrt{EI_y GJ}\left(B_1 + \sqrt{1 + B_2 + B_1^2}\right)\right\}$$

$$\approx \frac{57000 C_b}{L_b}\sqrt{I_y J}\left\{B_1 + \sqrt{1 + B_2 + B_1^2}\right\} \tag{5.16}$$

where

$$B_1 = \frac{\pi\beta_x}{2KL}\sqrt{\frac{EI_y}{GJ}} \approx 2.25\left(\frac{2I_{yc}}{I_y} - 1\right)\left(\frac{h}{L_b}\right)\sqrt{\frac{I_y}{J}} \tag{5.17}$$

$$B_2 = \frac{\pi^2 EC_w}{(KL)^2 GJ} \approx 25\left(1 - \frac{I_{yc}}{I_y}\right)\left(\frac{I_{yc}}{J}\right)\left(\frac{h}{L_b}\right)^2 \tag{5.18}$$

Based on Eqs. 5.16, 5.17, and 5.18, the LRFD code adopts Eqs. 5.3, 5.4, and 5.5 to compute the elastic lateral-torsional buckling of a monosymmetric beam.

The above derivation shows that the current LRFD formulas for a monosymmetric beam are actually based on a monosymmetric I-shaped beam. When the formulas (Eqs. 5.3 to 5.5) are applied to the type of section considered in this research, which is not accounted in the derivation of the formulas, the results are questionable.

5.3 Comparisons of Nominal Moment (Mn) Between the Exact and LRFD Methods

In this section, the differences between the exact nominal moments (M_n) and the ones by the LRFD formulas will be investigated. The exact nominal moment was evaluated by using the exact β_x, C_{wc}, and J. The exact β_x, C_{wc}, and J are calculated by the program which is based on the numerical procedure as presented in Section 4.3.

Forty-five sections listed in the current ASD and LRFD manuals are used for the comparisons between the exact and LRFD methods. The unbraced lengths of beams vary from 60 to 70

feet which depends on the size of the section. The results of the seventeen sections listed in the ASD manual are recorded in Table 5-1 and plotted in Figure 5-3. The results of the twenty-eight sections listed in the LRFD manual are recorded in Table 5-2 and plotted in Figure 5-4. Three of the forty-five sections were selected and their M_n versus L_b curves by both the exact and the LRFD methods are recorded in Tables 5-3 to 5-5 and plotted in Figure 5-5 to 5-7. From these Tables and Figures, it can be seen that the exact M_n can be up to 23% higher than the one with LRFD formulas.

In conclusion, the current LRFD formulas to predict the elastic lateral-torsional buckling of a wide flange beam with a channel cap is too conservative in most of the forty-five sections. Based on this investigation, improvements of the current LRFD formulas for the predictions of lateral-torsional buckling are definitely needed.

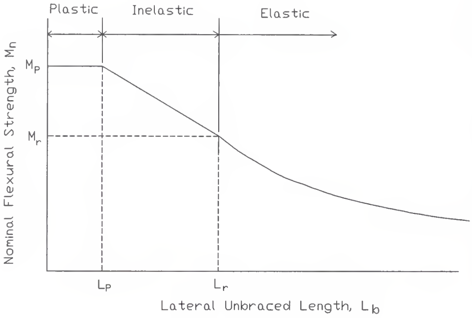

Figure 5-1. Schematic plot of M_n versus L_b in LRFD.

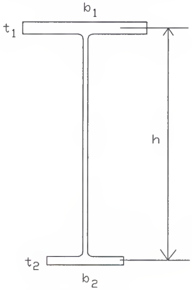

Figure 5-2. Monosymmetric I-shaped section.

Table 5-1. M_n versus A_c/A_w for the sections listed in the ASD manual.

W	C	A_c/A_w	Span	(%)
36X194	* 18x42.7	0.221	70	86.4
30x173	* 18x42.7	0.248	70	83.9
36x170	* 18x42.7	0.252	65	86.4
30x132	15x33.9	0.256	60	85.7
33x152	* 18x42.7	0.282	65	85.5
27x146	* 18x42.7	0.294	70	82.6
27x114	15x33.9	0.297	65	84.3
24x62	12X20.7	0.335	60	86.7
24x104	* 18x42.7	0.412	70	81.5
21x101	* 18x42.7	0.423	70	80.1
18x76	15X33.9	0.447	70	79.3
14x43	12x20.7	0.483	70	81.6
16x67	15x33.9	0.506	70	78.7
24x62	15x33.9	0.547	70	85.8
14x61	15X33.9	0.556	70	78.7
18x76	* 18x42.7	0.565	70	79.0
16x67	* 18x42.7	0.640	70	78.2

<u>Note</u>:
F_y = 50 ksi
W - Wide flange; C - Channel
* MC - Miscellaneous channel
A_c - Area of channel; A_w - Area of wide flange
Span - Span length (feet); M_n - Nominal moment
M_{n1} - Nominal moment by LRFD
M_{n2} - Exact nominal moment
(%) = Lowest % = M_{n1} / M_{n2} * 100

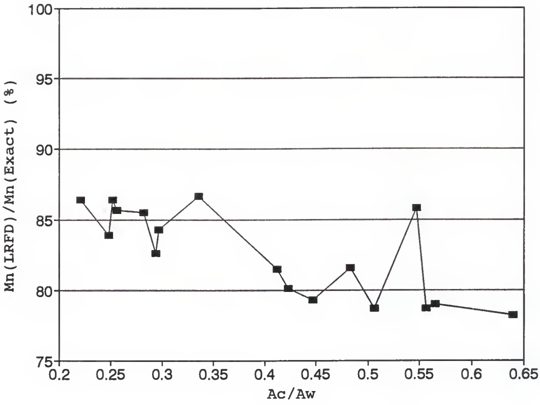

Figure 5-3. M_n(LRFD)/M_n(exact) versus A_c/A_w for the sections listed in the ASD manual and C_b = 1.

Table 5-2. M_n versus A_c/A_w for the sections listed in the LRFD manual.

W	C	A_c/A_w	Span	(%)
36X150	15X33.9	0.225	70	87.2
33X141	15X33.9	0.239	70	86.0
24X84	12X20.7	0.247	70	86.0
36X150	* 18X42.7	0.285	70	86.3
33X118	15X33.9	0.287	70	86.8
30X116	15X33.9	0.291	70	85.3
33X141	* 18X42.7	0.303	70	85.2
24X68	12X20.7	0.303	60	85.7
21X68	12X20.7	0.305	60	84.6
21X62	12X20.7	0.333	60	84.6
30X99	15X33.9	0.342	70	86.3
27X94	15X33.9	0.360	70	84.2
33X118	* 18X42.7	0.363	70	86.3
30X116	* 18X42.7	0.368	70	84.7
27X84	15X33.9	0.402	70	84.9
24X84	15X33.9	0.403	70	82.8
18X50	12X20.7	0.414	70	82.4
30X99	* 18X42.7	0.433	70	86.0
24X68	15X33.9	0.496	70	84.0
21X68	15X33.9	0.498	70	82.5
14X30	10X15.3	0.507	65	82.6
21X62	15X33.9	0.544	70	82.9
16X36	12X20.7	0.575	70	82.7
12X26	10X15.3	0.587	70	77.0
18X50	15X33.9	0.678	70	82.1
14X30	12X20.7	0.688	70	82.8
12X26	12X20.7	0.796	70	79.4
16X36	15X33.9	0.940	70	84.3

<u>Note</u>:
F_y = 50 ksi
W - Wide flange; C - Channel
* MC - Miscellaneous channel
A_c - Area of channel; A_w - Area of wide flange
Span - Span length (feet); M_n - Nominal moment
M_{n1} - Nominal moment by LRFD
M_{n2} - Exact nominal moment
(%) = Lowest % = M_{n1} / M_{n2} * 100

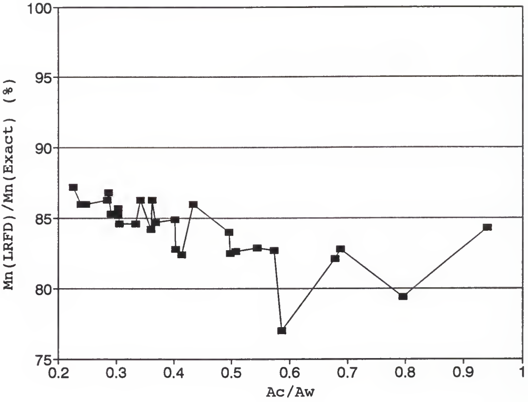

Figure 5-4. M_n(LRFD)/M_n(exact) versus A_c/A_w for the sections listed in the LRFD manual and C_b = 1.

Table 5-3. M_n versus L_b for the section of W30x173 with MC18x42.7, A_c/A_w=0.248.

L_b	M_{n1}	M_{n2}	(%)
0.00	3019.5	3019.5	100.0
19.32	3019.5	3019.5	100.0
44.36	2498.8	2408.4	96.4
48.71	2408.4	2067.2	85.8
48.86	2397.3	2057.3	85.8
50.00	2313.1	1982.2	85.7
51.67	2199.7	1881.1	85.5
53.33	2096.1	1789.0	85.3
55.00	2001.3	1704.7	85.2
56.67	1914.1	1627.3	85.0
58.33	1833.7	1556.2	84.9
60.00	1759.4	1490.6	84.7
61.67	1690.6	1429.8	84.6
63.33	1626.8	1373.6	84.4
65.00	1567.3	1321.3	84.3

<u>Note</u>:
F_y = 50 ksi
L_b (ft) - Unbraced length
M_n (k-ft) - Nominal moment
M_{n2} (k-ft) - Nominal moment by LRFD
M_{n1} (k-ft) - Exact nominal moment
(%) = M_{n2} / M_{n1} * 100

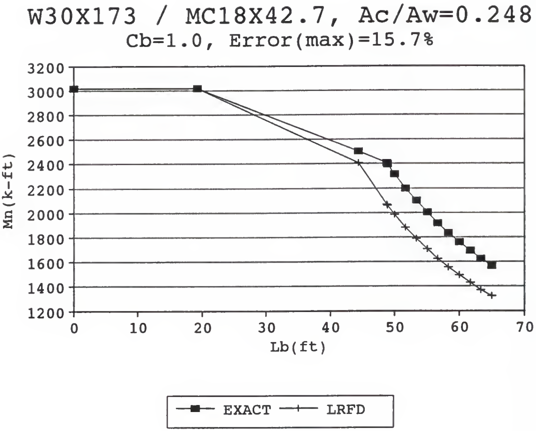

Note:
The EXACT curve is exact only in the elastic range and a straight line adopted by the LRFD specification is used for the inelastic range.

Figure 5-5. M_n versus L_b curves.

Table 5-4. M_n versus L_b for the section of W12x26 with C10x15.3, A_c/A_w=0.587.

L_b	M_{n1}	M_{n2}	(%)
0.00	194.5	194.5	100.0
11.39	194.5	194.5	100.0
32.84	160.1	151.1	94.4
37.50	152.7	122.4	80.2
38.46	151.1	117.7	77.9
40.00	142.3	110.7	77.8
41.67	133.8	104.0	77.8
43.33	126.2	98.0	77.7
45.00	119.3	92.7	77.6
46.67	113.1	87.8	77.6
48.33	107.5	83.4	77.5
50.00	102.4	79.4	77.5
51.67	97.7	75.7	77.5
53.33	93.4	72.3	77.4
55.00	89.5	69.2	77.4

<u>Note</u>:
F_y = 50 ksi
L_b (ft) - Unbraced length
M_n (k-ft) - Nominal moment
M_{n2} (k-ft) - Nominal moment by LRFD
M_{n1} (k-ft) - Exact nominal moment
(%) = M_{n2} / M_{n1} * 100

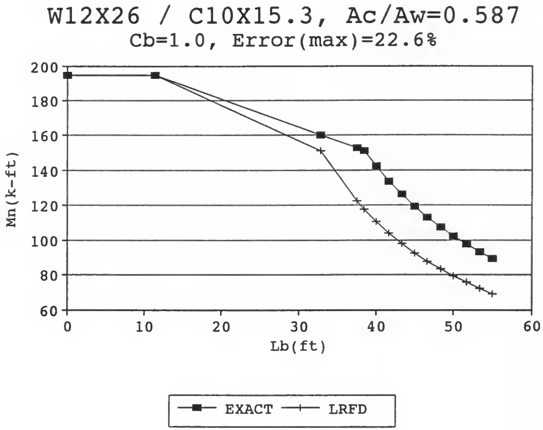

<u>Note</u>:
The EXACT curve is exact only in the elastic range and a straight line adopted by the LRFD specification is used for the inelastic range.

Figure 5-6. M_n versus L_b curves.

Table 5-5. M_n versus L_b for the section of W12x26 with C12x20.7, A_c/A_w=0.796.

L_b	M_{n1}	M_{n2}	(%)
0.00	202.0	202.0	100.0
13.98	202.0	202.0	100.0
45.82	162.3	153.2	94.3
52.64	153.8	124.0	80.6
53.20	153.2	122.0	79.7
55.00	145.8	116.1	79.6
56.67	139.6	111.1	79.6
58.33	133.8	106.5	79.6
60.00	128.5	102.2	79.5
61.67	123.6	98.3	79.5
63.33	119.0	94.6	79.5
65.00	114.7	91.1	79.5
66.67	110.7	87.9	79.4
68.33	107.0	84.9	79.4
70.00	103.4	82.1	79.4

<u>Note</u>:
F_y = 50 ksi
L_b (ft) - Unbraced length
M_n (k-ft) - Nominal moment
M_{n2} (k-ft) - Nominal moment by LRFD
M_{n1} (k-ft) - Exact nominal moment
(%) = M_{n2} / M_{n1} * 100

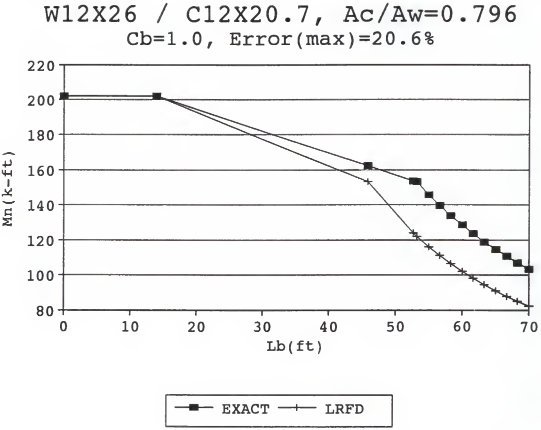

Note:
The EXACT curve is exact only in the elastic range and a straight line adopted by the LRFD specification is used for the inelastic range.

Figure 5-7. M_n versus L_b curves.

CHAPTER 6
PROPOSED MODELS

6.1 Introduction

The nominal moment (M_n) of a wide flange beam with a channel cap, as shown in Figure 6-1, by the current LRFD approach could have conservative results as high as 23% as discussed in Chapter 5. The conservative results are expectable because the LRFD uses the formulas derived based on a monosymmetric I-shaped section as shown in Figure 6-2. The difficulties associated with the section properties (β_x and C_{wc}) are the main reasons why the LRFD provides simplified but conservative formulas to compute the nominal moment of all monosymmetric beams, including the type of section considered in this research.

Alternatively, the designer could calculate the exact nominal moment of a wide flange beam with a channel cap with the help of the program presented in Section 4.3. However, the program may not be available to every designer.

The primary emphasis in this chapter is to develop simple and rational models of β_x, C_{wc}, and J for the evaluations of the nominal moment of a wide flange beam with a channel cap. In the following sections, a brief treatment of the models presented by other researchers will be discussed in Section

6.2, followed by the author's proposed models in Section 6.3. The approximate design based on the proposed models are presented at the end of the chapter.

6.2 Proposed Models by Kitipornchai and Trahair

In 1980, Kitipornchai and Trahair [1980] proposed their approximate models for their "lipped" section as shown in Figure 6-3, which closely approximates the case of this research, a wide flange with a channel cap. The notations used in the models are also referred to Figure 6-3.

6.2.1 The β_x Model

The proposed β_x model is given by:

$$\beta_x = 0.9h\left(\frac{2I_{yc}}{I_y} - 1\right)\left(1-(\frac{I_y}{I_x})^2\right)\left(1 + \frac{D_L}{2D}\right) \tag{6.1}$$

where

$$h = h_U + e\ , \quad e = (D_L^2\ B_C^2\ T_L)\ /\ (4\rho I_y)\ , \quad \rho = I_{yc}\ /\ I_y \tag{6.2}$$

The D, D_L, B_C, and T_L are defined and shown in Figure 6-3. The h_u is the distance between the center lines of the "unlipped" flanges and e is the distance between the shear center of the "lipped" flange and the center line of the "unlipped" flange. The I_x and I_y are the moments of inertia about X and Y axis, respectively. The I_{yc} is the moment of inertia of the compressive area about Y axis. The parameter h is evaluated using Eq. 6.2. The I_x, however, is not obtainable without knowing the centroid of the section.

This model is applied to the forty-five sections, which are listed in the current ASD and LRFD manuals. The results of the seventeen sections listed in the ASD manual and the twenty-eight sections listed in the LRFD manual are recorded in Tables 6-1 and 6-2, respectively. These two tables are combined and plotted in Figure 6-4. It can be seen from Figure 6-4 that the model gives good results when the ratio of A_c to A_w is less than 0.45 with a maximum error of -4.1%. However, when the ratio of A_c to A_w is greater than 0.45, the estimated error is increased with a maximum error of -19% when the ratio of A_c to A_w equals 0.796.

6.2.2 The C_{wc} Model

The proposed Cwc model is given by the following equation:

$$C_{wc} = a^2 I_{yc} + b^2 I_{yt} \tag{6.3}$$

where

$$a = (1-\rho) h \ , \quad b = \rho \ h \ , \quad I_{yt} = I_y - I_{yc} \tag{6.4}$$

$$h = h_U + e \ , \quad \rho = I_{yc} \ / \ I_y \ , \quad e = (D_L^2 \ B_C^2 \ T_L) \ / \ (4 \rho I_y) \tag{6.5}$$

The D_L, B_C, T_L, e, h_u, I_y, and I_{yc} are identical to the ones defined in the β_x model. Although some efforts are needed for the calculation of the model, it is quite straightforward.

This model is applied to the forty-five sections as mentioned in Section 6.2.1 and the results of the seventeen sections in the ASD manual and the twenty-eight sections in

the LRFD manual are recorded in Tables 6-3 and 6-4, respectively. These two tables are combined and plotted in Figure 6-5. It can be seen from Figure 6-5 that the model gives a good result when the ratio of A_c to A_w is less than 0.64 with a maximum error of -6%. The estimated error gets higher, as much as -12%, when the ratio of A_c to A_w exceeds 0.640.

There is another section property, the torsional section constant (J), which is also required for the calculation of the elastic nominal moment (M_n). However, Kitipornchai and Trahair did not include the model for it in their paper.

6.3 Proposed Models by the Author

From the preceding section, it has been seen that the models proposed by Kitipornchai and Trahair have some defects when the ratio of A_c to A_w is getting higher. Furthermore, the calculation of the β_x model needs the value of I_x, which involves the determination of the location of the centroid. In this section, the proposed β_x model will be presented first and followed by the C_{wc} and the J models.

6.3.1 The β_x Model

According to Kitipornchai and Trahair [1980], the β_x model, as related to Figure 6-3, is given by:

$$\beta_x = 0.9h\left(\frac{2I_{yc}}{I_y} - 1\right)\left(1-(\frac{I_y}{I_x})^2\right)\left(1 + \frac{D_L}{2D}\right) \tag{6.6}$$

Eliminating the term with I_x, the β_x becomes

$$\beta_x = 0.9h\left(\frac{2I_{yc}}{I_y} - 1\right)\left(1 + \frac{D_L}{2D}\right) \tag{6.7}$$

To simplify the equation, let h = D. The Eq. 6.7 becomes

$$\beta_x = 0.9D\left(\frac{2I_{yc}}{I_y} - 1\right)\left(1 + \frac{D_L}{2D}\right)$$

$$= 0.9\left(\frac{2I_{yc}}{I_y} - 1\right)\left(D + \frac{D_L}{2}\right) \tag{6.8}$$

$$= 0.9\,(2\rho - 1)\left(D + \frac{D_L}{2}\right), \quad \rho = \frac{2I_{yc}}{I_y} \tag{6.9}$$

By applying Eq. 6.9 to the forty-five sections listed in the AISC manual, the author found that the β_x model represented by Eq. 6.10 gives good approximations.

$$\beta_x = 0.87\,(2\rho - 1)\left(D + \frac{D_L}{2}\right), \quad \rho = \frac{2I_{yc}}{I_y} \tag{6.10}$$

where

$$I_y = I_{yw} + I_{xc}\,, \qquad I_{yc} = \frac{I_{yw}}{2} + I_{xc}$$

The section dimensions D and D_L are shown in Figure 6-1. The D is the overall depth of the section. The D_L is the flange width of channel. The I_y is the moment of inertia about weak axis and defined as the sum of I_{yw} and I_{xc}. The I_{yw} is the moment of inertia of the wide flange section about weak axis and I_{xc} is the moment of inertia of the channel section about strong axis. The I_{yc} is the moment of inertia of the

compression area about weak axis which is defined as the sum of I_{xc} and half of I_{yw}.

The proposed model as given by Eq. 6.10 is a simple and rational one involving no calculation of I_x. It is obvious from Eq. 6.10 that the use of the β_x model is quite straightforward without complications.

The developed β_x model, as given in Eq. 6.10, is applied to the forty-five sections as mentioned in Section 6.2.1. The results of the seventeen sections in the ASD manual and the twenty-eight sections in the LRFD manual are given in Tables 6-5 and 6-6, respectively. These two tables are combined and plotted in Figure 6-6. It can be seen from Figure 6-6 that the model give maximum errors of -4.1% to +3.2%. The estimated maximum error is relative small compared with the one by Kitipornchai and Trahair, which is -19%.

6.3.2 The C_{wc} Model

The objective of this section is to develop a reasonably accurate approach of calculating the warping section constant (C_{wc}), using a simple model which can be expressed in terms of known section properties or dimensions which are listed in the AISC manual.

The author used the program, which was discussed in Section 4.3, to calculate the exact values of warping section constants (C_{wc}) of a wide flange with a channel cap. The program is applied to the forty-five sections in the

AISC manual and the ratios of C_{wc} to C_w are recorded in Tables 6-7 and 6-8, respectively. These two tables are then combined and the ratios of C_{wc}/C_w are plotted against the ratios of A_c/A_w, as shown in Figure 6-7. The C_w, A_c, and A_w are the warping section constant of wide flange, the area of channel, and the area of wide flange, respectively.

By applying the multiple linear regression technique of statistics to the data of Figure 6-7, a curve (or model) was found to fit the data of Figure 6-7. The fitting curve (r^2 = 0.95) can be represented by:

$$C_{wc} = C_w\left(0.79 + 1.79\sqrt{\frac{A_c}{A_w}}\right), \qquad 0.2 \le \frac{A_c}{A_w} \le 0.95 \tag{6.11}$$

The resulting curve superimposed on the data of Figure 6-7 is shown in Figure 6-8. The model as given by Eq. 6.11 requires no calculation of section properties or parameters and use only C_w and the A_c/A_w as the independent variables. These variables A_c, A_w, and C_w are already given in the AISC Steel Manual.

The model is applied to the forty-five sections as discussed in Section 6.2.1 and the results of the seventeen sections in the ASD manual and the twenty-eight sections in the LRFD manual are recorded in Tables 6-9 and 6-10, respectively. These two tables are combined and plotted in Figure 6-9. It can be observed that the model gives results with errors of -3% to +5% in most of sections. There are only two extremely cases with errors -6.8% and +7.4%. The

estimated errors are small compared with the ones by Kitipornchai and Trahair with a maximum error of -12%.

6.3.3 The J model

The computation of the torsional section constant (J) is easier than β_x and C_{wc}. Figure 6-10 gives the details of the section modeled into torsional plate elements with sides b_i and t_i. The b_i and t_i are the length and thickness of the plate element, respectively. The section is composed of thin, flat elements which lend themselves to the numerical procedure. The torsional section constant is, therefore, evaluated by the numerical procedure and is given by:

$$J = \int_A r^2 dA = \frac{1}{3} \sum_{o}^{n} b_i\ t_i^3 \tag{6.12}$$

where n is the number of plate elements.

A further modification on Eq. 6.12 has been done by the author for the need of the practical designer. The modified formula of J is calculated based on the section properties and dimensions of wide flanges and channel caps and they are listed in both ASD and LRFD manuals. The proposed J is given by Eq. 6.13.

$$J = J_w + J_c + \frac{1}{3}B(t_1+t_2)^3 - \frac{1}{3}B(t_1^3+t_2^3)$$

$$= J_w + J_c + Bt_1t_2(t_1+t_2) \tag{6.13}$$

The J_w and J_c are the torsional section constants for the wide flange and the channel, respectively. The B is the

flange width of the wide flange, t_1 the web thickness of the channel, t_2 the flange thickness of the wide flange. The values of all these variables are given in the AISC manual.

The model is applied to the forty-five sections as discussed in Section 6.2.1 and the results of the seventeen sections in the ASD manual and the twenty-eight sections in the LRFD manual are recorded in Tables 6-11 and 6-12, respectively. These two tables are combined and plotted in Figure 6-11. It can be seen from Figure 6-11 that the model over estimates the value of J by +2.1% to +8.2%.

6.4 The Approximate Design Using the Proposed Models

The curve of the nominal moment (M_n) versus the unbraced length (L_b) will be examined in this section by using the proposed models as provided in Sections 6.3.

The elastic nominal moment (M_n) using the models proposed by the author can now be summarized by the following equations.

$$M_n = \frac{\pi C_b}{KL} \left[\sqrt{EI_y GJ} \; (B_1 + \sqrt{1 + B_2 + B_1^2}\,) \right] \tag{6.14}$$

where

$$B_1 = \frac{\pi \beta_x}{2KL}\sqrt{\frac{EI_y}{GJ}} \qquad B_2 = \frac{\pi^2 EC_{wc}}{(KL)^2 GJ} \tag{6.15}$$

$$\beta_x = 0.87\,(2\rho - 1)\left(D + \frac{D_L}{2}\right), \quad \rho = \frac{2I_{yc}}{I_y} \tag{6.16}$$

$$I_y = I_{yw} + I_{xc}\ , \qquad I_{yc} = \frac{I_{yw}}{2} + I_{xc} \tag{6.17}$$

$$C_{wc} = C_w\left(0.79 + 1.79\sqrt{\frac{A_c}{A_w}}\right), \qquad 0.2 \le \frac{A_c}{A_w} \le 0.95 \tag{6.18}$$

$$J = J_w + J_c + Bt_1t_2(t_1+t_2) \tag{6.19}$$

A straight line, which is adopted by the current LRFD method, is used for the inelastic nominal moment between the plastic moment (M_p) and the limiting moment (M_r). A typical plot of M_n versus L_b of a beam in LRFD method is shown in Figure 5-1.

The forty-five sections as mentioned in Section 6.2.1 are used to examine the differences between the exact nominal moments (M_n) and the ones based on the proposed models. The exact nominal moment has been discussed and presented in Section 4.3.

The unbraced lengths of beams vary from 60 to 70 feet which depends on the size of the section. The results of the seventeen sections in the ASD manual and the twenty-eight sections in the LRFD manual are recorded in Tables 6-13 and 6-14, respectively. These two tables are combined and plotted in Figure 6-12. It can be found from Figure 6-12, that the model gives estimated errors of -2.5% to +1.8%.

Three of the forty-five sections are selected and their M_n versus L_b curves based on the exact solution and the ones

proposed by the author are recorded and plotted in Table 6-15 and Figure 6-13, Table 6-16 and Figure 6-14, and Table 6-17 and Figure 6-15, respectively.

Based on Tables 6-13 , 6-14, and Figure 6-12, it can be seen that the proposed models, as given in Eqs. 6.16 to 6.19, are not only simple but also reasonably accurate. The section properties or dimensions used in these models are I_{yc}, I_y, D, D_L, A_c, A_w, B, t_1, and t_2. The I_{yc} and I_y can be easily calculated by using Eq. 6.17. The D, D_L, B, t_1, t_2, A_c, and A_w are the dimensions and areas of the wide flange and the channel. All the values of these parameters are listed in the AISC manual.

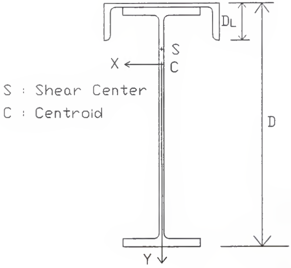

Figure 6-1. Section coordinate system.

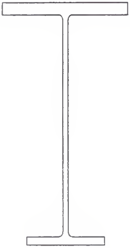

Figure 6-2. Monosymmetric I-shaped section.

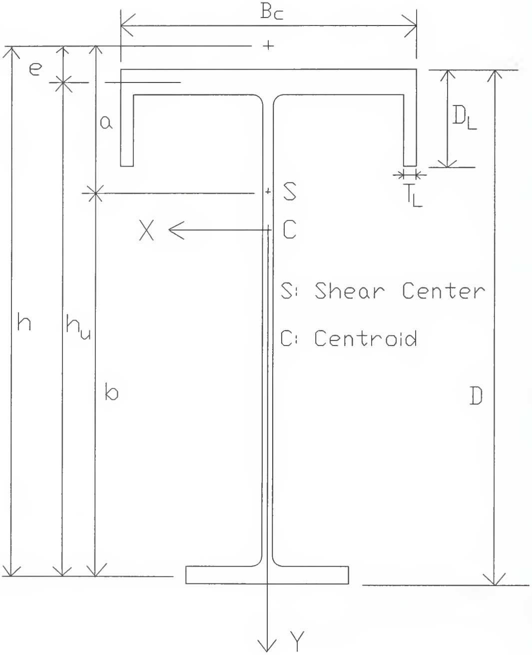

Figure 6-3. I-shaped section with lipped flanges.

Table 6-1. W-Sections with channels listed in the ASD manual.

W		C	A_c/A_w	β_{x1}	β_{x2}	Ratio
36X194	*	18x42.7	0.221	20.60	20.54	0.997
30x173	*	18x42.7	0.248	13.86	13.81	0.997
36x170	*	18x42.7	0.252	21.81	21.71	0.996
30x132		15x33.9	0.256	17.83	17.71	0.994
33x152	*	18x42.7	0.282	21.45	21.35	0.996
27x146	*	18x42.7	0.294	14.52	14.43	0.994
27x114		15x33.9	0.297	17.42	17.32	0.994
24x62		12X20.7	0.335	18.31	18.07	0.987
24x104	*	18x42.7	0.412	15.85	15.60	0.985
21x101	*	18x42.7	0.423	14.27	13.88	0.973
18x76		15X33.9	0.447	11.99	11.50	0.959
14x43		12x20.7	0.483	10.15	9.43	0.929
16x67		15x33.9	0.506	11.61	10.81	0.931
24x62		15x33.9	0.547	20.69	20.66	0.999
14x61		15X33.9	0.556	10.12	8.45	0.836
18x76	*	18x42.7	0.565	13.86	12.70	0.916
16x67	*	18x42.7	0.640	13.01	10.88	0.836

<u>Note</u>:
W - Wide flange; C - Channel; * MC - Misc. channel
A_c - Area of channel; A_w - Area of wide flange
β_{x1} - Exact coefficient of monosymmetry (in)
β_{x2} - Proposed coefficient of monosymmetry (in)
Ratio = β_{x2} / β_{x1}

Table 6-2. W-Sections with channels listed in the LRFD manual.

W		C	A_c/A_w	β_{x1}	β_{x2}	Ratio
36X150		15X33.9	0.225	18.27	18.19	0.996
33X141		15X33.9	0.239	17.75	17.64	0.994
24X84		12X20.7	0.247	13.48	13.26	0.983
36X150	*	18X42.7	0.285	23.02	22.93	0.996
33X118		15X33.9	0.287	19.68	19.59	0.995
30X116		15X33.9	0.291	18.90	18.78	0.994
33X141	*	18X42.7	0.303	22.07	21.98	0.996
24X68		12X20.7	0.303	14.97	14.73	0.984
21X68		12X20.7	0.305	13.78	13.54	0.983
21X62		12X20.7	0.333	14.26	14.01	0.982
30X99		15X33.9	0.342	20.26	20.20	0.997
27X94		15X33.9	0.360	18.65	18.52	0.993
33X118	*	18X42.7	0.363	23.57	23.54	0.999
30X116	*	18X42.7	0.368	22.27	22.23	0.998
27X84		15X33.9	0.402	19.35	19.23	0.994
24X84		15X33.9	0.403	17.99	17.84	0.991
18X50		12X20.7	0.414	13.61	13.30	0.977
30X99	*	18X42.7	0.433	23.18	23.20	1.001
24X68		15X33.9	0.496	18.86	18.70	0.991
21X68		15X33.9	0.498	17.09	16.86	0.987
14X30		10X15.3	0.507	10.80	10.36	0.959
21X62		15X33.9	0.544	17.33	17.05	0.984
16X36		12X20.7	0.575	13.32	12.77	0.959
12X26		10X15.3	0.587	9.89	9.16	0.926
18X50		15X33.9	0.678	15.62	14.87	0.952
14X30		12X20.7	0.688	12.05	10.99	0.912
12X26		12X20.7	0.796	10.87	8.87	0.816
16X36		15X33.9	0.940	14.36	12.05	0.840

<u>Note</u>:
W - Wide flange; C - Channel; * MC - Misc. channel
A_c - Area of channel; A_w - Area of wide flange
β_{x1} - Exact coefficient of monosymmetry (in)
β_{x2} - Proposed coefficient of monosymmetry (in)
Ratio = β_{x2} / β_{x1}

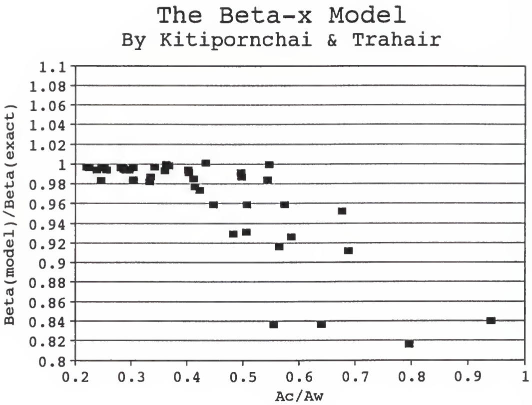

Figure 6-4. β_x(model)/β_x(exact) versus A_c/A_w.

Table 6-3. W-sections with channels listed the ASD manual.

W		C	A_c/A_w	C_{wc1}	C_{wc2}	Ratio
36X194	*	18x42.7	0.221	195,615	197,304	1.009
30x173	*	18x42.7	0.248	201,928	203,488	1.008
36x170	*	18x42.7	0.252	170,230	171,094	1.005
30x132		15x33.9	0.256	72,260	72,782	1.007
33x152	*	18x42.7	0.282	128,022	128,345	1.003
27x146	*	18x42.7	0.294	129,010	129,566	1.004
27x114		15x33.9	0.297	49,421	49,595	1.004
24x62		12X20.7	0.335	9,051	8,911	0.985
24x104	*	18x42.7	0.412	65,510	64,905	0.991
21x101	*	18x42.7	0.423	49,820	49,222	0.988
18x76		15X33.9	0.447	22,136	21,900	0.989
14x43		12x20.7	0.483	3,999	3,860	0.965
16x67		15x33.9	0.506	14,635	14,322	0.979
24x62		15x33.9	0.547	10,077	9,631	0.956
14x61		15X33.9	0.556	9,933	9,583	0.965
18x76	*	18x42.7	0.565	24,701	23,766	0.962
16x67	*	18x42.7	0.640	16,388	15,407	0.940

Note:
W - Wide flange; C - Channel; * MC - Misc. channel
A_c - Area of channel; A_w - Area of wide flange
C_{wc1} - Exact warping section constant (in^6)
C_{wc2} - Proposed warping section constant (in^6)
Ratio = C_{wc2} / C_{wc1}

Table 6-4. W-sections with channels listed the LRFD manual.

W		C	A_c/A_w	C_{wc1}	C_{wc2}	Ratio
36X150		15X33.9	0.225	13,2114	133,117	1.008
33X141		15X33.9	0.239	105,605	106,414	1.008
24X84		12X20.7	0.247	21,634	21,690	1.003
36X150	*	18X42.7	0.285	146,167	146,334	1.001
33X118		15X33.9	0.287	83,080	83,223	1.002
30X116		15X33.9	0.291	61,752	61,916	1.003
33X141	*	18X42.7	0.303	116,761	116,735	1.000
24X68		12X20.7	0.303	16,733	16,641	0.994
21X68		12X20.7	0.305	12,301	12,237	0.995
21X62		12X20.7	0.333	11,064	10,962	0.991
30X99		15X33.9	0.342	49,336	49,146	0.996
27X94		15X33.9	0.360	39,606	39,454	0.996
33X118	*	18X42.7	0.363	91,024	90,330	0.992
30X116	*	18X42.7	0.368	67,602	66,939	0.990
27X84		15X33.9	0.402	34,221	33,922	0.991
24X84		15X33.9	0.403	25,162	24,906	0.990
18X50		12X20.7	0.414	6,066	5,929	0.977
30X99	*	18X42.7	0.433	53,558	52,586	0.982
24X68		15X33.9	0.496	19,164	18,751	0.979
21X68		15X33.9	0.498	14,140	13,758	0.973
14X30		10X15.3	0.507	1,826	1,757	0.962
21X62		15X33.9	0.544	12,647	12,230	0.967
16X36		12X20.7	0.575	3,162	3,001	0.949
12X26		10X15.3	0.587	1,306	1,238	0.948
18X50		15X33.9	0.678	6,931	6,495	0.937
14X30		12X20.7	0.688	2,042	1,883	0.923
12X26		12X20.7	0.796	1,476	1,323	0.897
16X36		15X33.9	0.940	3,654	3,215	0.880

Note:
W - Wide flange; C - Channel; * MC - Misc. channel
A_c - Area of channel; A_w - Area of wide flange
C_{wc1} - Exact warping section constant (in^6)
C_{wc2} - Proposed warping section constant (in^6)
Ratio = C_{wc2} / C_{wc1}

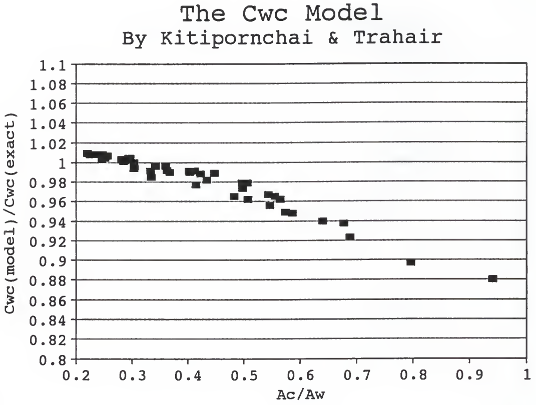

Figure 6-5. C_{wc}(model)/C_{wc}(exact) versus A_c/A_w.

Table 6-5. W-Sections with channels listed in the ASD manual.

W		C	A_c/A_w	β_{x1}	β_{x2}	Ratio
36X194	*	18x42.7	0.221	20.60	20.18	0.980
30x173	*	18x42.7	0.248	13.86	13.75	0.992
36x170	*	18x42.7	0.252	21.81	21.28	0.976
30x132		15x33.9	0.256	17.83	17.38	0.975
33x152	*	18x42.7	0.282	21.45	20.93	0.976
27x146	*	18x42.7	0.294	14.52	14.40	0.992
27x114		15x33.9	0.297	17.42	16.99	0.975
24x62		12X20.7	0.335	18.31	17.49	0.956
24x104	*	18x42.7	0.412	15.85	15.70	0.991
21x101	*	18x42.7	0.423	14.27	14.29	1.002
18x76		15X33.9	0.447	11.99	11.91	0.994
14x43		12x20.7	0.483	10.15	9.93	0.978
16x67		15x33.9	0.506	11.61	11.63	1.002
24x62		15x33.9	0.547	20.69	20.26	0.979
14x61		15X33.9	0.556	10.12	10.38	1.026
18x76	*	18x42.7	0.565	13.86	14.08	1.016
16x67	*	18x42.7	0.640	13.01	13.43	1.032

Note:
W - Wide flange; C - Channel; * MC - Misc. channel
A_c - Area of channel; A_w - Area of wide flange
β_{x1} - Exact coefficient of monosymmetry (in)
β_{x2} - Proposed coefficient of monosymmetry (in)
Ratio = β_{x2} / β_{x1}

Table 6-6. W-Sections with channels listed in the LRFD manual.

W		C	A_c/A_w	β_{x1}	β_{x2}	Ratio
36X150		15X33.9	0.225	18.27	17.77	0.973
33X141		15X33.9	0.239	17.75	17.29	0.974
24X84		12X20.7	0.247	13.48	12.98	0.963
36X150	*	18X42.7	0.285	23.02	22.38	0.973
33X118		15X33.9	0.287	19.68	19.08	0.970
30X116		15X33.9	0.291	18.90	18.37	0.972
33X141	*	18X42.7	0.303	22.07	21.52	0.975
24X68		12X20.7	0.303	14.97	14.34	0.958
21X68		12X20.7	0.305	13.78	13.25	0.962
21X62		12X20.7	0.333	14.26	13.68	0.959
30X99		15X33.9	0.342	20.26	19.64	0.969
27X94		15X33.9	0.360	18.65	18.11	0.971
33X118	*	18X42.7	0.363	23.57	22.95	0.974
30X116	*	18X42.7	0.368	22.27	21.77	0.977
27X84		15X33.9	0.402	19.35	18.75	0.969
24X84		15X33.9	0.403	17.99	17.53	0.974
18X50		12X20.7	0.414	13.61	13.10	0.962
30X99	*	18X42.7	0.433	23.18	22.66	0.978
24X68		15X33.9	0.496	18.86	18.36	0.973
21X68		15X33.9	0.498	17.09	16.76	0.981
14X30		10X15.3	0.507	10.80	10.36	0.959
21X62		15X33.9	0.544	17.33	16.98	0.980
16X36		12X20.7	0.575	13.32	12.87	0.967
12X26		10X15.3	0.587	9.89	9.52	0.962
18X50		15X33.9	0.678	15.62	15.50	0.992
14X30		12X20.7	0.688	12.05	11.77	0.977
12X26		12X20.7	0.796	10.87	10.71	0.986
16X36		15X33.9	0.940	14.36	14.49	1.009

<u>Note</u>:
W - Wide flange; C - Channel; * MC - Misc. channel
A_c - Area of channel; A_w - Area of wide flange
β_{x1} - Exact coefficient of monosymmetry (in)
β_{x2} - Proposed coefficient of monosymmetry (in)
Ratio = β_{x2} / β_{x1}

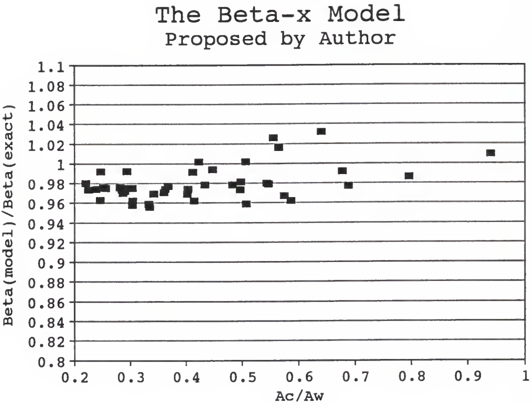

Figure 6-6. β_x(model)/β_x(exact) versus A_c/A_w.

Table 6-7. W-Sections with channels listed in the ASD manual.

W		C	A_c/A_w	C_{wc}	C_w	Ratio
36X194	*	18x42.7	0.221	195615	116000	1.686
30x173	*	18x42.7	0.248	201928	129000	1.565
36x170	*	18x42.7	0.252	170230	98500	1.728
30x132		15x33.9	0.256	72260	42100	1.716
33x152	*	18x42.7	0.282	128022	71700	1.786
27x146	*	18x42.7	0.294	129010	77200	1.671
27x114		15x33.9	0.297	49421	27600	1.791
24x62		12X20.7	0.335	9051	4620	1.959
24x104	*	18x42.7	0.412	65510	35200	1.861
21x101	*	18x42.7	0.423	49820	26200	1.902
18x76		15X33.9	0.447	22136	11700	1.892
14x43		12x20.7	0.483	3999	1950	2.051
16x67		15x33.9	0.506	14635	7300	2.005
24x62		15x33.9	0.547	10077	4620	2.181
14x61		15X33.9	0.556	9933	4710	2.109
18x76	*	18x42.7	0.565	24701	11700	2.111
16x67	*	18x42.7	0.640	16388	7300	2.245

Note:
W - Wide flange; C - Channel; * MC - Misc. channel
A_c - Area of channel; A_w - Area of wide flange
C_{wc} - Exact warping section constant (in^6)
C_w - Wide flange warping section constant (in^6)
Ratio = C_{wc} / C_w

Table 6-8. W-Sections with channels listed in the LRFD manual.

W	C	A_c/A_w	C_{wc}	C_w	Ratio
36X150	15X33.9	0.225	132114	82200	1.607
33X141	15X33.9	0.239	105605	64400	1.640
24X84	12X20.7	0.247	21633	12800	1.690
36X150	* 18X42.7	0.285	146167	82200	1.778
33X118	15X33.9	0.287	83079	48300	1.720
30X116	15X33.9	0.291	61752	34900	1.769
33X141	* 18X42.7	0.303	116761	64400	1.813
24X68	12X20.7	0.303	16733	9430	1.774
21X68	12X20.7	0.305	12301	6760	1.820
21X62	12X20.7	0.333	11064	5960	1.856
30X99	15X33.9	0.342	49335	26800	1.841
27X94	15X33.9	0.360	39605	21300	1.859
33X118	* 18X42.7	0.363	91023	48300	1.885
30X116	* 18X42.7	0.368	67601	34900	1.937
27X84	15X33.9	0.402	34221	17900	1.912
24X84	15X33.9	0.403	25162	12800	1.966
18X50	12X20.7	0.414	6065	3040	1.995
30X99	* 18X42.7	0.433	53557	26800	1.998
24X68	15X33.9	0.496	19163	9430	2.032
21X68	15X33.9	0.498	14140	6760	2.092
14X30	10X15.3	0.507	1826	887	2.059
21X62	15X33.9	0.544	12646	5960	2.122
16X36	12X20.7	0.575	3162	1460	2.166
12X26	10X15.3	0.587	1305	607	2.151
18X50	15X33.9	0.678	6931	3040	2.280
14X30	12X20.7	0.688	2041	887	2.302
12X26	12X20.7	0.796	1475	607	2.431
16X36	15X33.9	0.940	3653	1460	2.503

Note:
W - Wide flange; C - Channel; * MC - Misc. channel
A_c - Area of channel; A_w - Area of wide flange
C_{wc} - Exact warping section constant (in^6)
C_w - Wide flange warping section constant (in^6)
Ratio = C_{wc} / C_w

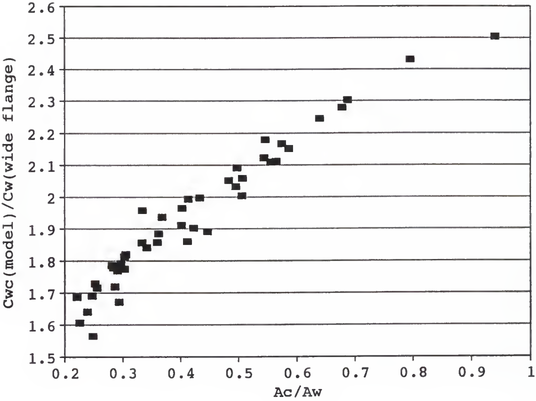

Figure 6-7. C_{wc}(model)/C_{wc} (wide flange) versus A_c/A_w.

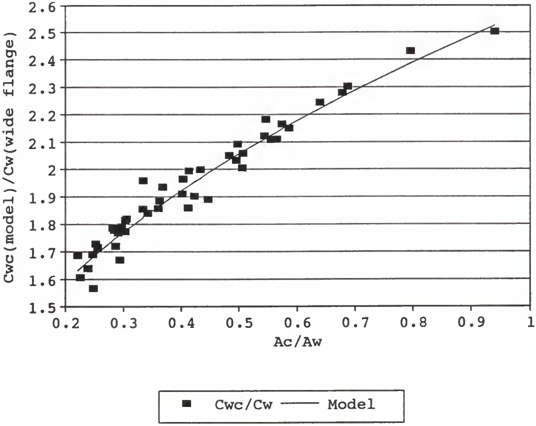

Figure 6-8. C_{wc}(exact)/C_w(wide flange) versus A_c/A_w.

Table 6-9. W-sections with channels listed in the ASD manual.

W		C	A_c/A_w	C_{wc1}	C_{wc2}	Ratio
36X194	*	18x42.7	0.221	195,615	189,264	0.968
30x173	*	18x42.7	0.248	201,928	216,909	1.074
36x170	*	18x42.7	0.252	170,230	166,324	0.977
30x132		15x33.9	0.256	72,260	71,391	0.988
33x152	*	18x42.7	0.282	128,022	124,783	0.975
27x146	*	18x42.7	0.294	129,010	135,878	1.053
27x114		15x33.9	0.297	49,421	48,742	0.986
24x62		12X20.7	0.335	9,051	8,433	0.932
24x104	*	18x42.7	0.412	65,510	68,239	1.042
21x101	*	18x42.7	0.423	49,820	51,193	1.028
18x76		15X33.9	0.447	22,136	23,239	1.050
14x43		12x20.7	0.483	3,999	3,967	0.992
16x67		15x33.9	0.506	14,635	15,058	1.029
24x62		15x33.9	0.547	10,077	9,767	0.969
14x61		15X33.9	0.556	9,933	10,009	1.008
18x76	*	18x42.7	0.565	24,701	24,985	1.011
16x67	*	18x42.7	0.640	16,388	16,217	0.990

Note:
W - Wide flange; C - Channel; * MC - Misc. channel
A_c - Area of channel; A_w - Area of wide flange
C_{wc1} - Exact warping section constant (in^6)
C_{wc2} - Proposed warping section constant (in^6)
Ratio = C_{wc2} / C_{wc1}

Table 6-10. W-sections with channels listed in the LRFD manual.

W		C	A_c/A_w	C_{wc1}	C_{wc2}	Ratio
36X150		15X33.9	0.225	13,2114	134784	1.020
33X141		15X33.9	0.239	105,605	107281	1.016
24X84		12X20.7	0.247	21,634	21488	0.993
36X150	*	18X42.7	0.285	146,167	143497	0.982
33X118		15X33.9	0.287	83,080	84476	1.017
30X116		15X33.9	0.291	61,752	61283	0.992
33X141	*	18X42.7	0.303	116,761	114318	0.979
24X68		12X20.7	0.303	16,733	16740	1.000
21X68		12X20.7	0.305	12,301	12017	0.977
21X62		12X20.7	0.333	11,064	10862	0.982
30X99		15X33.9	0.342	49,336	49237	0.998
27X94		15X33.9	0.360	39,606	39689	1.002
33X118	*	18X42.7	0.363	91,024	90254	0.992
30X116	*	18X42.7	0.368	67,602	65489	0.969
27X84		15X33.9	0.402	34,221	34446	1.007
24X84		15X33.9	0.403	25,162	24661	0.980
18X50		12X20.7	0.414	6,066	5904	0.973
30X99	*	18X42.7	0.433	53,558	52738	0.985
24X68		15X33.9	0.496	19,164	19331	1.009
21X68		15X33.9	0.498	14,140	13879	0.982
14X30		10X15.3	0.507	1,826	1831	1.003
21X62		15X33.9	0.544	12,647	12578	0.995
16X36		12X20.7	0.575	3,162	3134	0.991
12X26		10X15.3	0.587	1,306	1311	1.005
18X50		15X33.9	0.678	6,931	6880	0.993
14X30		12X20.7	0.688	2,042	2017	0.988
12X26		12X20.7	0.796	1,476	1448	0.982
16X36		15X33.9	0.940	3,654	3686	1.009

Note:
W - Wide flange; C - Channel; * MC - Misc. channel
A_c - Area of channel; A_w - Area of Wide flange
C_{wc1} - Exact warping section constant (in^6)
C_{wc2} - Proposed warping section constant (in^6)
Ratio = C_{wc2} / C_{wc1}

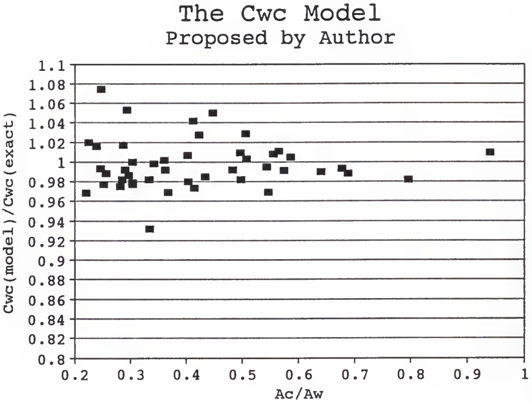

Figure 6-9. C_{wc}(model)/C_{wc}(exact) versus A_c/A_w.

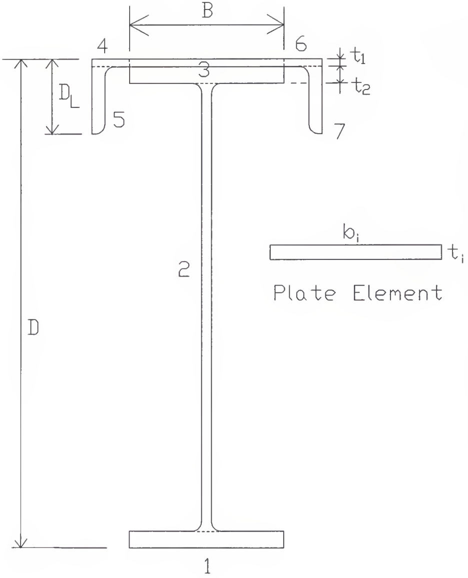

Figure 6-10. Torsional plate elements.

Table 6-11. W-Sections with channels listed in the ASD manual.

W		C	A_c/A_w	Js	Jm	Ratio
36X194	*	18x42.7	0.221	34.328	35.176	1.025
30x173	*	18x42.7	0.248	26.854	27.410	1.021
36x170	*	18x42.7	0.252	24.738	25.560	1.033
30x132		15x33.9	0.256	16.115	16.645	1.033
33x152	*	18x42.7	0.282	21.238	21.893	1.031
27x146	*	18x42.7	0.294	20.460	20.861	1.020
27x114		15x33.9	0.297	12.914	13.332	1.032
24x62		12X20.7	0.335	2.923	3.101	1.061
24x104	*	18x42.7	0.412	10.864	11.114	1.023
21x101	*	18x42.7	0.423	11.726	11.970	1.021
18x76		15X33.9	0.447	6.900	7.092	1.028
14x43		12x20.7	0.483	2.210	2.390	1.082
16x67		15x33.9	0.506	6.124	6.309	1.030
24x62		15x33.9	0.547	4.120	4.375	1.062
14x61		15X33.9	0.556	5.611	5.915	1.054
18x76	*	18x42.7	0.565	7.717	7.876	1.021
16x67	*	18x42.7	0.640	6.882	7.035	1.022

<u>Note</u>:
W - Wide flange; C - Channel; * MC - Misc. channel
A_c - Area of channel; A_w - Area of wide flange
Js - Exact torsional section constant (in^4)
Jm - Proposed torsional section constant (in^4)
Ratio = Jm / Js

Table 6-12. W-Sections with channels listed in the LRFD manual.

W		C	A_C/A_W	Js	Jm	Ratio
36X150		15X33.9	0.225	16.414	17.153	1.045
33X141		15X33.9	0.239	16.122	16.744	1.039
24X84		12X20.7	0.247	5.939	6.130	1.032
36X150	*	18X42.7	0.285	17.665	18.371	1.040
33X118		15X33.9	0.287	9.660	10.194	1.055
30X116		15X33.9	0.291	11.414	11.910	1.043
33X141	*	18X42.7	0.303	17.368	17.956	1.034
24X68		12X20.7	0.303	3.354	3.522	1.050
21X68		12X20.7	0.305	4.183	4.365	1.043
21X62		12X20.7	0.333	3.318	3.482	1.049
30X99		15X33.9	0.342	7.352	7.787	1.059
27X94		15X33.9	0.360	8.089	8.459	1.046
33X118	*	18X42.7	0.363	10.578	11.079	1.047
30X116	*	18X42.7	0.368	12.416	12.879	1.037
27X84		15X33.9	0.402	6.137	6.482	1.056
24X84		15X33.9	0.403	7.702	7.970	1.035
18X50		12X20.7	0.414	2.534	2.636	1.040
30X99	*	18X42.7	0.433	8.127	8.529	1.049
24X68		15X33.9	0.496	4.711	4.956	1.052
21X68		15X33.9	0.498	5.670	5.929	1.046
14X30		10X15.3	0.507	0.915	0.979	1.070
21X62		15X33.9	0.544	4.666	4.907	1.052
16X36		12X20.7	0.575	1.427	1.513	1.060
12X26		10X15.3	0.587	0.834	0.877	1.052
18X50		15X33.9	0.678	3.738	3.918	1.048
14X30		12X20.7	0.688	1.153	1.237	1.073
12X26		12X20.7	0.796	1.067	1.130	1.059
16X36		15X33.9	0.940	2.393	2.557	1.069

<u>Note</u>:
W - Wide flange; C - Channel; * MC - Misc. channel
A_C - Area of channel; A_W - Area of wide flange
Js - Exact torsional section constant (in^4)
Jm - Proposed torsional section constant (in^4)
Ratio = Jm / Js

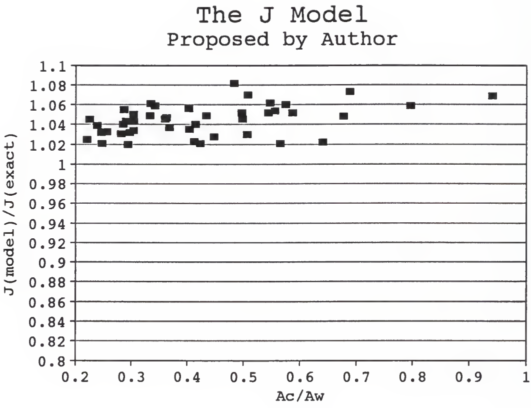

Figure 6-11. J(model)/J(exact) versus A_c/A_w.

Table 6-13. M_n versus A_c/A_w for W-sections with channels listed in the ASD manual.

W	C	A_c/A_w	L_b	Error(%)
36X194	* 18x42.7	0.221	70	-1.1 to -0.3
30x173	* 18x42.7	0.248	70	+0.1 to +0.5
36x170	* 18x42.7	0.252	65	-1.2 to -0.3
30x132	15x33.9	0.256	60	-1.1 to -0.3
33x152	* 18x42.7	0.282	65	-1.2 to -0.3
27x146	* 18x42.7	0.294	70	+0.0 to +0.1
27x114	15x33.9	0.297	65	-1.1 to -0.3
24x62	12X20.7	0.335	60	-2.5 to -0.9
24x104	* 18x42.7	0.412	70	-0.1 to 0.0
21x101	* 18x42.7	0.423	70	+0.1 to +0.3
18x76	15X33.9	0.447	70	0.0 to +0.1
14x43	12x20.7	0.483	70	+0.1 to +1.3
16x67	15x33.9	0.506	70	+0.1 to +0.5
24x62	15x33.9	0.547	70	-0.8 to +0.1
14x61	15X33.9	0.556	70	+0.3 to +1.8
18x76	* 18x42.7	0.565	70	+0.1 to +0.7
16x67	* 18x42.7	0.640	70	+0.2 to +1.2

Note:
F_y = 50 ksi
W - Wide flange; C - Channel; * MC - Misc. channel
A_c - Area of channel; A_w - Area of wide flange
L_b - Unbraced length (feet); M_n - Nominal moment
M_{n1} - Exact nominal moment
M_{n2} - Nominal moment by proposed models
Error (%) = $(M_{n2} - M_{n1}) / M_{n1} * 100$

Table 6-14. M_n versus A_c/A_w for W-sections with channels listed in the LRFD manual.

W		C	A_c/A_w	L_b	Error(%)
36X150		15X33.9	0.225	70	-0.8 to -0.1
33X141		15X33.9	0.239	70	-0.9 to -0.2
24X84		12X20.7	0.247	70	-1.8 to -0.7
36X150	*	18X42.7	0.285	70	-1.4 to -0.4
33X118		15X33.9	0.287	70	-1.1 to -0.3
30X116		15X33.9	0.291	70	-1.3 to -0.4
33X141	*	18X42.7	0.303	70	-1.3 to -0.7
24X68		12X20.7	0.303	60	-2.1 to -1.0
21X68		12X20.7	0.305	60	-1.9 to -0.5
21X62		12X20.7	0.333	60	-2.0 to -0.5
30X99		15X33.9	0.342	70	-1.4 to -0.4
27X94		15X33.9	0.360	70	-1.2 to -0.5
33X118	*	18X42.7	0.363	70	-1.3 to -0.5
30X116	*	18X42.7	0.368	70	-1.2 to -0.5
27X84		15X33.9	0.402	70	-1.2 to -0.3
24X84		15X33.9	0.403	70	-1.2 to -0.5
18X50		12X20.7	0.414	70	-2.0 to -0.8
30X99	*	18X42.7	0.433	70	-1.0 to -0.2
24X68		15X33.9	0.496	70	-1.1 to -0.2
21X68		15X33.9	0.498	70	-0.6 to +0.1
14X30		10X15.3	0.507	65	-1.2 to +0.2
21X62		15X33.9	0.544	70	-0.5 to +0.1
16X36		12X20.7	0.575	70	-0.4 to +1.4
12X26		10X15.3	0.587	70	-2.5 to -0.8
18X50		15X33.9	0.678	70	+0.1 to +0.6
14X30		12X20.7	0.688	70	-0.4 to +0.6
12X26		12X20.7	0.796	70	-1.6 to -1.3
16X36		15X33.9	0.940	70	+0.4 to +1.8

<u>Note</u>:
F_y = 50 ksi
W - Wide flange; C - Channel; * MC - Misc. channel
A_c - Area of channel; A_w - Area of wide flange
L_b - Unbraced length (feet); M_n - Nominal moment
M_{n1} - Exact nominal moment
M_{n2} - Nominal moment by proposed models
Error (%) = $(M_{n2} - M_{n1}) / M_{n1} * 100$

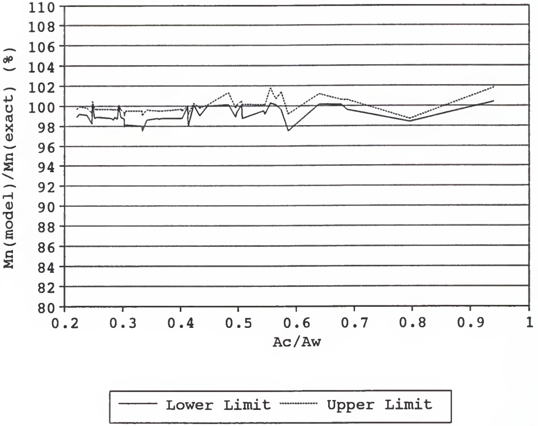

Figure 6-12. M_n(model)/M_n(exact) versus A_c/A_w.

Table 6-15. M_n versus L_b for W36x150 with C15x33.9, A_c/A_w=.225, Fy = 50 ksi.

L_b	M_{n1}	M_{n2}	M_{n3}	Percent
0.00	2945.3	2945.3	2945.3	100.0
16.28	2945.3	2945.3	2945.3	100.0
34.62	2351.8	2280.8	2347.0	99.8
36.64	2286.2	2063.3	2280.8	99.2
36.81	2280.8	2047.1	2263.4	99.2
38.33	2128.9	1907.5	2113.5	99.3
40.00	1981.8	1772.4	1968.3	99.3
41.67	1851.4	1652.9	1839.6	99.4
43.33	1735.4	1546.5	1725.0	99.4
45.00	1631.6	1451.5	1622.5	99.4
46.67	1538.3	1366.2	1530.3	99.5
48.33	1454.1	1289.3	1447.1	99.5
50.00	1377.8	1219.7	1371.8	99.6
51.67	1308.4	1156.5	1303.2	99.6
53.33	1245.2	1098.9	1240.6	99.6
55.00	1187.2	1046.3	1183.3	99.7
56.67	1134.1	998.0	1130.7	99.7
58.33	1085.1	953.6	1082.3	99.7
60.00	1039.9	912.7	1037.5	99.8
61.67	998.1	874.8	996.1	99.8
63.33	959.3	839.7	957.7	99.8
65.00	923.2	807.2	921.9	99.9
66.67	889.6	776.9	888.6	99.9
68.33	858.2	748.6	857.5	99.9
70.00	828.8	722.2	828.4	99.9

Note:
M_n - Nominal moment (k-ft)
L_b - Unbraced length (ft)
M_{n1} - Exact nominal moment
M_{n2} - Nominal moment by LRFD
M_{n3} - Nominal moment by proposed models
Percent (%) = M_{n3} / M_{n1}

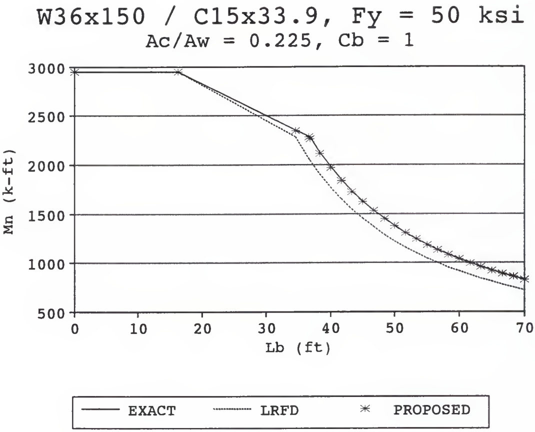

Note:
The EXACT curve is exact only in the elastic range and a straight line adopted by the LRFD specification is used for the inelastic range.

Figure 6-13. M_n versus L_b.

Table 6-16. M_n versus L_b for W27x84 with C15x33.9, A_c/A_w=.402, Fy = 50 ksi.

L_b	M_{n1}	M_{n2}	M_{n3}	Percent
0.00	1312.1	1312.1	1312.1	100.0
16.78	1312.1	1312.1	1312.1	100.0
40.95	1026.6	985.7	1023.2	99.7
44.09	989.5	866.5	985.7	98.8
44.41	985.7	855.5	973.6	98.8
45.00	964.2	836.4	952.6	98.8
46.67	907.3	785.7	897.0	98.9
48.33	856.0	740.1	846.8	98.9
50.00	809.6	698.8	801.3	99.0
51.67	767.4	661.3	760.0	99.0
53.33	729.0	627.2	722.4	99.1
55.00	693.8	596.1	687.9	99.2
56.67	661.6	567.5	656.3	99.2
58.33	631.9	541.3	627.2	99.3
60.00	604.6	517.2	600.4	99.3
61.67	579.3	494.9	575.6	99.4
63.33	555.9	474.2	552.6	99.4
65.00	534.1	455.1	531.2	99.5
66.67	513.9	437.3	511.3	99.5
68.33	495.0	420.7	492.7	99.5
70.00	477.3	405.2	475.4	99.6

<u>Note</u>:
M_n - Nominal moment (k-ft)
L_b - Unbraced length (ft)
M_{n1} - Exact nominal moment
M_{n2} - Nominal moment by LRFD
M_{n3} - Nominal moment by proposed models
Percent (%) = M_{n3} / M_{n1}

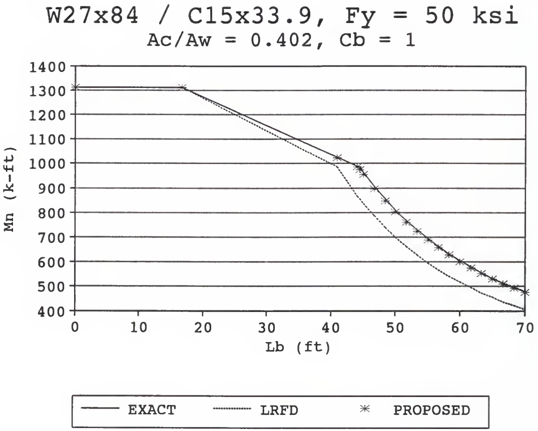

<u>Note</u>:
The EXACT curve is exact only in the elastic range and a straight line adopted by the LRFD specification is used for the inelastic range.

Figure 6-14. M_n versus L_b.

Table 6-17. M_n versus L_b for W12x26 with C12x20.7, A_c/A_w=.796, Fy = 50 ksi.

L_b	M_{n1}	M_{n2}	M_{n3}	Percent
0.00	202.0	202.0	202.0	100.0
13.98	202.0	202.0	202.0	100.0
45.82	162.3	153.2	161.8	99.6
52.64	153.8	124.0	153.2	98.4
53.20	153.2	122.0	150.8	98.5
55.00	145.8	116.1	143.6	98.5
56.67	139.6	111.1	137.5	98.5
58.33	133.8	106.5	131.8	98.5
60.00	128.5	102.2	126.6	98.5
61.67	123.6	98.3	121.8	98.6
63.33	119.0	94.6	117.3	98.6
65.00	114.7	91.1	113.1	98.6
66.67	110.7	87.9	109.2	98.6
68.33	107.0	84.9	105.5	98.6
70.00	103.4	82.1	102.0	98.6

Note:
M_n - Nominal moment (k-ft)
L_b - Unbraced length (ft)
M_{n1} - Exact nominal moment
M_{n2} - Nominal moment by LRFD
M_{n3} - Nominal moment by proposed models
Percent (%) = M_{n3} / M_{n1}

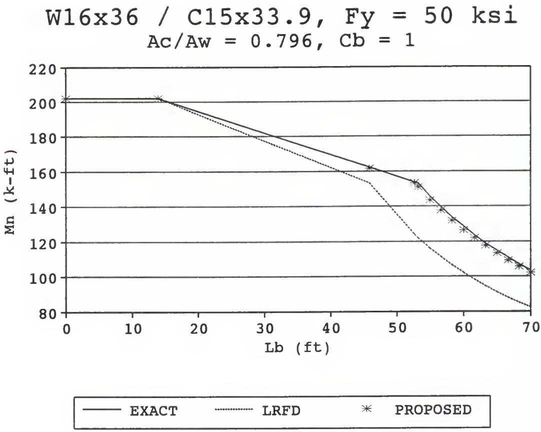

Note:
The EXACT curve is exact only in the elastic range and a straight line adopted by the LRFD specification is used for the inelastic range.

Figure 6-15. M_n versus L_b.

CHAPTER 7
LABORATORY TESTING

7.1 Introduction

This chapter presents an experimental investigation of the lateral-torsional buckling of molded fiberglass and rolled steel beams. The testing was conducted as part of this research and consisted of two phases of testing.

Phase one. Testing in phase one consisted of tests of sixteen small-scale molded fiberglass beams and was the preliminary test of phase two. Eight were wide flange beams without channel caps and the rest were wide flange beams with channel caps. All sixteen fiberglass beams failed in the elastic range.

Phase two. Testing in phase two consisted of tests of eighteen steel beams. Eight of them were rolled wide flange beams without channel caps and the remaining ten were rolled wide flange beams with channel caps. Eight rolled steel wide flange beams and two rolled steel wide flange beams with channel caps were observed to fail in the elastic range. Ten wide flange beams with channel caps were found to fail by either yielding or inelastic buckling.

Specially designed roller supports allowed the end cross sections of each test beam to rotate about the major and minor

axes and to warp freely, but restrained them against twisting about the longitudinal axis of the beam. Details of end supports are shown in Figure 7-1.

The load was applied through the loading frame as either a point concentrated load or a flat concentrated load, as shown in Figures 7-2a and 7-2b, respectively. A flat concentrated load is a load applied through a beam bearing flat against the top flange as opposed to a ball-joint. It was observed in these tests that a point load and a flat load created significantly different results under the same loading conditions. Subsidiary tests including twenty-two tensile coupon tests were conducted to determine steel nominal yield stresses.

In the following sections, a brief treatment of the tests of the molded fiberglass beams will be discussed in Section 7.2 followed by the tests of the steel beams in Section 7.3. A summary is presented at the end of the chapter.

7.2 Phase One Testing

7.2.1 General

Phase one testing was performed to obtain preliminary information prior to implementing phase two which included eighteen tests of full-scale steel beams. This testing was to investigate the lateral-torsional buckling of small-scale molded fiberglass beams. Each test was carried out on a simply supported fiberglass beam with a concentrated gravity load applied at the midspan as shown in Figure 7-3. The load was

applied in an essentially static manner, in large increments in the beginning, then small increments, and finally very small increments as the buckling load was approached. The beam was loaded to failure in each test. The end supports allowed the end cross sections of each test beam to rotate about the major and minor axes and to warp freely, but restrained them against twisting about longitudinal axis. The details of end supports are shown in Figure 7-4.

7.2.2 Tests of Wide Flange Beams Without Channel Caps

A total of eight nominally identical fiberglass wide flange beams without channel caps were tested and their sections were identified as W 4 x 2 x 1/4 x 1/4 according to the EXTREN Fiberglass Design Manual [1989] which was provided by the Morrison Molded Fiberglass Company, Bristol, Virginia. The schematic plot of the test setup and beam cross-section for the wide flange beams without channels are shown in Figures 7-3.

According to the EXTREN Fiberglass Design Manual [1989], the ultimate flexural stress of the laterally unsupported beam is given by the following equations.

$$F_u' = \frac{C_1}{S_x}\sqrt{N^2+\frac{d^2B^2}{4}} \leq F_u \tag{7.1}$$

where

$$N = \frac{\pi}{K_yL_u}\sqrt{EI_yGJ}\ , \quad B = \frac{\pi^2 EI_y}{(K_yL_u)^2}$$

The F_u' is the ultimate flexural stress of laterally unsupported beams. The F_u is the ultimate flexural stress of laterally supported beams. The K_y and C_1 reflect the beams end conditions in the Y axis. The L_u is the unbraced length of the beam.

In each test, the beam was loaded to failure and all buckled elastically. One of the buckled beams is shown in Figure 7-5a. The test results and the ones based on Eq. 7.1 are summarized in Table 7-1. The L_u in Eq. 7.1 is equal to 119 inches. The K_y and C_1 are taken from Table B-1 of the EXTREN Fiberglass Design Manual [1989]. It can be seen from Table 7-1 that the average buckling load from tests is about 28% higher than the one based on Eq. 7.1.

7.2.3 Tests of Wide Flange Beams With Channel Caps

The combined section (the wide flange with the channel cap) was made by gluing the channel cap to the wide flange along the beam. A total of eight fiberglass wide flange beams with channel caps were tested. There are only two different combined sections as shown in Figure 7-6.

Each beam was loaded to failure and all buckled elastically. One of the buckled beams is shown in Figure 7-5b. There is no available formula provided by the above-mentioned manual to evaluate the ultimate flexural stress (F_u') of a beam with a singly symmetric section which includes the case of this research. Because of this drawback, the theoretical buckling load of a singly symmetric beam is calculated by

using Eqs. 4.1 and 4.2 which are applicable to any beam with a singly symmetric section. The test results are included in Table 7-2. From Table 7-2, it can be seen that the buckling capacity of a wide flange beam with a channel cap is much higher than the one without a channel cap.

The tests on this small-scale model beams are used as a foundation of full-scale steel beam tests. However, they do not properly represent full-scale beams because of their different material properties and methods of manufacture, and consequent differences in their residual stress distribution.

7.3 Phase Two Testing

7.3.1 General

This section presents an experimental investigation of the lateral-torsional buckling of rolled steel beams. A total of eighteen beams were tested. The test beams spanned between end roller supports mounted on the cross beams of two H-frames, which were bolted to a reaction floor as shown in Figure 7-7.

Designed roller supports allowed the end cross sections of each test beam to rotate about the major and minor axes and to warp freely, but restrained them against twisting about longitudinal axis. Details of end supports are shown in Figure 7-1. Eight of the eighteen tests were conducted with wide flange beams without channel caps and the remaining ten were wide flange beams with channel caps.

The load versus horizontal and vertical deflections were recorded when the tests were proceeding. Standard tensile tests of twenty-two coupons were conducted to determine the steel nominal strength.

7.3.2 Gravity Load Simulator

Each test was carried out on a full-scale simply supported beam with a concentrated load applied at the top flange as shown in Figure 7-8. The load was applied in an essentially static manner, in large increments in the beginning, then small increments, and finally very small increments as the buckling load was approached. The concentrated load was applied vertically through a loading frame as shown in Figure 7-9. The frame was connected to the upper end of a tension actuator, with the pressure controlled by a hand pump. The lower end of the tension actuator was connected to the upper end of a load cell where the load (or pressure) readings were measured. The lower end of the load cell was then connected to a gravitational load simulator. Details of the loading frame, actuator, load cell, and gravity load simulator are shown in Figures 7-8 and 7-9.

The gravity load simulator was similar to the ones developed and used at the Fritz Engineering Laboratory at Lehigh University [1967]. The test arrangement which included the loading frame, actuator, load cell, and gravity load simulator ensured that the applied load remained vertical, even when the test beam twisted and deflected laterally.

7.3.3 Tests of Wide Flange Beams Without Channel Caps

A total of eight wide flange beams without channel caps were tested. Each of them was tested with a point concentrated load applied at the mid point or the third point of the beam. The schematic plot of the test setup and beam cross-section for the wide flange beams without channels are shown in Figure 7-10.

All eight beams failed in the elastic range. A typical buckled beam is shown in Figure 7-11. Both the test and the theoretical buckling loads are summarized in Table 7-3. The theoretical buckling loads are calculated based on Eqs. 3.13 and 3.14, which are the formulas for elastic nominal moments of doubly symmetric beams. The yield stresses of wide flanges are determined based on the tensile coupon tests and listed in Table 7-5.

7.3.4 Tests of Wide Flange Beams With Channel Caps

The combined section (the wide flange with the channel cap) was made by welding the channel cap to the wide flange on site using 1/4-in. intermittent fillet welds at every 24-in. from the mid point of the beam to the end supports. The 1/4-in. intermittent fillet welds were applied on each side of the top flange tips of the wide flange and they were 3-in. long between the end supports and 12-in. long over the end supports. The method of intermittent fillet welds was courteously provided by William E. Moor II of Ferro Products Corporation, Charleston, West Virginia.

A total of ten wide flange beams with channel caps were tested. Eight of them were conducted with a point concentrated load applied either at the mid point or at the third point of the beam. The remaining two were conducted with a flat concentrated load applied either at the mid point or at the third point of the beam. The point and flat concentrated loads are shown in Figures 7-2a and 7-2b, respectively. The schematic plot of the test setup, beam cross-section, and the end supports for the wide flange beams with channels are shown in Figures 7-1 and 7-12. Based on the tensile coupon tests, it is found that the yield stresses of wide flanges and channel caps are different and their values are listed in Table 7-6.

All ten tests failed either in yielding or in inelastic buckling. A typical buckled beam is shown in Figure 7-10b. Both the test and the theoretical buckling loads are summarized in Table 7-4. The theoretical buckling loads are based on Eqs. 4.1 and 4.2, which are the formulas for elastic nominal moments of monosymmetric beams.

7.3.5 Load-Deflection Curves

The horizontal and vertical deflections of the beam section at the mid point or at the third point of the beam were measured with LVDTs as shown in Figure 7-13. The load versus horizontal and vertical deflections were recorded and included in Appendix C.

7.3.6 Tensile Coupon Tests

Twenty-two coupons were taken from the tested beams near the end supports where the stresses were small, and cut from either the centers of the channel webs or the midheights of the wide flange webs.

A typical tensile coupon is shown in Figure 7-14. Twenty-two tension tests were carried out to determine the nominal steel strength. The average steel yield stresses determined from these tests are given in Tables 7-5 and 7-6.

7.4 Summary

7.4.1 Equivalent Moment Factor (C_b)

The critical moment for a beam under uniform moment has been derived in Chapter 3. If the moment in the beam is not constant throughout, the critical moment for the beam will be larger. This means that the beam under uniform moment is the most severe loading condition. Thus, the beam under any other loading condition may resist a greater critical moment. An equivalent moment factor (C_b) has been introduced by the some researchers and specifications including the LRFD to account the effect of non-uniform moment, and it can be represented by

$$M_{cr} = C_b\, M_{ocr}\ , \quad C_b \geq 1 \tag{7.2}$$

where M_{cr} is the critical moment for a beam under non-uniform moment, M_{ocr} the critical moment for a beam under uniform moment, and M_{cr} is greater than or equal to M_{ocr}.

According to Nethercot and Rockey [1971], The C_b for a beam with a doubly symmetric section can be given by

$$C_b = A/B \ \ or \ \ A \ \ or \ \ A*B \tag{7.3}$$

where the values of A and B depend on the location of the load applied along the beam. For the case of the concentrated load applied at the midspan, the values of A and B are given by

$$A = 1.35\ , \qquad B = 1.0 + 0.649\ W - 0.180\ W^2 \tag{7.4}$$

where

$$W = \frac{\pi}{L}\sqrt{\frac{EC_w}{GJ}}$$

The A/B is for the load applied at the top flange, the A for the load at the shear center, and the A*B for the load at the bottom flange. Nethercot and Rockey provided the values of A and B for several loading cases in their paper. More recently, Chen and Lui [1988] also gave the values of A and B for a total of seven cases in their book. There are still many other loading cases for which A and B were not determined. An empirical C_b formula used for any loading case was introduced by Kirby and Nethercot [1979], and it was given by

$$C_b = \frac{12}{3\,(M_1/M_{max})\ +\ 4\,(M_2/M_{max})\ +\ 3\,(M_3/M_{max})\ +\ 2} \tag{7.5}$$

where M_1, M_2, and M_3 are the moments at the quarter point, midpoint, and three-quarter point of the beam, respectively, and M_{max} is the maximum moment of the beam. The value of C_b as given in Eq. 7.5 is valid only if the load is applied through the shear center. If the location of the applied load is not at the shear center, the value of C_b will be different.

All equivalent moment factor (C_b) have been discussed so far are only valid for a beam with a doubly symmetric section. The C_b for a beam with a singly symmetric section can not be determined based on what is known today.

7.4.2 Test Results of Wide Flange Beams Without Channel Caps

The test results of steel wide flange beams without channel caps have been given in Table 7-3 and part of them are relisted in Table 7-7 to compare between the values of C_b.

Since the beams are doubly symmetric, the formulas for the C_b presented in Section 7.4.1 are applied. The values of A/B listed in Table 7-7 are calculated on the basis of the load applied at the mid point even for the case with the load applied at the third point of the beam. The reason for this is that the C_b formula is not available for the case with the load applied at the third point of the beam. From Table 7-7, it can be seen that all the test C_b values are greater than the values of A/B which are the equivalent moment factors for the load applied at the top flange. This test results indicate that the values of A/B computed by using Eq. 7-4 give consistent but rather conservative results.

7.4.3 Test Results of Wide Flange Beams With Channel Caps

Although there is no available formula to calculate the C_b for a beam with a singly symmetric section as has been discussed in Section 7.4.1, the comparisons between the test C_b and the A/B based on Eq. 7-4 are still provided. The comparisons are included in Table 7-8 with part of the data from Table 7-4. It can be seen in Table 7-8 that all the test C_b values, except for beams WC-01 and WC-02, are greater than the values of A/B. These results point out that the values of A/B computed by using Eq. 7-4 are closer to the values of the test C_b than in the doubly symmetric cases.

Figure 7-1. Details of end support.

(a)

(b)

Figure 7-2. Beam loading.
a) Point load; b) Flat load.

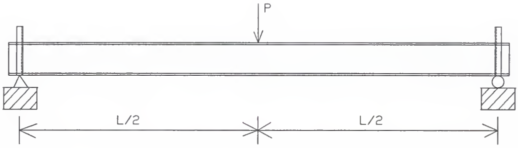

(a)

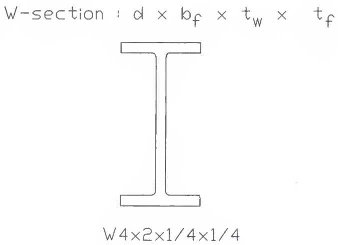

(b)

Figure 7-3. Beam setup and cross-section.
a) Simply supported wide flange beam without channel cap; b) Cross-section of wide flange beam without channel cap.

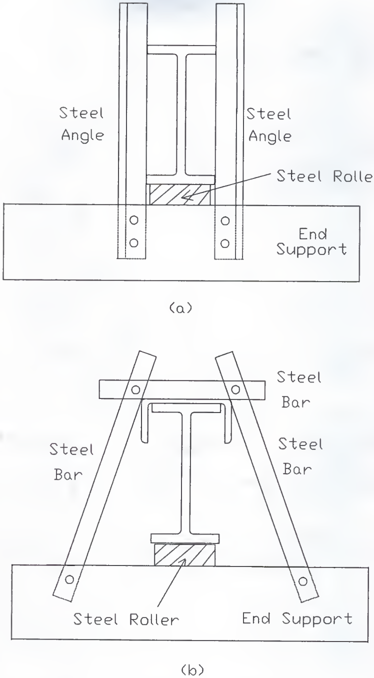

Figure 7-4. Details of end supports.
a) End support of wide flange beam without channel cap; b) End support of wide flange beam with channel cap.

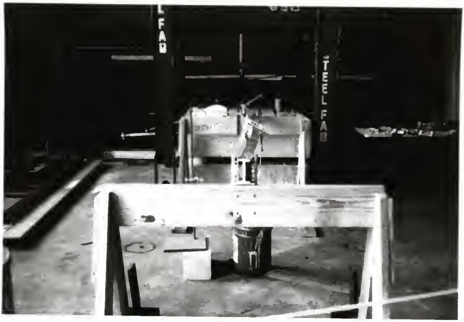

(a)

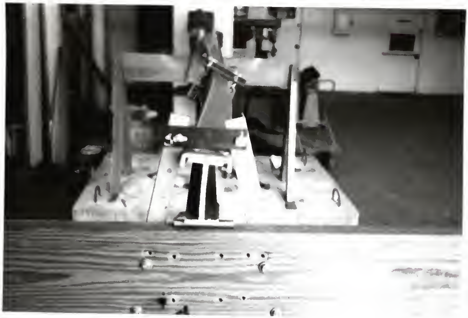

(b)

Figure 7-5. Buckled beam shapes.
a) Buckled wide flange beam without channel cap;
b) Buckled wide flange beam with channel cap.

Table 7-1. W-sections without channels (fiberglass Beams).

Beam	W-Section	P_u	P_e	C_b
1	W 4 x 2 x 1/4 x 1/4	210	153	1.373
2	W 4 x 2 x 1/4 x 1/4	186	153	1.216
3	W 4 x 2 x 1/4 x 1/4	193	153	1.261
4	W 4 x 2 x 1/4 x 1/4	194	153	1.268
5	W 4 x 2 x 1/4 x 1/4	187	153	1.222
6	W 4 x 2 x 1/4 x 1/4	201	153	1.314
7	W 4 x 2 x 1/4 x 1/4	195	153	1.275
8	W 4 x 2 x 1/4 x 1/4	196	153	1.281

Note:

- W-Section dimensions = W d x b_f x t_w x t_f
- Simply supported with a concentrated load applied at the midspan.
- P_u (pounds) is the test buckling load and P_e (pounds) is the theoretical buckling load based on C_b = 1.
- C_b = C_b from test = P_u / P_e.

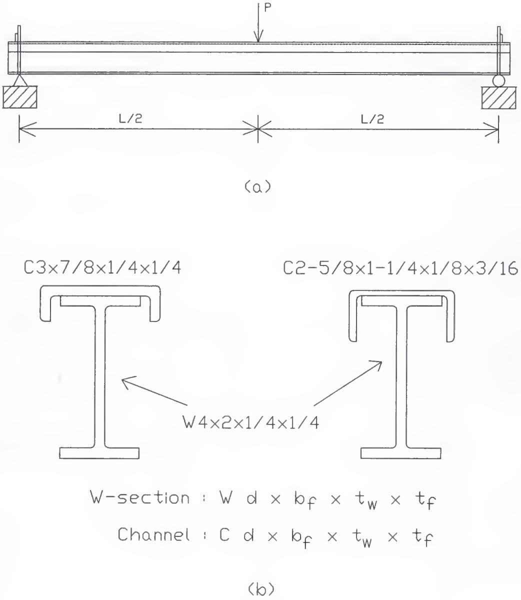

Figure 7-6. Beam setup and cross-section.
a) Simply supported wide flange beam with channel cap; b) Cross-section of wide flange beam with channel cap.

Table 7-2. W-sections with channels (fiberglass beams).

Beam	W-Section	C-Section	P_u	P_e
1	W 4x2x1/4x1/4	C2-5/8x1-1/4x1/8x2/16	1086	424
2	W 4x2x1/4x1/4	C2-5/8X1-1/4X1/8X3/16	1146	424
3	W 4x2x1/4x1/4	C2-5/8X1-1/4X1/8X3/16	1179	424
4	W 4x2x1/4x1/4	C2-5/8X1-1/4X1/8X3/16	1176	424
5	W 4x2x1/4x1/4	C 3 X 7/8 X 1/4 X 1/4	1352	584
6	W 4x2x1/4x1/4	C 3 X 7/8 X 1/4 X 1/4	1241	584
7	W 4x2x1/4x1/4	C 3 X 7/8 X 1/4 X 1/4	1364	584
8	W 4x2x1/4x1/4	C 3 X 7/8 X 1/4 X 1/4	1332	584

Note:
- W-Section dimensions = W d x b_f x t_w x t_f
  C-Section dimensions = C d x b_f x t_w x t_f
- Simply supported with a concentrated load applied at the midspan.
- P_u (pounds) is the test buckling load and P_e (pounds) is the theoretical buckling load based on C_b = 1.
- P_e is calculated based on E = 2.8 x 10^3 ksi and G = .425 x 10^3 ksi.

Figure 7-7. Beam setup.

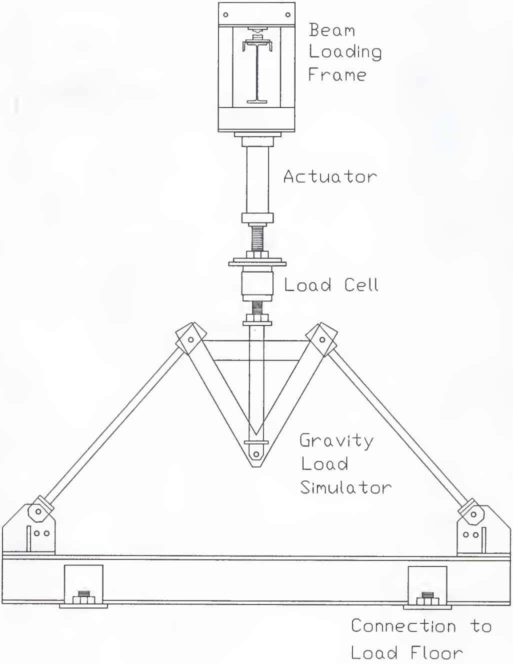

Figure 7-8. Loading device.

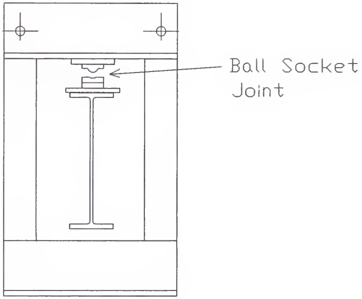

(a)

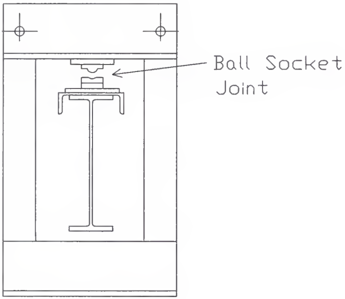

(b)

Figure 7-9. Beam loading frame.
a) Wide flange beam without channel cap;
b) Wide flange beam with channel cap.

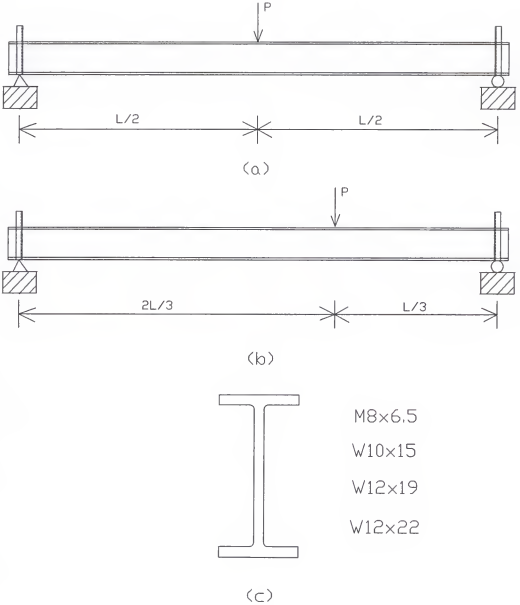

Figure 7-10. Beam setups and cross-section.
a) Simply supported wide flange beam without channel cap, p at center; b) Simply supported wide flange beam without channel cap, p at 1/3 of the span; c) Cross-section of wide flange beam without channel cap.

Figure 7-11. Beam buckled shapes.

Table 7-3. W-sections without channels (steel beams).

Beam	W	L	Load	P_u	P_e	C_b
W-01	W12x19	24′	@1/2	3.50	2.44	1.43
W-02	W12x22	18′	@1/3	10.50	7.29	1.44
W-03	W10x15	18′	@1/3	4.20	3.40	1.24
W-04	W12x19	18′	@1/3	10.00	5.28	1.89
W-05	W12x19	12′	@1/2	15.80	12.80	1.23
W-06	W10x15	12′	@1/2	9.00	8.15	1.10
W-07	M8x6.5	12′	@1/2	1.80	1.08	1.67
W-08	M8x6.5	12′	@1/2	1.50	1.08	1.39

Note:
- Load applied at 1/2 L or at 1/3 L.
- P_u (kips) is the test buckling load and P_e (kips) is the theoretical buckling load based C_b = 1.
- C_b = C_b from test = P_u / P_e.

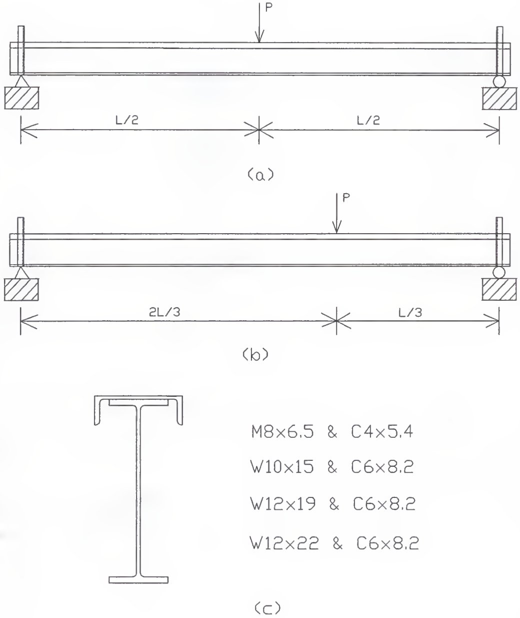

Figure 7-12. Beam setups and cross-section.
a) Simply supported wide flange beam with channel cap, p at center; b) Simply supported wide flange beam with channel cap, p at 1/3 of the span; c) Cross-section of wide flange beam with channel cap.

Table 7-4. W-sections with channels (steel beams).

Beam	W	C	L	Load	P_u	P_e	C_b
WC-01	W12X19	C6X8.2	24′	@1/2	12.0	12.90	0.93
WC-1A	W12X19	C6X8.2	18′	@1/2	19.0	N/A	N/A
WC-02	W12X22	C6X8.2	18′	@1/3	30.5	33.30	0.93
WC-2A	W12X22	C6X8.2	18′	@1/3	39.0	N/A	N/A
WC-03	W10X15	C6X8.2	18′	@1/3	22.9	18.40	1.23
WC-04	W12X19	C6X8.2	18′	@1/3	35.5	28.80	1.23
WC-05	W12X19	C6X8.2	12′	@1/2	49.5	49.90	0.99
WC-06	W10X15	C6X8.2	12′	@1/2	32.5	28.20	1.15
WC-07	M8X6.5	C4X5.4	12′	@1/2	10.0	8.16	1.23
WC-08	M8X6.5	C4X5.4	12′	@1/2	9.0	8.16	1.10

Note:
- Load applied at 1/2 L or at 1/3 L.
- P_u (kips) is the test buckling load and P_e (kips) is the theoretical buckling load based on C_b = 1.
- C_b = C_b from test = P_u / P_e.
- N/A = Not avaiable.

Table 7-5. W-sections without channels (steel beams).

Beam	W	L	F_y
W-01	W12x19	24′	62.1
W-02	W12x22	18′	62.0
W-03	W10x15	18′	53.3
W-04	W12x19	18′	62.1
W-05	W12x19	12′	62.1
W-06	W10x15	12′	53.3
W-07	M8x6.5	12′	40.0
W-08	M8x6.5	12′	40.0

<u>Note</u>:
- W: Wide flange
- L: Span length (ft)
- F_y: Test yielding stress of wide flange based on the average of two specimen (ksi)

Table 7-6. W-sections With channels (steel beams).

Beam	W	F_{y1}^{*}	C	F_{y2}^{*}	L
WC-01	W12X19	62.1	C6X8.2	62.6	24′
WC-1A	W12X19	62.1	C6X8.2	62.6	18′
WC-02	W12X22	62.0	C6X8.2	48.0	18′
WC-2A	W12X22	62.0	C6X8.2	48.0	18′
WC-03	W10X15	53.3	C6X8.2	48.1	18′
WC-04	W12X19	62.1	C6X8.2	50.3	18′
WC-05	W12X19	62.1	C6X8.2	63.6	12′
WC-06	W10X15	53.3	C6X8.2	49.6	12′
WC-07	M8X6.5	40.0	C4X5.4	45.4	12′
WC-08	M8X6.5	40.0	C4X5.4	45.4	12′

<u>Note</u>:

- W: Wide flange; C: Channel
- L: Span length (ft)
- F_{y1}: Test yielding stress of wide flange (ksi)
- F_{y2}: Test yielding stress of channel (ksi)
- *: Average of two specimen

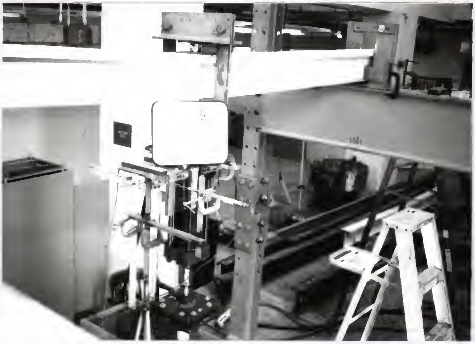

Figure 7-13. Setup of LVDTs.

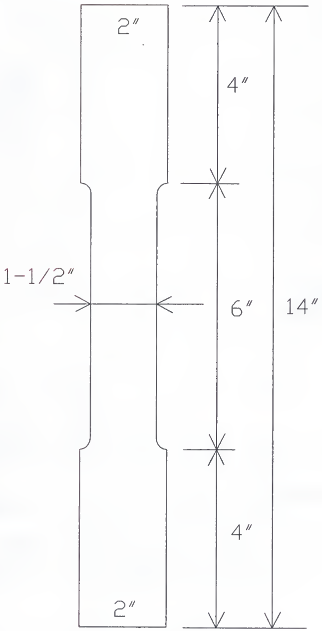

Figure 7-14. Steel tensile coupon.

Table 7-7. W-sections without channels (steel beams).

Beam	W	L	Load	C_b Test	C_b A/B	C_b A	C_b A*B
W-01	W12x19	24'	@1/2	1.43	1.064	1.350	1.713
W-02	W12x22	18'	@1/3	1.44	1.032	1.350	1.766
W-03	W10x15	18'	@1/3	1.24	1.014	1.350	1.798
W-04	W12x19	18'	@1/3	1.89	1.007	1.350	1.810
W-05	W12x19	12'	@1/2	1.23	0.925	1.350	1.970
W-06	W10x15	12'	@1/2	1.10	0.931	1.350	1.958
W-07	M8x6.5	12'	@1/2	1.67	1.026	1.350	1.777
W-08	M8x6.5	12'	@1/2	1.39	1.026	1.350	1.777

Note:

- Average C_b for load @ 1/2 L -- 1.364
  Average A/B for load @ 1/2 L -- 0.994; 1.364/0.994 = 1.37
  Average C_b for load @ 1/3 L -- 1.523
  Average A/B for load @ 1/3 L -- 1.018; 1.523/1.018 = 1.50
- Load applied at 1/2 L or at 1/3 L.
- P_u (kips) is the test buckling load and
  P_e (kips) is the theoretical buckling load based on C_b = 1.
- Test = C_b from test = P_u / P_e.
- A/B = calculated C_b for the load applied at the top flange.
- A = calculated C_b for the load applied at the shear center.
- A*B = calculated C_b for the load applied at the bottom flange.
- Elastic buckling: W-01, W-02, W-03, W-04, W-05, W-06, W-07, and W-08.

Table 7-8. W-sections with channels (steel beams).

Beam	W	C	Load	C_b Test	C_b A/B	C_b A	C_b A*B
WC-01	W12X19	C6X8.2	@1/2	0.93	1.069	1.350	1.705
WC-02	W12X22	C6X8.2	@1/3	0.93	1.030	1.350	1.770
WC-03	W10X15	C6X8.2	@1/3	1.23	1.031	1.350	1.767
WC-04	W12X19	C6X8.2	@1/3	1.23	1.013	1.350	1.800
WC-05	W12X19	C6X8.2	@1/2	0.99	0.930	1.350	1.959
WC-06	W10X15	C6X8.2	@1/2	1.15	0.948	1.350	1.922
WC-07	M8X6.5	C4X5.4	@1/2	1.23	1.067	1.350	1.708
WC-08	M8X6.5	C4X5.4	@1/2	1.10	1.067	1.350	1.708

Note:
- Average C_b for load @ 1/2 L -- 1.080
  Average A/B for load @ 1/2 L-- 1.016; 1.080/1.016 = 1.06
  Average C_b for load @ 1/3 L -- 1.130
  Average A/B for load @ 1/3 L -- 1.025; 1.130/1.025 = 1.10
- Load applied at 1/2 L or at 1/3 L.
- P_u (kips) is the test buckling load and P_e (kips) is the theoretical buckling load based on C_b = 1.
- Test = C_b from test = P_u / P_e.
- A/B = calculated C_b for the load applied at the top flange.
- A = calculated C_b for the load applied at the shear center.
- A*B = calculated C_b for the load applied at the bottom flange.
- Elastic buckling: WC-01 and WC-02.
- Inelastic buckling : WC-04, WC-05, and WC-08.
- Yielding: WC-03, WC-06, and WC-07.

CHAPTER 8

SUMMARY, CONCLUSIONS, AND DESIGN RECOMMENDATIONS

8.1 Summary

8.1.1 Moment Strength Curve

The nominal moment (M_n) of a beam is subdivided into elastic, inelastic, and plastic ranges. In the elastic and inelastic ranges, the lateral instability is assumed to be the dominating factor. In the plastic range, deformation capacity is the significant factor. A straight line, which is adopted by the current LRFD specification, is used for the inelastic nominal moment between the plastic moment (M_p) and the limiting moment (M_r). A typical plot of M_n versus L_b of a beam is shown in Figure 5-1.

The theoretical solution of lateral-torsional buckling has been derived and presented in Chapter 3. For the needs of design professionals, a simplified but reasonably accurate solution has been developed as an alternate to the theoretical one and is presented in Chapter 6. These two approaches are now summarized as shown below. All the notations used in the following formulas have been defined in Figure 5-1, Chapter 3, and Chapter 6.

1. Theoretical approach. This approach has been presented in Chapter 4 and can be summarized as follow.

Plastic yielding. If L_b is less than or equal to L_p, the nominal moment is given by

$$M_n = M_p \tag{8.1}$$

Inelastic lateral-torsional buckling. If L_b is larger than L_p and less than L_r, the nominal moment according to the LRFD specification is given by

$$M_n = C_b\left[M_p - (M_p - M_r)\left(\frac{L_b - L_p}{L_r - L_p}\right)\right] \leq M_p \tag{8.2}$$

Elastic lateral-torsional buckling. If L_b is larger than or equal to L_r, the nominal moment is given by

$$M_{cr} = \frac{\pi C_b}{KL}\left\{\sqrt{EI_y GJ}\ \left(B_1 + \sqrt{1 + B_2 + B_1^2}\ \right)\right\} \tag{8.3}$$

where

$$B_1 = \frac{\pi\beta_x}{2KL}\sqrt{\frac{EI_y}{GJ}} \qquad B_2 = \frac{\pi^2 EC_{wc}}{(KL)^2 GJ} \tag{8.3a}$$

$$\beta_x = \frac{1}{I_x}\int_A y(x^2 + y^2)\,dA - 2(Y_s - Y_c) \tag{8.3b}$$

$$C_{wc} = \int_o^L W_n^2 t\,ds\ , \qquad J = \int_A r^2 dA \tag{8.3c}$$

$$W_n = \frac{1}{A}\int_o^L W_o t\,ds - W_o \qquad W_o = \int_o^s \rho_o\,ds \tag{8.3d}$$

The analytical solution of lateral-torsional buckling for the wide flange beam with channel cap was derived based on the

energy method and was presented in Chapter 3. The difficulties associated with the use of the formulas as given in Eqs. 8.3 to 8.3d are the section properties which include the coefficients of monosymmetry parameter (β_x), the warping section constant (C_{wc}), and the torsional constant (J).

A computer program (LTBMN) was originally written in BASIC language by Professor T. V. Galambos of the University of Minnesota and converted to FORTRAN language by Dr. Thomas Sputo, a consulting engineer in Gainesville, Florida. The program was initially developed for evaluating the section warping constant (C_{wc}) only. The author has enhanced the program and made it to be able to generate the beam strength curve (M_n versus L_b) and calculate other section properties which include β_x, J, the plastic section modules (Z_p), and other parameters which are required in this research. Since the type of section considered in this research is composed of flat, thin elements, the program is able to be written based on a numerical procedure.

The program was used to compute the section properties of the forty-five combined sections listed in the current AISC manual, the exact values of β_x, C_{wc}, and J are listed in Tables 4-1 and 4-2.

2. Simplified approach. For those who do not have access to the program, a simplified approach is proposed as an alternative to the theoretical one. All the notations used in Eqs. 8.6 to 8.6e have been defined and shown in Chapter 6.

Plastic yielding. If L_b is less than or equal to L_p, the nominal moment is given by

$$M_n = M_p \tag{8.4}$$

Inelastic lateral-torsional buckling. If L_b is larger than L_p and less than L_r, the nominal moment according to the LRFD specification is given by

$$M_n = C_b\left[M_p - (M_p - M_r)\left(\frac{L_b - L_p}{L_r - L_p}\right)\right] \le M_p \tag{8.5}$$

Elastic lateral-torsional buckling. If L_b is larger than or equal to L_r, the nominal moment is given by

$$M_n = \frac{\pi C_b}{KL}\left[\sqrt{EI_y GJ}\ \left(B_1 + \sqrt{1 + B_2 + B_1^2}\ \right)\right] \tag{8.6}$$

where

$$B_1 = \frac{\pi \beta_x}{2KL}\sqrt{\frac{EI_y}{GJ}} \qquad B_2 = \frac{\pi^2 EC_{wc}}{(KL)^2 GJ} \tag{8.6a}$$

$$\beta_x = 0.87\ (2\rho - 1)\left(D + \frac{D_L}{2}\right), \quad \rho = \frac{2I_{yc}}{I_y} \tag{8.6b}$$

$$I_y = I_{yw} + I_{xc}\ , \quad I_{yc} = \frac{I_{yw}}{2} + I_{xc} \tag{8.6c}$$

$$C_{wc} = C_w\left(0.79 + 1.79\sqrt{\frac{A_c}{A_w}}\right), \quad 0.2 \le \frac{A_c}{A_w} \le 0.95 \tag{8.6d}$$

$$J = J_w + J_c + Bt_1 t_2 (t_1 + t_2) \tag{8.6e}$$

The proposed models for β_x, C_{wc}, and J, as given in Eqs. 8.6b, 8.6d, and 8.6e, have been developed and presented in Chapter 6. The models were applied to the forty-five sections in the current AISC manual and the results were compared with the ones computed by the program (LTBMN), these are shown in Figures 6-6, 6-9, and 6-11, respectively.

It can be seen from Figure 6-6 that the model of β_x can predict the results with maximum errors of -4.1% to +3.2%. From Figure 6-9, the model of C_{wc} gives results with errors of -3% to +5% in most of the forty-five sections. There are only two extreme cases with errors -6.8% and +7.4%. From Figure 6-11, the model of J overestimates the results by +2.1% to +8.2%.

When the proposed models of β_x, C_{wc}, and J are applied to the forty-five sections to compute the nominal moment, it can be found that the proposed method gives the predictions of the nominal moments with estimated errors of -3% to +2% as shown in Figure 6-12. Thus, a simplified but reasonably accurate approach is provided. The main advantage of this proposed approach is that the calculations of β_x, C_{wc}, and J are now simplified by using parameters given.

It has been discussed in Chapter 6 that the derivations of the models are on the basis of the forty-five sections in the current AISC manual. The models can also be applied to sections not included in the current AISC manual, such as the sections used in the tests, the results are recorded in Tables

8-1 to 8-7 and plotted in Figures 8-1 to 8-7, respectively. It can be observed from Figures 8-1 to 8-7 that the results compare well with the exact ones and with maximum errors within 2%.

8.1.2 Equivalent Moment Factor (C_b)

A beam under uniform moment is the worst loading condition. Thus, the beam under any other loading condition may resist a greater critical moment. An equivalent moment factor (C_b) has been introduced to account for the effect of non-uniform moment. it can be represented by the following equation.

$$M_{cr} = C_b \, M_{ocr} \ , \quad C_b \geq 1 \tag{8.7}$$

where M_{cr} is the critical moment for a beam under non-uniform moment, M_{ocr} the critical moment for a beam under uniform moment, and M_{cr} is greater than or equal to M_{ocr}.

8.1.2.1 Equivalent Moment Factors of Wide Flange Beams Without Channel Caps

The scattered test results of rolled wide flange beams without channel caps compared with the ones computed by the program (LTBMN) are plotted in Figure 8-8 and their tested C_b values are given in Table 7-7. Figure 8-8 is plotted with two nondimensional parameters, the M_n/M_p and the square root of M_p/M_e, where M_n is the nominal moment, M_p the plastic moment, and M_e the elastic moment. It is interesting to find that the four different sections (W12x19, W12x22, W10x15, and M8x6.5) have consistent beam strength curves as shown in Figure 8-8.

It can also be seen that all the beams fail in the elastic range.

For the five cases of load at the midspan, it can be seen from Table 7-7 that the calculated values of C_b (A/B) are less than the tested values of C_b (P_u/P_e) by 15% to 39%. For the three cases of load at the third point of the span, it can be seen that the calculated values of C_b (A/B) are less than the tested values of C_b (P_u/P_e) by 18% to 47%.

It should be noted that all the calculated values of C_b (A/B) are calculated on the basis of a single point load applied at the midspan because there is no available formulas for the calculations of C_b (A/B) for the case of a single point load applied at the third point of the span. The calculated value of C_b (A/B) provided is conservative for the case of load applied at the third point of the span.

8.1.2.2 Equivalent Moment Factors of Wide Flange Beams With Channel Caps

The scattered test results of rolled wide flange beams with channel caps compared with the theoretical formulas are plotted in Figure 8-9 and their tested C_b values are given in Table 7-8. Figure 8-9 is also plotted with two nondimensional parameters, M_n/M_p and the square root of M_p/M_e. Again, it can be found that the four different sections (W12x19 with C6x82, W12x22 with C6x8.2, W10x15 with C6x8.2, and M8x6.5 with C6x8.2) have very consistent beam strength curves as shown in Figure 8-9.

From Figure 8-9 and Table 7-8, it can be seen that beams WC-01 and WC-02 fail in the elastic range and all the remaining beams fail either in the inelastic range or in plastic yielding. Two beams (WC-1A and WC-2A) subjected to flat loads, which loads applied through a beam bearing flat against the top flange as opposed to a ball-joint, are conducted and the results are much greater then the ones in WC-01 and WC-02, respectively.

For beam WC-01, the case of load at the midspan and the elastic failure, the calculated value of C_b (A/B) is greater than the tested value of C_b (P_u/P_e) by 15%. For beam WC-02, the case of load at the third point of the span and the elastic failure, the calculated value of C_b (A/B) is greater than the tested value of C_b (P_u/P_e) by 11%. For the cases of load at the midspan (WC-05, WC-06, WC-07, and WC-08), the calculated values of C_b (A/B) are less than the tested values of C_b (P_u/P_e) by 3% to 18%. For the cases of load at the third point of the span (WC-03 and WC-04), the calculated values of C_b (A/B) are less than the tested values of C_b (P_u/P_e) by 16% to 18%.

It should be noted that the calculated values of C_b (A/B) provided in Table 7-8 are calculated on the basis of a single point load applied at the midspan. Furthermore, the values of A and B are derived on the basis of the doubly symmetric section. When these A and B are applied to sections with

singly symmetry including the type of section considered in this research, the results are questionable.

Based on the results presented in Table 7-8, the calculated values of C_b (A/B) are overestimated for the cases WC-01 and WC-02. However, the calculated values of C_b (A/B) are slightly underestimated in the remaining cases.

8.2 Conclusions and Recommendations

Lateral-torsional buckling of a beam is a complex problem, especially for a beam with monosymmetric section. The current LRFD specification [1986] provides a simplified but conservative method to deal with monosymmetric beams which includes the case of this research i.e. a wide flange beam with channel cap. As discussed in Chapter 4, the formulas provided for monosymmetric beams in LRFD are actually based on the beam with 3-plate section as shown in Figure 1-1b. When the formulas provided by LRFD are applied to a wide flange beam with channel cap, the results are very conservative with the estimated error being as much as 23% as discussed in Chapter 5.

A simplified and reasonably accurate method has been developed in this study to deal with the elastic lateral-torsional buckling of the wide flange beam with channel cap. Based on the discussions in Section 8.1.1 and the models presented in Eqs. 8.6b to 8.6e, it can be concluded that the proposed approach is not only simplified but also reasonably accurate for the design professions.

The equivalent bending factor (C_b) was not the initial objective of this study. However, C_b was determined from the laboratory test data. For the beam without channel cap, the calculated values of C_b (A/B), which are derived based on the doubly symmetric section with midspan loading, are greatly underestimated for all cases except W-06 as shown in Table 7-7 and Figure 8-8.

For the beam with channel cap, it is evident from the laboratory testing as given in Table 7-8 and Figure 8-9 that the experimental C_b values in the elastic range (WC-01 and WC-02) are less than the calculated values of C_b (A/B) derived based on the doubly symmetric section with midspan loading. The experimental C_b values in the inelastic range for the beam with channel cap are closer to the calculated values of C_b (A/B) than that for the beam without channel cap and as shown in Tables 7-7 and 7-8. Thus, based on the experimental values of C_b as given in Table 7-8 and Figure 8-9, it has been found that the C_b is overestimated for the cases WC-01 and WC-02 (elastic range) and underestimated for the cases WC-04, WC-05, WC-06, WC-07 and WC-08 (inelastic range).

As specified in Chapter 7, the yielding stresses of wide flanges and channels are different and their values are listed in Table 7-6. Although there are differences in yielding stresses between wide flanges and channels, their M_n curves, which are plotted with two nondimensional parameters (M_n/M_p and the square root of M_p/M_e), are very consistent as shown in

Figure 8-9. The consistences of M_n/M_p versus square root of M_p/M_e curves can also be found in the cases of wide flange beams with different yielding stresses and as shown in Figure 8-8.

For a beam with different loading types, it is seen that the buckling load under a flat load is higher than that under a point load. Note that a flat load is applied through a beam bearing flat against the top flange as opposed to a ball-joint for a point load and is close to the actual load applied to beam in service. It can be seen from Table 7-4 that the difference in the buckling load for the cases WC-01 and WC-1A is 58%, while for the cases WC-02 and WC-2A is 28%.

8.3 Future Research Needs

Future research needs for a wide flange beam with a channel cap include the following.

1. More rational method to compute the equivalent bending factor (C_b) in both elastic and inelastic ranges, especially in the case of elastic range which has been shown low in the laboratory testing.
2. More case studies needed to see if all the M_n curves are consistent as shown in Figures 8-8 and 8-9.
3. Exact residual stress distributions due to Intermittent fillet welds along the beam should be found out.

4. Effects of different load locations including load applied at the top of channel cap, at the shear center, and at the bottom of flange should be studied.
5. Need more accurate equations to predict the inelastic part of behavior instead of using a straight line.
6. More studies are needed to find the effect of different yield strengths of wide flanges and channels, used in the same beam.

Table 8-1. Comparison between theory and model, section W12x19 with C6x8.2, F_y=62.3 ksi.

L_b	M_n	LRFD	Model	Percent
0.00	165.6	165.6	165.6	100.0
2.62	165.6	165.6	165.6	100.0
4.17	165.6	165.6	165.6	100.0
6.29	165.6	165.6	165.6	100.0
6.82	163.7	163.3	163.6	100.0
8.33	157.9	156.6	157.8	99.9
10.00	151.6	149.3	151.3	99.8
12.50	142.2	138.3	141.7	99.7
15.87	129.5	123.5	128.7	99.4
17.22	124.3	107.4	123.5	97.9
17.44	123.5	105.1	120.9	97.9
20.00	98.6	83.7	96.9	98.3
23.79	74.9	63.4	74.1	98.8
25.00	69.5	58.7	68.7	99.0
26.67	63.0	53.2	62.5	99.2
30.00	52.9	44.6	52.7	99.5
33.33	45.5	38.3	45.4	99.8
35.00	42.5	35.8	42.4	99.9

Note:
L_b - Unbraced length (ft)
M_n - Theoretical nominal moment (k-ft)
LRFD - Moment using the LRFD specification (k-ft)
Model - Moment using the proposed model (k-ft)
Percent - Model / M_n

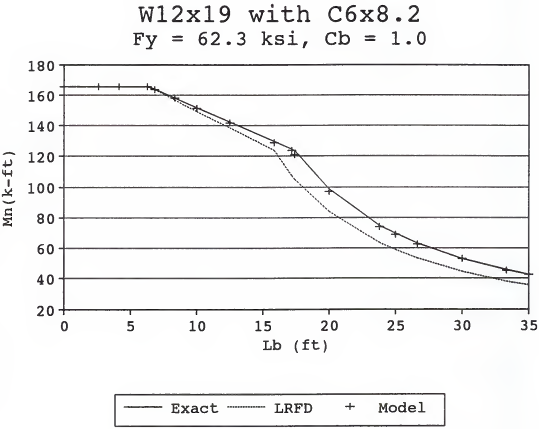

Note:
The EXACT curve is exact only in the elastic range and a straight line adopted by the LRFD specification is used for the inelastic range.

Figure 8-1. M_n versus L_b curves.

Table 8-2. Comparison between theory and model, section W12x22 with C6x8.2, F_y=55.0 ksi.

L_b	M_n	LRFD	Model	Percent
0.00	170.5	170.5	170.5	100.0
2.87	170.5	170.5	170.5	100.0
4.17	170.5	170.5	170.5	100.0
6.53	170.5	170.5	170.5	100.0
7.84	165.8	164.9	165.7	99.9
10.00	157.9	155.6	157.7	99.8
12.50	148.9	144.9	148.5	99.7
15.00	139.8	134.2	139.3	99.6
16.26	135.3	128.8	134.6	99.5
17.82	129.6	110.9	128.8	98.1
18.04	128.8	108.8	126.4	98.1
20.00	109.6	92.3	107.8	98.4
22.50	91.5	77.0	90.3	98.7
25.00	78.3	65.7	77.5	98.9
30.00	60.4	50.5	60.0	99.4
35.00	48.9	40.9	48.8	99.7

Note:
L_b - Unbraced length (ft)
M_n - Theoretical nominal moment (k-ft)
LRFD - Moment using the LRFD specification (k-ft)
Model - Moment using the proposed model (k-ft)
Percent - Model / M_n

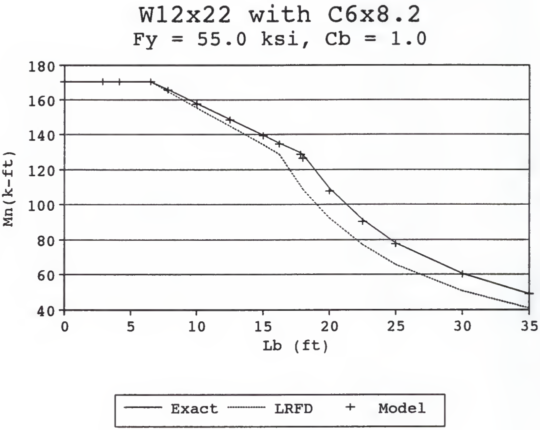

<u>Note</u>:
The EXACT curve is exact only in the elastic range and a straight line adopted by the LRFD specification is used for the inelastic range.

Figure 8-2. M_n versus L_b curves.

Table 8-3. Comparison between theory and model, section W10x15 with C6x8.2, F_y=50.7 ksi.

L_b	M_n	LRFD	Model	Percent
0.00	89.1	89.1	89.1	100.0
2.87	89.1	89.1	89.1	100.0
4.17	89.1	89.1	89.1	100.0
7.18	89.1	89.1	89.1	100.0
7.85	88.1	87.9	88.1	100.0
10.00	84.8	84.0	84.7	100.0
12.50	80.9	79.5	80.9	99.9
15.00	77.1	75.1	77.0	99.9
17.81	72.8	70.0	72.7	99.8
20.38	68.9	65.4	68.7	99.7
22.50	65.6	55.8	65.4	99.1
22.63	65.4	55.3	64.8	99.1
25.00	56.1	47.4	55.7	99.4
27.50	48.5	41.0	48.4	99.7
30.00	42.7	36.1	42.7	99.9
32.50	38.0	32.1	38.1	100.2
35.00	34.2	28.9	34.4	100.4

Note:
L_b - Unbraced length (ft)
M_n - Theoretical nominal moment (k-ft)
LRFD - Moment using the LRFD specification (k-ft)
Model - Moment using the proposed model (k-ft)
Percent - Model / M_n

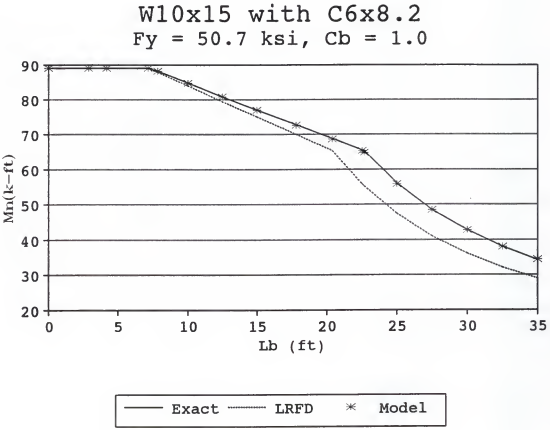

Note:
The EXACT curve is exact only in the elastic range and a straight line adopted by the LRFD specification is used for the inelastic range.

Figure 8-3. M_n versus L_b curves.

Table 8-4. Comparison between theory and model, section W12x19 with C6x8.2, F_y=56.2 ksi.

L_b	M_n	LRFD	Model	Percent
0.00	149.4	149.4	149.4	100.0
2.76	149.4	149.4	149.4	100.0
6.62	149.4	149.4	149.4	100.0
7.32	147.2	146.8	147.2	100.0
8.33	144.0	143.1	143.9	99.9
10.00	138.7	136.9	138.5	99.9
12.50	130.7	127.6	130.3	99.7
15.00	122.7	118.3	122.2	99.6
16.85	116.8	111.4	116.2	99.5
17.79	113.9	101.6	113.2	99.4
18.34	112.1	96.6	111.4	98.0
18.56	111.4	94.7	109.3	98.1
20.00	98.6	83.7	96.9	98.3
22.50	81.8	69.3	80.6	98.6
25.00	69.5	58.7	68.7	99.0
27.50	60.2	50.8	59.7	99.2
30.00	52.9	44.6	52.7	99.5
32.50	47.2	39.7	47.0	99.7
35.00	42.5	35.8	42.4	99.9

<u>Note</u>:
L_b - Unbraced length (ft)
M_n - Theoretical nominal moment (k-ft)
LRFD - Moment using the LRFD specification (k-ft)
Model - Moment using the proposed model (k-ft)
Percent - Model / M_n

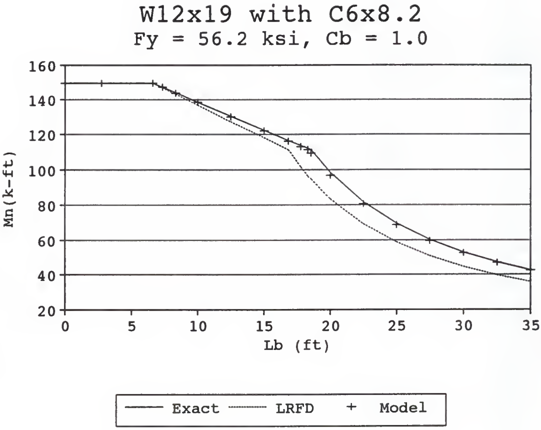

Note:
The EXACT curve is exact only in the elastic range and a straight line adopted by the LRFD specification is used for the inelastic range.

Figure 8-4. M_n versus L_b curves.

Table 8-5. Comparison between theory and model, section W12x19 with C6x8.2, F_y=62.9 ksi.

L_b	M_n	LRFD	Model	Percent
0.00	167.2	167.2	167.2	100.0
2.61	167.2	167.2	167.2	100.0
6.26	167.2	167.2	167.2	100.0
6.77	165.3	164.9	165.2	100.0
8.33	159.3	158.0	159.1	99.9
10.00	152.9	150.5	152.6	99.8
11.72	146.3	142.8	145.8	99.7
15.78	130.7	124.7	129.9	99.4
17.12	125.5	108.5	124.7	97.8
17.34	124.7	106.1	122.0	97.9
20.00	98.6	83.7	96.9	98.3
22.50	81.8	69.3	80.6	98.6
25.00	69.5	58.7	68.7	99.0
27.50	60.2	50.8	59.7	99.2
30.00	52.9	44.6	52.7	99.5
32.50	47.2	39.7	47.0	99.7
35.00	42.5	35.8	42.4	99.9

Note:
L_b - Unbraced length (ft)
M_n - Theoretical nominal moment (k-ft)
LRFD - Moment using the LRFD specification (k-ft)
Model - Moment using the proposed model (k-ft)
Percent - Model / M_n

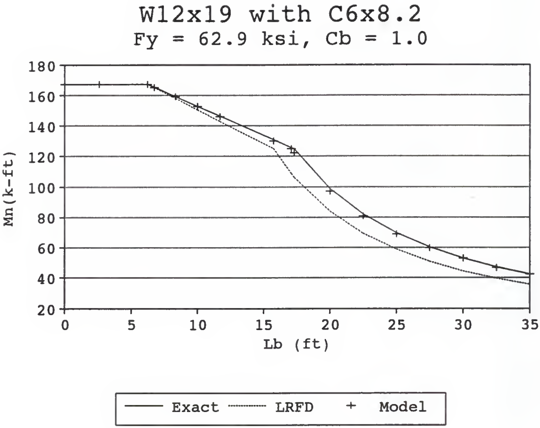

<u>Note</u>:
The EXACT curve is exact only in the elastic range and a straight line adopted by the LRFD specification is used for the inelastic range.

Figure 8-5. M_n versus L_b curves.

Table 8-6. Comparison between theory and model, section W10x15 with C6x8.2, F_y=51.5 ksi.

L_b	M_n	LRFD	Model	Percent
0.00	90.5	90.5	90.5	100.0
2.85	90.5	90.5	90.5	100.0
4.17	90.5	90.5	90.5	100.0
7.12	90.5	90.5	90.5	100.0
7.76	89.5	89.3	89.5	100.0
10.00	86.0	85.2	85.9	100.0
11.77	83.2	81.9	83.1	99.9
15.00	78.1	76.0	78.0	99.9
17.50	74.2	71.4	74.0	99.8
20.18	69.9	66.4	69.8	99.7
22.27	66.7	56.7	66.4	99.0
22.41	66.4	56.2	65.8	99.0
25.00	56.1	47.4	55.7	99.4
27.50	48.5	41.0	48.4	99.7
30.00	42.7	36.1	42.7	99.9
32.50	38.0	32.1	38.1	100.2
35.00	34.2	28.9	34.4	100.4

<u>Note</u>:
L_b - Unbraced length (ft)
M_n - Theoretical nominal moment (k-ft)
LRFD - Moment using the LRFD specification (k-ft)
Model - Moment using the proposed model (k-ft)
Percent - Model / M_n

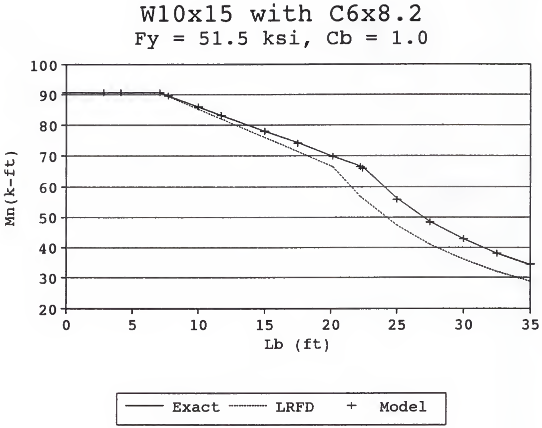

Note:
The EXACT curve is exact only in the elastic range and a straight line adopted by the LRFD specification is used for the inelastic range.

Figure 8-6. M_n versus L_b curves.

Table 8-7. Comparison between theory and model, section M8x6.5 with C4x5.4, F_y=42.7 ksi.

L_b	M_n	LRFD	Model	Percent
0.00	27.3	27.3	27.3	100.0
1.70	27.3	27.3	27.3	100.0
4.80	27.3	27.3	27.3	100.0
5.40	27.3	27.3	27.3	100.0
7.50	26.1	26.0	26.1	100.0
10.00	24.8	24.4	24.8	100.0
11.72	23.9	23.4	23.9	99.9
15.00	22.2	21.4	22.1	99.9
17.50	20.8	19.8	20.8	99.9
18.49	20.3	19.2	20.3	99.9
20.48	19.2	16.5	19.2	99.6
20.54	19.2	16.4	19.1	99.6
22.50	16.8	14.3	16.8	99.9
25.00	14.4	12.3	14.4	100.4
27.50	12.6	10.8	12.6	100.7
30.00	11.1	9.6	11.2	101.0
32.50	10.0	8.6	10.1	101.3
35.00	9.0	7.8	9.2	101.5

<u>Note</u>:
L_b - Unbraced length (ft)
M_n - Theoretical nominal moment (k-ft)
LRFD - Moment using the LRFD specification (k-ft)
Model - Moment using the proposed model (k-ft)
Percent - Model / M_n

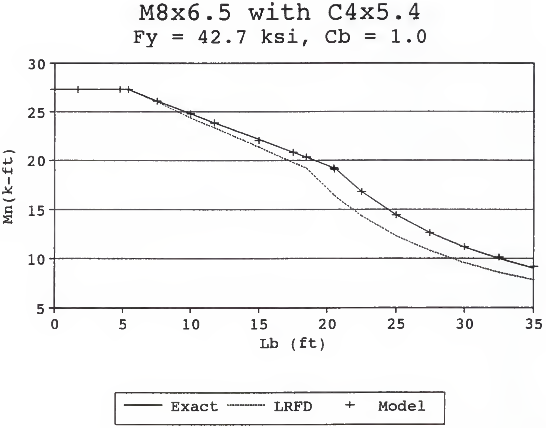

Note:
The EXACT curve is exact only in the elastic range and a straight line adopted by the LRFD specification is used for the inelastic range.

Figure 8-7. M_n versus L_b curves.

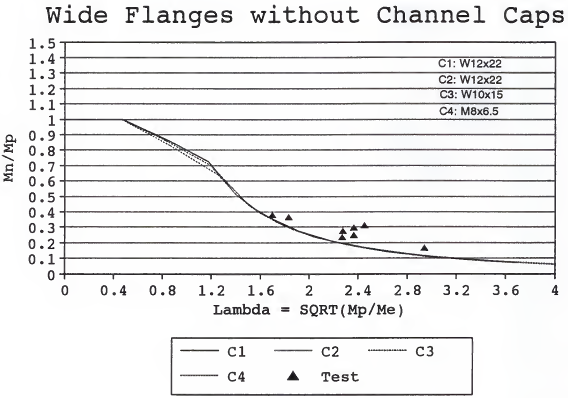

Figure 8-8. Test results of wide flange beams without channel caps, where M_p is plastic moment, M_e is elastic moment, and M_n is nominal moment. The M_e and M_n are calculated based on $C_b = 1$.

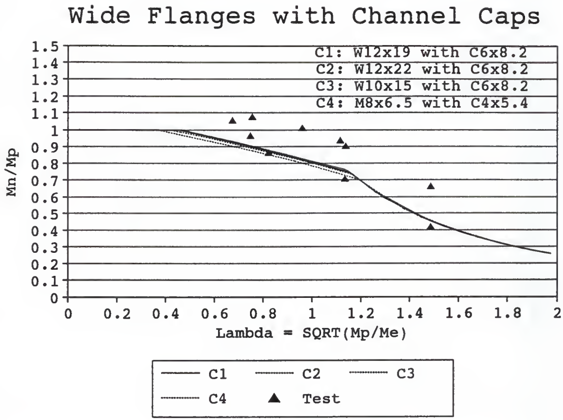

Figure 8-9. Test results of wide flange beams with channel caps, where M_p is plastic moment, M_e is elastic moment, and M_n is nominal moment. The M_e and M_n are calculated based on $C_b = 1$.

APPENDIX A

USER'S GUIDE FOR THE NOMINAL MOMENT PROGRAM (LTBMN)

1. CONTROL INFORMATION - ONE CARD
   ISC, FY, CB

   ISC -- 1 for considering residual stress = 10.0 ksi.
   2 for considering residual stress = 16.5 ksi.
   FY --- Steel yielding stress (ksi).
   CB --- Equivalent bending coefficient.

2. WIDE FLANGE DIMENSIONS - ONE CARD
   WA,WD,WTW,WBF,WTF

   WA --- Area of wide flange.
   WD --- Depth of wide flange.
   WTW -- Web thickness of wide flange.
   WBF -- Flange width of wide flange.
   WTF -- Flange thickness of wide flange.

3. UNBRACED LENGTHS FOR WIDE FLANGE BEAMS - SET OF CARDS
   DSPTN
   DSLB(I)

   DSPTN ---- Number of unbraced lengths.
   DSLB(I) -- Set of unbraced lengths of wide flange beams.

4. CHANNEL CAP DIMENSIONS - ONE CARD
   CA,CD,CTW,CBF,CTF

   CA --- Area of channel cap.
   CD --- Depth of channel cap.
   CTW -- Web thickness of channel cap.
   CBF -- Flange width of channel cap.
   CTF -- Flange thickness of channel cap.

5. SECTION PROPERTIES OF WIDE FLANGES WITH CHANNEL CAPS - ONE CARD
   CIW, IYW, JW, IXC, JC

   CIW -- Warping constant of wide flange.
   IYW -- Moment inertia about Y axis of wide flange.
   JW --- Torsional constant of wide flange.

IXC -- Moment inertia about X axis of channel cap.
JC --- Torsional constant of channel cap.

6. UNBRACED LENGTHS OF WIDE FLANGE BEAMS WITH CHANNEL CAPS - SET OF CARDS
SSPTN
SSLBS(I)

SSPTN ----- Number of unbraced lengths.
SSLBS(I) -- Set of unbraced lengths of wide flange beams with channel caps.

DESIGN EXAMPLES

Example One

Problem:

A simply supported wide flange beam with channel cap without bracing between end supports has a central concentrated load acting at its top surface. Determine the critical buckling moment of the beam.

Given:

Section - W30x173 with MC18x42.7, $A_c/A_w = 0.248$, $E = 29{,}000$ ksi, $G = 11{,}200$ ksi, $L_b = 55'$, $C_b = 1.0$, and $K = 1.0$.

W30x173 - dimensions: $A = 50.80$ in^2, $d = 30.44$ in, $t_w = 0.655$ in, $b_f = 14.985$ in, and $t_f = 1.065$ in.

MC18x42.7 - dimensions: $A = 12.60$ in^2, $d = 18.00$ in, $t_w = 0.450$ in, $b_f = 3.950$ in, and $t_f = 0.625$ in.

Solution:

1. The Theoretical Approach:

According to Chapter 3, the elastic critical buckling moment can be expressed by

$$M_{cr} = \frac{\pi C_b}{KL_b} \left\{ \sqrt{EI_y GJ} \ \left(B_1 + \sqrt{1 + B_2 + B_1^2} \right) \right\} \tag{B.1}$$

where

$$B_1 = \frac{\pi \beta_x}{2KL_b}\sqrt{\frac{EI_y}{GJ}} , \qquad B_2 = \frac{\pi^2 EC_{wc}}{(KL_b)^2 GJ} \tag{B.2}$$

From the output of the LTBMN program,

L_p = 231.87 in, L_r = 584.53 in, β_x = 13.86 in, C_{wc} = 201,928 in^6, J = 26.854 in^4, and I_y = 1,145 in^4.

L_b = 55′ = 660" > L_r, thus the beam will buckle elastically and Eqs. B.1 and B.2 are applied.

From Eq. B.2 and the known values of β_x, C_{wc}, J, K, G, E, and I_y, B_1 = 0.3467 and B_2 = 0.4412.

Substituting B_1 and B_2 into Eq. B.1 and M_{cr} = 24,015 k-in.

2. The LRFD Approach:

According to the Table A.F.1.1 in LRFD [1986], the elastic critical buckling moment can be written by

$$M_{cr} = \frac{57000C_b}{L_b}\sqrt{I_yJ}\left\{B_1 + \sqrt{1 + B_2 + B_1^{\,2}}\right\} \qquad (B.3)$$

where

$$B_1 = 2.25\left(\frac{2I_{yc}}{I_y} - 1\right)\left(\frac{h}{L_b}\right)\sqrt{\frac{I_y}{J}} \qquad (B.4)$$

$$B_2 = 25\left(1 - \frac{I_{yc}}{I_y}\right)\left(\frac{I_{yc}}{J}\right)\left(\frac{h}{L_b}\right)^2 \qquad (B.5)$$

From Eqs. F1-4 and F1-6 in LRFD [1986], L_p = 231.87 in and L_r = 532.36 in.

L_b = 55′ = 660" > L_r, thus the beam will buckle elastically and Eqs. B.3, B.4, and B.5 are applied.

$I_{yc} = I_{yw}/2 + I_{xc}$ = 853.0 in^4

$I_y = I_{yw} + I_{xc}$ = 1,152 in^4

$h = d - 2*t_f$ = 28.31 in

From Eqs. B.4 and B.5 and the known values of I_{yc}, I_y, h, L_b, and J, B_1 = 0.3875 and B_2 = 0.6161.

Substituting B_1 and B_2 into Eq. B.1 and M_{cr} = 20,456 k-in.

3. The Proposed Approach:

According to Chapter 6, the elastic critical buckling moment can be expressed by

$$M_{cr} = \frac{\pi C_b}{KL_b}\left[\sqrt{EI_yGJ}\ \left(B_1 + \sqrt{1 + B_2 + B_1^2}\ \right)\right] \tag{B.6}$$

where

$$B_1 = \frac{\pi\beta_x}{2KL_b}\sqrt{\frac{EI_y}{GJ}}\ , \qquad B_2 = \frac{\pi^2 EC_{wc}}{(KL_b)^2 GJ} \tag{B.7}$$

$$\beta_x = 0.87\ (2\rho - 1)\left(D + \frac{D_L}{2}\right), \quad \rho = \frac{2I_{yc}}{I_y} \tag{B.8}$$

$$I_y = I_{yw} + I_{xc}\ , \qquad I_{yc} = \frac{I_{yw}}{2} + I_{xc} \tag{B.9}$$

$$C_{wc} = C_w\left(0.79 + 1.79\sqrt{\frac{A_c}{A_w}}\right), \qquad 0.2 \le \frac{A_c}{A_w} \le 0.95 \tag{B.10}$$

$$J = J_w + J_c + Bt_1t_2(t_1+t_2) \tag{B.11}$$

From Eqs. F1-4 and F1-6 in LRFD [1986], L_p = 231.87 in and L_r = 586.27 in.

L_b = 55′ = 660" > L_r, thus the beam will buckle elastically and Eqs. B.6 to B.11 are applied.

Using Eq. B.8 and the known values of D, D_L, I_{yc}, and I_y , β_x = 13.75.

Using Eq. B.10 and A_c/A_w = 0.248, C_{wc} = 217,619 in^6.

Using Eq. B.11 and the known values of J_c, J_w, t_1, and t_2, J = 27.41 in^4.

From Eq. B.7 and the known values of β_x , C_{wc}, J, E, G, I_y, L_b, and K, B_1 = 0.3414 and B_2 = 0.4659.

Substituting B_1 and B_2 into Eq. B.6 and M_{cr} = 24,113 k-in.

Summary: (C_b = 1.0)

			(k-in)	Error(%)
The Theoretical Approach:	M_{cr}	=	24,015	0.0
The LRFD Approach:	M_{cr}	=	20,456	-14.8
The Proposed Approach:	M_{cr}	=	24,113	+0.4

<u>Example Two</u>

Problem:

A simply supported wide flange beam with channel cap without bracing between end supports has a central concentrated load acting at its top surface. Determine the critical buckling moment of the beam.

Given:

Section - W12x26 with C10x15.3, A_c/A_w = 0.587, E = 29,000 ksi, G = 11,200 ksi, L_b = 45', C_b = 1.0, and K = 1.0.

W12x26 - dimensions: A = 7.65 in^2, d = 12.22 in, t_w = 0.230 in, b_f = 6.490 in, and t_f = 0.380 in.

C10x15.3 - dimensions: A = 4.49 in^2, d = 10.00 in, t_w = 0.240 in, b_f = 2.60 in, and t_f = 0.436 in.

Solution:

1. The Theoretical Approach:

According to Chapter 3, the elastic critical buckling moment can be expressed by

$$M_{cr} = \frac{\pi C_b}{KL_b} \left\{ \sqrt{EI_y GJ} \left(B_1 + \sqrt{1 + B_2 + B_1^2} \right) \right\} \tag{B.1}$$

where

$$B_1 = \frac{\pi \beta_x}{2KL_b} \sqrt{\frac{EI_y}{GJ}} , \qquad B_2 = \frac{\pi^2 E C_{wc}}{(KL_b)^2 GJ} \tag{B.2}$$

From the output of the LTBMN program,

L_p = 136.68 in, L_r = 461.49 in, β_x = 9.90 in, C_{wc} = 1,306 in^6, J = 0.834 in^4, and I_y = 84.3 in^4.

L_b = 45′ = 540" > L_r, thus the beam will buckle elastically and Eqs. B.1 and B.2 are applied.

From Eq. B.2 and the known values of β_x, C_{wc}, J, K, G, E, and I_y, B_1 = 0.4657 and B_2 = 0.1372.

Substituting B_1 and B_2 into Eq. B.1 and M_{cr} = 1,432 k-in.

2. The LRFD Approach:

According to the Table A.F.1.1 in LRFD [1986], the elastic critical buckling moment can be written by

$$M_{cr} = \frac{57000 C_b}{L_b} \sqrt{I_y J} \left\{ B_1 + \sqrt{1 + B_2 + B_1^2} \right\} \tag{B.3}$$

where

$$B_1 = 2.25\left(\frac{2 I_{yc}}{I_y} - 1\right)\left(\frac{h}{L_b}\right)\sqrt{\frac{I_y}{J}} \tag{B.4}$$

$$B_2 = 25\left(1 - \frac{I_{yc}}{I_y}\right)\left(\frac{I_{yc}}{J}\right)\left(\frac{h}{L_b}\right)^2 \tag{B.5}$$

From Eqs. F1-4 and F1-6 in LRFD [1986], L_p = 136.68 in and L_r = 394.03 in.

L_b = 45′ = 540" > L_r, thus the beam will buckle elastically and Eqs. B.3, B.4, and B.5 are applied.

$I_{yc} = I_{yw}/2 + I_{xc}$ = 72.20 in^4

$I_y = I_{yw} + I_{xc}$ = 76.99 in^4

$h = d - 2*t_f$ = 11.46 in

From Eqs. B.4 and B.5 and the known values of I_{yc}, I_y, h, L_b, and J, B_1 = 0.5136 and B_2 = 0.0993.

Substituting B_1 and B_2 into Eq. B.1 and M_{cr} = 1,112 k-in.

3. The Proposed Approach:

According to Chapter 6, the elastic critical buckling moment can be expressed by

$$M_{cr} = \frac{\pi C_b}{KL_b}\left[\sqrt{EI_y GJ}\ \left(B_1 + \sqrt{1 + B_2 + B_1^2}\ \right)\right] \tag{B.6}$$

where

$$B_1 = \frac{\pi \beta_x}{2KL_b}\sqrt{\frac{EI_y}{GJ}}\ , \qquad B_2 = \frac{\pi^2 EC_{wc}}{(KL_b)^2 GJ} \tag{B.7}$$

$$\beta_x = 0.87\ (2\rho - 1)\left(D + \frac{D_L}{2}\right), \qquad \rho = \frac{2I_{yc}}{I_y} \tag{B.8}$$

$$I_y = I_{yw} + I_{xc}\ , \qquad I_{yc} = \frac{I_{yw}}{2} + I_{xc} \tag{B.9}$$

$$C_{wc} = C_w\left(0.79 + 1.79\sqrt{\frac{A_c}{A_w}}\right), \qquad 0.2 \le \frac{A_c}{A_w} \le 0.95 \tag{B.10}$$

$$J = J_w + J_c + Bt_1t_2(t_1+t_2) \tag{B.11}$$

From Eqs. F1-4 and F1-6 in LRFD [1986], L_p = 136.68 in and L_r = 450.01 in.

L_b = 45′ = 540" > L_r, thus the beam will buckle elastically and Eqs. B.6 to B.11 are applied.

Using Eq. B.8 and the known values of D, D_L, I_{yc}, and I_y , $\beta_x = 10.48$.

Using Eq. B.10 and $A_c/A_w = 0.587$, $C_{wc} = 1315.7\ in^6$.

Using Eq. B.11 and the known values of J_c, J_w, t_1, and t_2, $J = 0.877\ in^4$.

From Eq. B.7 and the known values of β_x , C_{wc}, J, E, G, I_y, L_b, and K, $B_1 = 0.4596$ and $B_2 = 0.1315$.

Substituting B_1 and B_2 into Eq. B.6 and $M_{cr} = 1{,}379$ k-in.

Summary: ($C_b = 1.0$)

		(k-in)	Error(%)
The Theoretical Approach:	M_{cr} =	1,432	0.0
The LRFD Approach:	M_{cr} =	1,112	-22.4
The Proposed Approach:	M_{cr} =	1,379	-3.7

Example Three

Problem:

A simply supported wide flange beam with channel cap without bracing between end supports has a central concentrated load acting at its top surface. Determine the critical buckling moment of the beam.

Given:

Section - W12x26 with C12x20.7, A_c/A_w = 0.796, E = 29,000 ksi, G = 11,200 ksi, L_b = 55', C_b = 1.0, and K = 1.0

W12x26 - dimensions: A = 7.65 in^2, d = 12.22 in, t_w = 0.230 in, b_f = 6.490 in, and t_f = 0.380 in.

C12x20.7 - dimensions: A = 6.09 in^2, d = 12.00 in, t_w = 0.282 in, b_f = 2.942 in, and t_f = 0.501 in.

Solution:

1. The Theoretical Approach:

According to Chapter 3, the elastic critical buckling moment can be expressed by

$$M_{cr} = \frac{\pi C_b}{KL_b} \left\{ \sqrt{EI_y GJ} \left(B_1 + \sqrt{1 + B_2 + B_1^2} \right) \right\} \tag{B.1}$$

where

$$B_1 = \frac{\pi \beta_x}{2KL_b} \sqrt{\frac{EI_y}{GJ}} , \qquad B_2 = \frac{\pi^2 EC_{wc}}{(KL_b)^2 GJ} \tag{B.2}$$

From the output of the LTBMN program,

L_p = 167.77 in, L_r = 638.36 in, β_x = 10.88 in, C_{wc} = 1,476 in^6, J = 1.067 in^4, and I_y = 145.8 in^4.

L_b = 55' = 660" > L_r, thus the beam will buckle elastically and Eqs. B.1 and B.2 are applied.

From Eq. B.2 and the known values of β_x, C_{wc}, J, K, G, E, and I_y, B_1 = 0.4869 and B_2 = 0.0812.

Substituting B_1 and B_2 into Eq. B.1 and M_{cr} = 1,750 k-in.

2. The LRFD Approach:

According to the Table A.F.1.1 in LRFD [1986], the elastic critical buckling moment can be written by

$$M_{cr} = \frac{57000 C_b}{L_b} \sqrt{I_y J} \left\{ B_1 + \sqrt{1 + B_2 + B_1^2} \right\} \tag{B.3}$$

where

$$B_1 = 2.25\left(\frac{2 I_{yc}}{I_y} - 1\right)\left(\frac{h}{L_b}\right)\sqrt{\frac{I_y}{J}} \tag{B.4}$$

$$B_2 = 25\left(1 - \frac{I_{yc}}{I_y}\right)\left(\frac{I_{yc}}{J}\right)\left(\frac{h}{L_b}\right)^2 \tag{B.5}$$

From Eqs. F1-4 and F1-6 in LRFD [1986], L_p = 167.77 in and L_r = 549.86 in.

L_b = 55' = 660" > L_r, thus the beam will buckle elastically and Eqs. B.3, B.4, and B.5 are applied.

$I_{yc} = I_{yw}/2 + I_{xc}$ = 133.80 in^4

$I_y = I_{yw} + I_{xc}$ = 138.6 in^4

$h = d - 2*t_f$ = 11.46 in

From Eqs. B.4 and B.5 and the known values of I_{yc}, I_y, h, L_b, and J, B_1 = 0.5230 and B_2 = 0.0521.

Substituting B_1 and B_2 into Eq. B.1 and M_{cr} = 1,393 k-in.

3. The Proposed Approach:

According to Chapter 6, the elastic critical buckling moment can be expressed by

$$M_{cr} = \frac{\pi C_b}{KL_b}\left[\sqrt{EI_yGJ}\ (B_1 + \sqrt{1 + B_2 + B_1^2}\ )\right] \tag{B.6}$$

where

$$B_1 = \frac{\pi\beta_x}{2KL_b}\sqrt{\frac{EI_y}{GJ}}\ , \qquad B_2 = \frac{\pi^2 EC_{wc}}{(KL_b)^2 GJ} \tag{B.7}$$

$$\beta_x = 0.87\ (2\rho - 1)\left(D + \frac{D_L}{2}\right), \qquad \rho = \frac{2I_{yc}}{I_y} \tag{B.8}$$

$$I_y = I_{yw} + I_{xc}\ , \qquad I_{yc} = \frac{I_{yw}}{2} + I_{xc} \tag{B.9}$$

$$C_{wc} = C_w\left(0.79 + 1.79\sqrt{\frac{A_c}{A_w}}\right), \qquad 0.2 \le \frac{A_c}{A_w} \le 0.95 \tag{B.10}$$

$$J = J_w + J_c + Bt_1t_2(t_1+t_2) \tag{B.11}$$

From Eqs. F1-4 and F1-6 in LRFD [1986], L_p = 167.77 in and L_r = 631.65 in.

L_b = 55′ = 660" > L_r, thus the beam will buckle elastically and Eqs. B.6 to B.11 are applied.

Using Eq. B.8 and the known values of D, D_L, I_{yc}, and I_y , $\beta_x = 11.31$.

Using Eq. B.10 and $A_c/A_w = 0.796$, $C_{wc} = 1{,}453$ in^6.

Using Eq. B.11 and the known values of J_c, J_w, t_1, and t_2, J = 1.130 in^4.

From Eq. B.7 and the known values of β_x , C_{wc}, J, E, G, I_y, L_b, and K, $B_1 = 0.4798$ and $B_2 = 0.0754$.

Substituting B_1 and B_2 into Eq. B.6 and $M_{cr} = 1{,}723$ k-in.

Summary: ($C_b = 1.0$)

		(k-in)	Error(%)
The Theoretical Approach:	M_{cr} =	1,750	0.0
The LRFD Approach:	M_{cr} =	1,393	-20.4
The Proposed Approach:	M_{cr} =	1,723	-1.5

APPENDIX B

LISTING OF THE NOMINAL MOMENT PROGRAM (LTBMN)

```
CCCCCCCCCCCCCCCCCCCCCCCCCCCCCCCCCCCCCCCCCCCCCCCCCCCCCCCCCCCCCCCCCCCC
C                                                                  C
C     PROGRAM FOR LATERAL-TORSIONAL BUCKLING OF DOUBLY AND SINGLY   C
C     SYMMETRIC BEAMS; DOUBLY SYMMETRIC BEAMS IN THIS PROGRAM ARE   C
C     I-SHAPED MEMBERS AND SINGLY SYMMETRIC BEAMS ARE WIDE FLANGE   C
C     BEAMS WITH CHANNEL CAPS.                                      C
C                                                                  C
C     -- (LTBMN.FOR) --                                            C
C                                                                  C
CCCCCCCCCCCCCCCCCCCCCCCCCCCCCCCCCCCCCCCCCCCCCCCCCCCCCCCCCCCCCCCCCCCC
C-----------------------------------------------------------
      MAIN PROGRAM
C-----------------------------------------------------------
      REAL IYW, JW, IXC, JC, IYS, JS
      REAL DSLB(30), SSLBS(30), SSLBA(30), SSLBM(30), SSLBT(30)
      INTEGER DSPTN, SSPTN
      DOUBLE PRECISION ALL
C
      COMMON /GENDATA/ ISC, FY, CB
      COMMON /WFSEC/ WA, WD, WTW, WBF, WTF
      COMMON /DSDATA/ DSPTN, DSLB
      COMMON /CHSEC/ CA, CD, CTW, CBF, CTF
      COMMON /WCDATA/ CIW, IYW, JW, IXC, JC
      COMMON /CWDATA/ IYS,JS,SXC,SXT,ZXS,BETAX,BETAXT,CW,CWT
      COMMON /SSDATA/ SSPTN, SSLBS, SSLBA, SSLBM, SSLBT
C
      OPEN (7,FILE='LTBMN.DAT')
      REWIND (7)
C
C     INPUT OF DOUBLLY SYMMETRIC SECTION
C
      READ(7,*)  ISC, FY, CB
      READ(7,*)  WA, WD, WTW, WBF, WTF
      READ(7,*)  DSPTN
      IF (DSPTN .GT. 0) THEN
      DO 100 I = 1, DSPTN
      READ(7,*)  DSLB(I)
  100 CONTINUE
      ENDIF
C
C     INPUT OF SINGLY SYMMETRIC SECTION
C
      READ(7,*)  CA, CD, CTW, CBF, CTF
      READ(7,*)  CIW, IYW, JW, IXC, JC
      READ(7,*) SSPTN
      IF (SSPTN .GT. 0)  THEN
      DO 120 I = 1, SSPTN
      READ(7,*) SSLBS(I), SSLBA(I), SSLBM(I), SSLBT(I)
  120 CONTINUE
      ENDIF
C
C     DOUBLLY SYMMETRIC SECTION
```

```
C
      CALL DSCRV
C
C     SINGLY SYMMETRIC SECTION
C
      CALL CWINP
      CALL WARPC
      CALL SSCRV
C
      CLOSE (7)
      STOP
      END
C
C--------------------------------------------------------------
C
      SUBROUTINE DSCRV
C
C--------------------------------------------------------------
C
C     NOMINAL MOMENT (Mn) OF DOUBLY SYMMETRIC SECTION
C
      REAL MCR(30), LES(30), MP, MR, LP, LR, IX, IY, JJ, ME(30)
      INTEGER DSPTN
C
      COMMON /GENDATA/ ISC, FY, CB
      COMMON /WFSEC/ WA, WD, WTW, WBF, WTF
      COMMON /DSDATA/ DSPTN, LES
C
      OPEN(8,FILE='DSCRV.OUT',STATUS='UNKNOWN')
      REWIND (8)
C
  905 FORMAT(/ ' OUTPUT OF DOUBLY SYMMETRIC SECTION (WIDE FLANGE) ')
  910 FORMAT(/ ' Unit: Kips, Inches ')
  915 FORMAT(/ '    Cb= ', F4.2, 3X, ' Fy(Ksi)= ', F5.1, '    ROLLED SECT
     *ION (Fr = 10 Ksi)'  )
  916 FORMAT(/ '    Cb= ', F4.2, 3X, ' Fy(Ksi)= ', F5.1, '    WELDED SECT
     *ION (Fr = 16.5 Ksi)')
  920 FORMAT(/ ' SECTION PROPERTIES ')
  922 FORMAT(/ '     d= ', F10.3, '    tw= ', F10.3, '     bf= ',  F10.3,
     *'    tf= ', F10.3)
  925 FORMAT(/ '    Ix= ', F10.2, '    Iy= ', F10.2, '     Zx= ', F10.2)
  927 FORMAT(/ '    Sx= ', F10.2, '    Sy= ', F10.2, '   Area= ', F10.2)
  928 FORMAT(/ '    Rx= ', F10.3, '    Ry= ', F10.3, '     Cw= ', F10.2,
     *'     J= ', F10.3)
  935 FORMAT(/ '    Mp= ', F10.2, '    Mr= ', F10.2)
  940 FORMAT(/ '    Lp= ', F10.2, '    Lr= ', F10.2/)
  945 FORMAT(/ ' NOMINAL MOMENT CURVE (Mn) --------------- ')
  950 FORMAT(/ '    PT  ', '    Lb         Mn    ')
  955 FORMAT(/ I5, F10.2, F11.1/)
C
      WRITE(8,905)
      WRITE(8,910)
      IF (ISC .EQ. 1) THEN
      WRITE(8,915) CB, FY
      ENDIF
      IF (ISC .EQ. 2) THEN
      WRITE(8,916) CB, FY
      ENDIF
      WRITE(8,920)
      WRITE(8,922) WD, WTW, WBF, WTF
```

```
C
C     PROPERTIES OF SECTION
C
      AA = 2.*WBF*WTF + (WD-2.*WTF)*WTW
      XX = WBF * WTF * (WD-WTF)/2.
      ZX = 2. * (1./8.*WTW*(WD-2.*WTF)**2 + XX)
      IX = 1./12.*WBF*(WD**3) - 1./12.*(WBF-WTW)*(WD-2.*WTF)**3
      RX = SQRT(IX/AA)
      SX = IX / (WD/2.)
      IY = 1./6.*WTF*(WBF**3) + 1./12.*(WD-2.*WTF)*(WTW**3)
      SY = IY / (WBF/2.)
      RY = SQRT(IY/AA)
      JJ = 2./3.*(WBF*WTF**3) + 1./3.*(WD-2.*WTF)*(WTW**3)
      CW = 1./4. * IY * (WD-WTF)**2
      WRITE(8,925) IX, IY, ZX
      WRITE(8,927) SX, SY, AA
      WRITE(8,928) RX, RY, CW, JJ
C
C     CALCULATE Mp AND Mr
C
      IF (ISC .EQ. 1) GO TO 50
      IF (ISC .EQ. 2) GO TO 60
   50 MP = ZX * FY
      MR = (FY-10.0) * SX
      GO TO 70
   60 MP = ZX * FY
      MR = (FY-16.5) * SX
   70 CONTINUE
      WRITE(8,935) MP, MR
C
C     CALCULATE Lp AND Lr (EXACT)
C
      LP = 300. * RY / SQRT(FY)
      XX = 29000. * JJ * AA / 2. * 11200.
      X1 = 3.14159 / SX * SQRT(XX)
      XX = (SX/11200./JJ)**2
      X2 = 4. * CW / IY * XX
      IF (ISC .EQ. 1) GO TO 100
      IF (ISC .EQ. 2) GO TO 110
  100 XX = 1. + X2*(FY-10.0)**2
      XX = 1. + SQRT(XX)
      LR = RY*X1/(FY-10.0)*SQRT(XX)
      GO TO 120
  110 XX = 1. + X2*(FY-16.5)**2
      XX = 1. + SQRT(XX)
      LR = RY*X1/(FY-16.5)*SQRT(XX)
  120 CONTINUE
      WRITE(8,940) LP, LR
C
C     NOMINAL MOMENT CURVE (Mn) -- DOUBLY SYMMETRIC SECTION
C
      IF ( DSPTN .EQ. 0 ) GO TO 220
      DO 200 I = 1, DSPTN
      IF (LES(I) .LE. LP) GO TO 150
      IF ( (LES(I) .GT. LP) .AND. (LES(I) .LE. LR) ) GO TO 160
      IF (LES(I) .GT. LR) GO TO 170
  150 MCR(I) = MP
      GO TO 200
  160 XX = (MR-MP)/(LR-LP) * (LES(I)-LP) + MP
      MCR(I) = CB * XX
```

```
      IF (MCR(I) .GE. MP) THEN
      MCR(I) = MP
      ENDIF
      GO TO 200
  170 CONTINUE
      XXX1 = (LES(I)/RY)**2
      XXX2 = X2 * (X1**2)
      XXX = 2.* (1.+XXX2/2./XXX1)
      MCR(I) = CB * SX * X1 / (LES(I)/RY) * SQRT(XXX)
  200 CONTINUE
      WRITE(8,945)
      WRITE(8,950)
      DO 210 I = 1, DSPTN
      WRITE(8, 955) I, LES(I), MCR(I)
  210 CONTINUE
  220 CONTINUE
C
      DO 225 I = 1, DSPTN
      XXX1 = (LES(I)/RY)**2
      XXX2 = X2 * (X1**2)
      XXX = 2.* (1.+XXX2/2./XXX1)
      ME(I) = CB * SX * X1 / (LES(I)/RY) * SQRT(XXX)
  225 CONTINUE
      WRITE(8,*) '  '
      WRITE(8,*) ' Lb  MCR, ME, LAMBDA, MCRS/Mp '
      WRITE(8,*) '  '
  946 FORMAT(F7.2, F10.1, F10.1, F10.3, F10.3)
      DO 620 I = 1, DSPTN
      XX1 = LES(I)/12.
      XX2 = MCR(I)/12.
      XX3 = ME(I)/12.
      XX4 = MP / ME(I)
      XX4 = SQRT(XX4)
      XX5 = MCR(I) / MP
      WRITE(8,946) XX1, XX2, XX3, XX4, XX5
  620 CONTINUE
C
      CLOSE (8)
C
      RETURN
      END
C
C-----------------------------------------------------------
C
      SUBROUTINE CWINP
C
C------------------------------------------------------------
C
C     GENERATE INPUT FOR SECTION PROPERTY PROGRAM INCLUDING
C     WARPING CONSTANT
C
      DIMENSION X(17), Y(17), ELE(20)
C
      COMMON /WFSEC/ WA, WD, WTW, WBF, WTF
      COMMON /CHSEC/ CA, CD, CTW, CBF, CTF
C
      OPEN (8,FILE='CWINP.OUT',STATUS='UNKNOWN')
      REWIND (8)
C
  900 FORMAT(4X, 5F8.4)
```

```
  910 FORMAT(4X, I2)
  912 FORMAT(4X, I2, '  ', F8.5, '   ', F8.5)
  914 FORMAT(4X, I2)
  916 FORMAT(4X, I2, I4, I4, F9.5)
C
C     Calculation
C
      X(1) = (CD - WBF)/2.
      Y(1) = WTF/2.
      X(2) = CD/2.
      Y(2) = Y(1)
      X(3) = X(2)
      Y(3) = WD + CTW - (WTF+CTW)/2.
      X(4) = X(1)
      Y(4) = Y(3)
      X(5) = X(1)
      Y(5) = WD + CTW - CTW/2.
      X(6) = CTF/2.
      Y(6) = Y(5)
      X(7) = X(6)
      Y(7) = WD + CTW - CBF
      X(8) = X(1) + WBF
      Y(8) = Y(1)
      X(9) = X(8)
      Y(9) = Y(3)
      X(10) = X(9)
      Y(10) = Y(5)
      X(11) = CD - CTF/2.
      Y(11) = Y(10)
      X(12) = X(11)
      Y(12) = Y(7)
C
      ELE(1) = WTF
      ELE(2) = WTW
      ELE(3) = WTF + CTW
      ELE(4) = 0.
      ELE(5) = CTW
      ELE(6) = CTF
      ELE(7) = ELE(1)
      ELE(8) = ELE(3)
      ELE(9) = 0.
      ELE(10) = ELE(5)
      ELE(11) = ELE(6)
C
      N = 12
      WRITE(8,910) N
      DO 10 I = 1, N
      WRITE(8,912) I, X(I), Y(I)
   10 CONTINUE
      K = 11
      WRITE(8,914) K
      K = 6
      WRITE(8,914) K
      K = 1
      WRITE(8,914) K
      K = 5
      WRITE(8,914) K
      K= 1
      K1 = 1
      K2 = 2
```

```
      WRITE(8,916) K, K1, K2, ELE(1)
      K = 2
      K1 = 2
      K2 = 3
      WRITE(8,916) K, K1, K2, ELE(2)
      K = 3
      K1 = 3
      K2 = 4
      WRITE(8,916) K, K1, K2, ELE(3)
      K = 4
      K1 = 4
      K2 = 5
      WRITE(8,916) K, K1, K2, ELE(4)
      K = 5
      K1 = 5
      K2 = 6
      WRITE(8,916) K, K1, K2, ELE(5)
      K = 6
      K1 = 6
      K2 = 7
      WRITE(8,916) K, K1, K2, ELE(6)
      K = 7
      K1 = 8
      K2 = 2
      WRITE(8,916) K, K1, K2, ELE(7)
      K = 8
      K1 = 9
      K2 = 3
      WRITE(8,916) K, K1, K2, ELE(8)
      K = 9
      K1 = 10
      K2 =  9
      WRITE(8,916) K, K1, K2, ELE(9)
      K = 10
      K1 = 11
      K2 = 10
      WRITE(8,916) K, K1, K2, ELE(10)
      K = 11
      K1 = 12
      K2 = 11
      WRITE(8,916) K, K1, K2, ELE(11)
      CLOSE (8)
      RETURN
      END
C
C-----------------------------------------------------------
C
      SUBROUTINE WARPC
C
C-----------------------------------------------------------
C
C     PROGRAM FOR PROPERTIES OF THIN-WALLED OPEN CROSS SECTIONS WAS
C     ORIGINALLY WRITTEN IN BASIC LANGUAGE BY PROFESSOR T. V. GALAMBOS
C
C     CONVERED TO FORTRAN LANGUAGE AND MODIFIED BY T. SPUTO  OCT 1988
C
C     MODIFIED AND EXPANDED BY TONY LUE IN MAY 1992
C
C     THEORY APPLIES TO THIN-WALLED, OPEN CROSS SECTIONS WITH STRAIGHT
C     ELEMENTS.
```

```
C
C     NOTE: ORIGIN OF COORDINATES IS LOWER LEFT CORNER.
C
      DIMENSION COSE(50),SINE(50),J1(50),I1(50),F(50),FO(50),AC(4),YC(4)
      DIMENSION LENGTH(50),RHO(50),RHOO(50),T(50),W(50),WO(50),WN(50)
      DIMENSION X(50),Y(50),X1(50),Y1(50),ZWEIG(50),XELE(6,2),YELE(6,2)
      REAL LENGTH, JTOR, L1, L2, IXX, IYY, IXY, IWX, IWY, IYYC, IYA,
     * IYW, IXC, JW, JC
      INTEGER ZWEIG
      DOUBLE PRECISION ALL
C
      COMMON /GENDATA/ ISC, FY, CB
      COMMON /WFSEC/ WA, WD, WTW, WBF, WTF
      COMMON /CHSEC/ CA, CD, CTW, CBF, CTF
      COMMON /WCDATA/ CIW, IYW, JW, IXC, JC
      COMMON /CWDATA/ IYY,JTOR,SXC,SXT,ZX,BETAX,BETAXT,CW,CWT
C
      OPEN (7,FILE='CWINP.OUT')
      OPEN (8,FILE='WAPC.OUT',STATUS='UNKNOWN')
      REWIND (7)
      REWIND (8)
      ACT = 0.
C
      NI = 7
      NO = 8
 1000 FORMAT ('PROPERTIES OF THIN WALLED OPEN CROSS SECTIONS: ')
 2000 FORMAT (A1)
 3000 FORMAT('A=', F6.2,'  d=', F6.2, '  tw=', F7.4, '  bf=', F7.4,
     $ '  tf=', F7.4/)
C
      WRITE(NO,2000)
      WRITE(NO,*) 'W-Section Dimensions '
      WRITE(NO,2000)
      WRITE(NO,3000) WA, WD, WTW, WBF, WTF
      WRITE(NO,*) 'Channel Dimensions '
      WRITE(NO,2000)
      WRITE(NO,3000) CA, CD, CTW, CBF, CTF
      WRITE(NO,1000)
      WRITE(NO,2000)
C
C  READ IN NUMBER OF COORDINATE POINTS ON CROSS SECTION
C
 1001 FORMAT ('NUMBER OF COORDINATE POINTS ON CROSS SECTION = ',I2)
      READ (NI,*) N
      WRITE (NO,1001) N
      WRITE (NO,2000)
C
C  READ IN THE COORDINATE POINTS
C
 1002 FORMAT ('NODAL POINT COORDINATES')
 1004 FORMAT ('I = ',I2,5X,'X = ',F8.4,5X,'Y = ',F8.4)
      WRITE(NO,1002)
      DO 20  I = 1, N
      READ(NI,*) K, X(I), Y(I)
      WRITE(NO,1004) I, X(I), Y(I)
   20 CONTINUE
      WRITE (NO,2000)
C
C  ELEMENTS MUST BE NUMBERED IN ORDER OF INTEGRATION:
C  NUMBEL -- Total number of elements
```

```
C  NOEND -- Total number of elements in the primary path
C  NOBRAN -- Total number of branches
C  ZWEIG(I) -- Total numer of elements in branche I
C
 1005 FORMAT('NUMBER OF ELEMENTS = ', I2)
 1006 FORMAT('NUMBER OF ELEMENTS IN THE PRIMARY PATH OF ',
     $    'INTEGRATION = ',I2)
 1007 FORMAT('NUMBER OF BRANCHES = ',I2)
 1008 FORMAT('NUMBER OF ELEMENTS IN BRANCH ',I2,' = ',I3)
 1010 FORMAT('ELEM NUM ',I2,' NODE I = ',I2,' NODE J = ',I2,'  THICKNESS
     $ = ',F7.4)
      READ(NI,*) NUMBEL
      WRITE(NO,1005) NUMBEL
      WRITE(NO,2000)
      READ(NI,*) NOEND
      WRITE(NO,1006) NOEND
      WRITE(NO,2000)
      NOBRAN = 0
      IF (NOEND.EQ.NUMBEL) GO TO 400
      READ(NI,*) NOBRAN
      WRITE(NO,1007) NOBRAN
      WRITE(NO,2000)
  400 CONTINUE
      IF(NOBRAN.EQ.1) ZWEIG(1) = NUMBEL - NOEND
      DO 450 I = 1, NOBRAN
      READ(NI,*) ZWEIG(I)
      WRITE(NO,1008) I, ZWEIG(I)
  450 CONTINUE
C
      DO 520 I = 1, NUMBEL
      READ(NI,*) K, I1(I), J1(I), T(I)
      WRITE(NO,1010) I, I1(I), J1(I), T(I)
  520 CONTINUE
C
C  COMPUTE CENTER OF GRAVITY  ( CENTROID OF SECTION )
C
C  NOTE: ORIGIN OF COORDINATES IS LOWER LEFT CORNER.
C
 1025 FORMAT('Coordinate 1 - origin is the lower left corner with ')
 1027 FORMAT('               principal axes, pos-x to right, pos-y up.')
 1029 FORMAT(/'Coordinate 2 - origin is the centroid of section with')
 1031 FORMAT('               principal axes, pos-x to left, pos-y down.
     $ '/)
 1033 FORMAT('Centroid: (XBAR,YBAR) with respect to Coordinate 1 '/)
 1034 FORMAT('Centroid of Compressive Area:(Xcc,Ycc) w.r.t. Coordinate
     $1'/)
 1035 FORMAT('Shear Center: (Xs,Ys) with respect to Coordinate 1 '/)
 1037 FORMAT('Shear Center: (Xo,Yo) with respect to Coordinate 2 '/)
 1039 FORMAT('Ixx, Iyy, and Ixy are with respect to Coordinate 2 '/)
 1040 FORMAT('Sxc, Sxt: elastic section modulus refered to compression a
     *nd tension flanges'/)
 1041 FORMAT('Iwx and Iwy are with respect to Coordinate 2 '/)
 1011 FORMAT('AREA= ',F10.5,'    XBAR= ',F10.5,'     YBAR= ',F10.5/)
 1043 FORMAT('                  ','     Xcc= ', F10.5,'      Ycc= ',F10.5
     $/)
 1012 FORMAT(' Ixx= ',F10.3,'     Iyy= ',F10.3,'      Ixy= ',F10.3,
     $'     J= ',F10.3/)
 1051 FORMAT(' Sxc= ',F10.3,'     Sxt= ',F10.3/)
 1013 FORMAT(' Iwx= ',F10.3,'     Iwy= ',F10.3,'       Xs= ',F10.4,
     $'   Ys= ',F10.4/)
```

```
 1015 FORMAT('                                               Xo= ',F10.4,
     $'    Yo= ',F10.4/)
 1014 FORMAT('Section Warping Constant (exact)   Cw = ', F15.4/)
 6008 FORMAT('Section Warping Constant (Trahair) Cw = ', F15.4/)
      AREA = 0.
      JTOR = 0.
      XMOM = 0.
      YMOM = 0.
      DO 880 I = 1, NUMBEL
      L1 = X(I1(I)) - X(J1(I))
      L2 = Y(I1(I)) - Y(J1(I))
      LENGTH(I) = SQRT(L1**2+L2**2)
      AREA = AREA + LENGTH(I)*T(I)
      JTOR = JTOR + (LENGTH(I)*T(I)**3)/3.
      XMOM = XMOM + LENGTH(I)*T(I)*(X(J1(I))+L1/2.)
      YMOM = YMOM + LENGTH(I)*T(I)*(Y(J1(I))+L2/2.)
  880 CONTINUE
      XBAR = XMOM/AREA
      YBAR = YMOM/AREA
C
C  COMPUTE CENTROID OF COMPRESSIVE AREA
C
      AC(1) = CBF*CTF
      AC(2) = AC(1)
      AC(3) = WBF*WTF
      AC(4) = (CD-2.*CTF) * CTW
      YC(1) = (WD+CTW) - CBF/2.
      YC(2) = YC(1)
      YC(3) = WD - WTF/2.
      YC(4) = WD + CTW/2.
      YMON = 0.
      AAA = 0.
      DO 890 I = 1, 4
      YMON = YMON + AC(I)*YC(I)
      AAA = AAA + AC(I)
  890 CONTINUE
      XCC = CD/2.
      YCC = YMON/AAA
C
      WRITE(NO,2000)
      WRITE(NO,1025)
      WRITE(NO,1027)
      WRITE(NO,1029)
      WRITE(NO,1031)
      WRITE(NO,1033)
      WRITE(NO,1034)
      WRITE(NO,1035)
      WRITE(NO,1037)
      WRITE(NO,1039)
      WRITE(NO,1040)
      WRITE(NO,1041)
      WRITE(NO,1011) AREA, XBAR, YBAR
      WRITE(NO,1043) XCC, YCC
C
C  RELOCATE TO NEUTRAL AXIS
C
      DO 960 I = 1, N
      X1(I) = -X(I) + XBAR
      Y1(I) = -Y(I) + YBAR
  960 CONTINUE
```

```
C
C  COMPUTE MOMENTS AND PRODUCTS OF INERTIA
C
      IXX = 0.
      IYY = 0.
      IXY = 0.
      DO 961 I = 1, NUMBEL
      IXX = IXX + (Y1(I1(I))**2 + Y1(I1(I))*Y1(J1(I)) + Y1(J1(I))**2)
     $*LENGTH(I)*T(I)/3.
      IYY = IYY + (X1(I1(I))**2 + X1(I1(I))*X1(J1(I)) + X1(J1(I))**2)
     $*LENGTH(I)*T(I)/3.
      IXY = IXY + (X1(I1(I))*Y1(I1(I)) + X1(J1(I))*Y1(J1(I)))
     $*LENGTH(I)*T(I)/3.
      IXY = IXY + (X1(I1(I))*Y1(J1(I)) + X1(J1(I))*Y1(I1(I)))
     $*LENGTH(I)*T(I)/6.
  961 CONTINUE
      SXC = IXX / (WD+CTW-YBAR)
      SXT = IXX / YBAR
      WRITE(NO,1012) IXX, IYY, IXY, JTOR
      WRITE(NO,1051) SXC, SXT
C
C  CALCULATE SHEAR CENTER (Xo,Yo)
C
 3001 FORMAT(3I5, 3F10.4/)
 3002 FORMAT(3I5, 4F10.4/)
 3003 FORMAT('    ', 4F10.4/)
 4001 FORMAT(I5, 3F10.4/)
      DO 963 I = 1, NUMBEL
      COSE(I) = (X1(J1(I)) - X1(I1(I))) / LENGTH(I)
      SINE(I) = (Y1(J1(I)) - Y1(I1(I))) / LENGTH(I)
      RHO(I) = -(Y1(I1(I))*COSE(I) - X1(I1(I))*SINE(I))
      F(I) = RHO(I)*LENGTH(I)
C     WRITE(NO,3001) I, I1(I), J1(I), LENGTH(I), RHO(I), F(I)
  963 CONTINUE
      W(I1(1)) = 0.
      DO 965 I = 1, NOEND
      W(J1(I)) = W(I1(I)) + F(I)
      IF (I .EQ. NOEND) GO TO 965
      W(I1(I+1)) = W(J1(I))
  965 CONTINUE
C
C     DO 966 I = 1, NOEND
C     WIXI = W(I1(I))*X1(I1(I))
C     WJXJ = W(J1(I))*X1(J1(I))
C     WIXJ = W(I1(I))*X1(J1(I))
C     WJXI = W(J1(I))*X1(I1(I))
C     WRITE(NO,3002) I,I1(I),J1(I),X1(I1(I)),X1(J1(I)),W(I1(I)),W(J1(I))
C     WRITE(NO,3003) WIXI, WJXJ, WIXJ, WJXI
C 966 CONTINUE
C
      DO 967 I = NOEND+1, NUMBEL
      DO 967 J = 1, NOBRAN
      DO 967 K = 1, ZWEIG(J)
      W(I1(I)) = W(J1(I)) - F(I)
  967 CONTINUE
C
C     DO 968 I = NOEND+1, NUMBEL
C     WIXI = W(I1(I))*X1(I1(I))
C     WJXJ = W(J1(I))*X1(J1(I))
C     WIXJ = W(I1(I))*X1(J1(I))
```

```
C     WJXI = W(J1(I))*X1(I1(I))
C     WRITE(NO,3002) I,I1(I),J1(I),X1(I1(I)),X1(J1(I)),W(I1(I)),W(J1(I))
C     WRITE(NO,3003) WIXI, WJXJ, WIXJ, WJXI
C 968 CONTINUE
C
C  COMPUTE WARPING PRODECT OF INERTIA
C
      IWX = 0.
      IWY = 0.
      DO 969 I = 1, NUMBEL
      IWX = IWX + (W(I1(I))*X1(I1(I))+W(J1(I))*X1(J1(I))) * LENGTH(I)
     $*T(I)/3.
      IWX = IWX + (W(I1(I))*X1(J1(I))+W(J1(I))*X1(I1(I))) * LENGTH(I)
     $*T(I)/6.
      IWY = IWY + (W(I1(I))*Y1(I1(I))+W(J1(I))*Y1(J1(I))) * LENGTH(I)
     $*T(I)/3.
      IWY = IWY + (W(I1(I))*Y1(J1(I))+W(J1(I))*Y1(I1(I))) * LENGTH(I)
     $*T(I)/6.
  969 CONTINUE
      XO = (IXY*IWX-IYY*IWY)/(IXY**2-IXX*IYY)
      YO = (IXX*IWX-IXY*IWY)/(IXY**2-IXX*IYY)
      XS = -XO + XBAR
      YS = -YO + YBAR
      WRITE(NO,1013) IWX, IWY, XS, YS
      WRITE(NO,1015) XO, YO
C
C  WARPING CONSTANT Cw (or Iw)
C
 5001 FORMAT(I5, 3F10.4/)
      DO 971 I = 1, NUMBEL
      RHOO(I) = -((Y1(I1(I))-YO)*COSE(I) - (X1(I1(I))-XO)*SINE(I))
      FO(I) = RHOO(I) * LENGTH(I)
  971 CONTINUE
      WO(I1(1)) = 0.
      DO 973 I = 1, NOEND
      WO(J1(I)) = WO(I1(I)) + FO(I)
      IF (I .EQ. NOEND) GO TO 973
      WO(I1(I+1)) = WO(J1(I))
  973 CONTINUE
      DO 975 I = NOEND+1, NUMBEL
      DO 975 J = 1, NOBRAN
      DO 975 K = 1, ZWEIG(J)
      WO(I1(I)) = WO(J1(I)) - FO(I)
  975 CONTINUE
      CF = 0.
      DO 977 I = 1, NUMBEL
      CF = CF + (WO(I1(I))+WO(J1(I)))*LENGTH(I)*T(I)
  977 CONTINUE
      CF= CF / (2.*AREA)
      DO 979 I = 1, NUMBEL
      WN(I1(I)) = CF - WO(I1(I))
      WN(J1(I)) = CF - WO(J1(I))
C     WRITE(NO,*) I, WN(I1(I)), WN(J1(I))
  979 CONTINUE
      CW = 0.
      DO 981 I = 1, NUMBEL
      CW = CW + (WN(I1(I))**2 + WN(I1(I))*WN(J1(I)) + WN(J1(I))**2) *
     $ LENGTH(I)*T(I)/3.
C     WRITE(NO,5001) I, CW, WN(I1(I)), WN(J1(I))
  981 CONTINUE
```

```
      WRITE(NO,1014) CW
C
C  THE CROSS-SECTIONAL PROPERTY  BETA-X
C
 6001 FORMAT(I3, 4F10.4/)
 6002 FORMAT(I3, 6F10.2/)
 6003 FORMAT(I3, 2F10.2/)
 6004 FORMAT('Section Property Beta-x  (exact)  = ', F9.4/)
 6005 FORMAT('Section Property Beta-x (Trahair) = ', F9.4/)
      XELE(1,1) = XBAR - CTF
      XELE(1,2) = XBAR
      YELE(1,1) = YBAR - (WD+CTW)
      YELE(1,2) = YBAR - (WD+CTW-CBF)
      XELE(2,1) = - WTW/2.
      XELE(2,2) = WTW/2.
      YELE(2,1) = YBAR - (WD-WTF)
      YELE(2,2) = YBAR - WTF
      XELE(3,1) = - XELE(1,2)
      XELE(3,2) = - XELE(1,1)
      YELE(3,1) = YELE(1,1)
      YELE(3,2) = YELE(1,2)
      XELE(4,1) = XBAR - (CD+WBF)/2.
      XELE(4,2) = XBAR - (CD-WBF)/2.
      YELE(4,1) = YBAR - WTF
      YELE(4,2) = YBAR
      XELE(5,1) = XELE(4,1)
      XELE(5,2) = XELE(4,2)
      YELE(5,1) = YBAR - WD
      YELE(5,2) = YBAR - (WD-WTF)
      XELE(6,1) = XBAR - (CD-CTF)
      XELE(6,2) = XBAR - CTF
      YELE(6,1) = YBAR - (WD+CTW)
      YELE(6,2) = YBAR - WD
      BETAX = 0.
      DO 995 I = 1, 6
      XX1 = (XELE(I,2))**3 - (XELE(I,1))**3
      XX2 = XELE(I,2) - XELE(I,1)
      YY1 = (YELE(I,2))**2 - (YELE(I,1))**2
      YY2 = (YELE(I,2))**4 - (YELE(I,1))**4
      TT1 = XX1/6. * YY1
      TT2 = XX2/4. * YY2
      TT = TT1 + TT2
      BETAX = BETAX + (TT1+TT2)
  995 CONTINUE
      BETAX = BETAX/IXX - 2.*YO
C
C      TRAHAIR'S APPROXIMATIONS (BETA-X AND CW)
C
      IYA = IYW + IXC
      IYYC = IYA - 1./12.*WTF*(WBF)**3
      PP = IYYC/IYA
      EE = (CBF**2)*(CD**2)*CTF/(4.*PP*IYA)
      HAS = YCC + EE - WTF/2.
      XXX = 0.9 * (2.*PP-1.) * (1.0 - (IYA/IXX)**2)
      DD = WD + CTW
      BETAXT = (XXX * (1.+CBF/2./DD)) * HAS
      AA = (1.-PP)*HAS
      BB = PP*HAS
      CWT = (AA**2)*IYYC + (BB**2)*(IYA-IYYC)
      WRITE(NO,6008) CWT
```

```
      WRITE(NO,6004) BETAX
      WRITE(NO,6005) BETAXT
C
C     CALCULATE Zx
C
 6100 FORMAT('Plastic Section Properties'/)
 6101 FORMAT('PNA location --- ', 'Case No =', I2, /)
 6102 FORMAT(' Ypc = ', F6.3, '   Ypt = ', F6.3, '    Zx =', F8.3/)
      AAC = CD*CTW + 2.*(CBF-CTW)*CTF
      AAW = 2.*WBF*WTF + (WD-2.*WTF)*WTW
      AAH = (AAC+AAW) / 2.
      AA1 = CD * CTW
      YY1 = 0.5 * CTW
      AA2 = (2.*CTF+WBF) * WTF
      YY2 = CTW + 0.5*WTF
      AA3 = (2.*CTF+WTW) * (CBF-CTW-WTF)
      YY3 = CTW + WTF + (CBF-CTW-WTF)/2.
      AA4 = (WD+CTW-CBF-WTF) * WTW
      YY4 = (WD+CTW-CBF-WTF)/2. + CBF
      AA5 = WBF * WTF
      YY5 = WD + CTW - 0.5*WTF
      IF (AAH .LE. AA1) GO TO 302
      IF ((AAH.GT.AA1) .AND. (AAH.LE.(AA1+AA2))) GO TO 304
      IF ((AAH.GT.(AA1+AA2)) .AND. (AAH.LE.(AA1+AA2+AA3))) GO TO 306
      IF (AAH .GT. (AA1+AA2+AA3)) GO TO 308
  302 J = 1
      YPX = AAH / CD
      ZXX = AAH*YPX/2. + (AA1-AAH)*(CTW-YPX)/2.
      ZXX = AA2*(YY2-YPX) + AA3*(YY3-YPX) + AA4*(YY4-YPX) + ZXX
      ZX = AA5*(YY5-YPX) + ZXX
      GO TO 310
  304 J = 2
      YPX = CTW + (AAH-AA1) / (2.*CTF+WBF)
      ZXX = AA1*(YPX-YY1) + (AAH-AA1)*(YPX-CTW)/2.
      ZXX = (AA1+AA2-AAH)*(CTW+WTF-YPX)/2. + ZXX
      ZX = AA3*(YY3-YPX) + AA4*(YY4-YPX) + AA5*(YY5-YPX) + ZXX
      GO TO 310
  306 J = 3
      YPX = CTW + WTF + (AAH-AA1-AA2) / (2.*CTF+WTW)
      ZXX = AA1*(YPX-YY1) + AA2*(YPX-YY2)
      ZXX = (AAH-AA1-AA2)*(YPX-CTW-WTF)/2. + ZXX
      ZXX = (AA1+AA2+AA3-AAH)*(CBF-YPX)/2. + AA4*(YY4-YPX) + ZXX
      ZX = AA5*(YY5-YPX) + ZXX
      GO TO 310
  308 J = 4
      YPX = CBF + (AAH-AA1-AA2-AA3) / WTW
      ZXX = AA1*(YPX-YY1) + AA2*(YPX-YY2) + AA3*(YPX-YY3)
      ZXX = (AAH-AA1-AA2-AA3)*(YPX-CBF)/2. + ZXX
      ZXX = (AA1+AA2+AA3+AA4-AAH)*(WD+CTW-YPX-WTF)/2. + ZXX
      ZX = AA5*(YY5-YPX) + ZXX
  310 CONTINUE
      YPCX = YPX
      YPTX = WD + CTW - YPX
      WRITE(8,6100)
      WRITE(8,6101) J
      WRITE(8,6102) YPCX, YPTX, ZX
C
      CLOSE (7)
      CLOSE (8)
C
```

```
      RETURN
      END
C
C-----------------------------------------------------------
C
      SUBROUTINE SSCRV
C
C-----------------------------------------------------------
C
C     NOMINAL MOMENT (Mn) OF SINGLY SYMMETRIC SECTION
C
      DIMENSION B1S(30), B2S(30), B1A(30), B2A(30), B1M(30), B2M(30),
     * B1T(30), B2T(30)
      REAL IYW, IXC, JW, JC, JS, JM, IYAC, JA, MR, IYS, IYA, IYTC,
     * JMON(30), MCRS(30), MCRA(30), MCRM(30), MCRT(30), MP, MCRE(30),
     * MCRSS(30), MCRAA(30), MCRMM(30), MCRTT(30), SSLBS(30), SSLBA(30),
     * SSLBM(30), SSLBT(30), LPS, LRS, LPA, LRA, LPM, LRM, LPT, LRT
      REAL PB1S(30), PB1A(30), PB1M(30), PB1T(30), PB2S(30), PB2A(30),
     * PB2M(30), PB2T(30), PMCRS(30), PMCRA(30), PMCRM(30), PMCRT(30),
     * AC(10), YC(10)
C
      INTEGER SSPTN
C
      COMMON /GENDATA/ ISC, FY, CB
      COMMON /WFSEC/ WA, WD, WTW, WBF, WTF
      COMMON /CHSEC/ CA, CD, CTW, CBF, CTF
      COMMON /WCDATA/ CIW, IYW, JW, IXC, JC
      COMMON /CWDATA/ IYS,JS,SXC,SXT,ZX,BETAX,BETAXT,CW,CWT
      COMMON /SSDATA/ SSPTN, SSLBS, SSLBA, SSLBM, SSLBT
C
      OPEN(8,FILE='SSCRV.OUT',STATUS='UNKNOWN')
      REWIND (8)
C
  902 FORMAT(/4X, ' Iy= ', F5.1, '  Ix= ', F5.1, ' Jw= ', F6.3, ' Jc= '
     *, F6.3, ' Cw2= ', F8.1, ' Js= ', F6.3)
  914 FORMAT(/6X,' Cb= ', F4.2, 5X, ' Fy (Ksi)= ', F5.1)
  907 FORMAT(/'UNIT: Kips, Inches ')
  915 FORMAT(/'            ',5X, '    Mp    ','     Mr    ', 2X, '    Lp
     *   ','    Lr     ')
  917 FORMAT(/' EXACT      ', 2F12.2, 2F10.2)
  918 FORMAT(/' AISC       ', 2F12.2, 2F10.2)
  919 FORMAT(/' MODEL      ', 2F12.2, 2F10.2)
  921 FORMAT(/' TRAHAIR    ', 2F12.2, 2F10.2)
  920 FORMAT(/ I5, 2F7.3)
  922 FORMAT(/'NOMINAL MOMENT CUREVE (Mn) ---------- ')
  931 FORMAT(/'EXACT APPROACH --- ')
  932 FORMAT(/'   Lb       B1      B2         Mn        B1(%)   B2(%)    M
     *n(%) ')
  933 FORMAT(/'AISC APPROACH --- ')
  935 FORMAT(/'MODEL APPROACH --- ')
  936 FORMAT(/'TRAHAIR APPROACH --- ')
  925 FORMAT(/ F7.2, 2F8.3, F12.1, 3F8.1, /)
  926 FORMAT(/ F7.2, 2F8.3, F12.1, 2F8.1, F9.1/)
  930 FORMAT(/'(Fy-10.0)*Sxc = ', F10.2, '  Fy*Sxt = ', F10.2)
  934 FORMAT(/'(Fy-16.5)*Sxc = ', F10.2, '  Fy*Sxt = ', F10.2)
C
C     Read Section Dimensions
C
      WRITE(8,*)  '                                                    '
      WRITE(8,*)  ' OUTPUT OF SINGLY SYMMETRIC SECTION ( WIDE FLANGE AND
```

```
     * CHANNEL)   '
      WRITE(8,*)  '                                          '
      WRITE(8,*)  '  EXACT:  J : Exact J                     '
      WRITE(8,*)  '          B1: Exact Beta-x is applied     '
      WRITE(8,*)  '          B2: Exact Cw is applied         '
      WRITE(8,*)  '                                          '
      WRITE(8,*)  '   AISC:  J = Jc + Jw -- from manual      '
      WRITE(8,*)  '          B1: Beta-x is not applied       '
      WRITE(8,*)  '          B2: Cw is not applied           '
      WRITE(8,*)  '                                          '
      WRITE(8,*)  '  MODEL:  J --  Calculated                '
      WRITE(8,*)  '          B1: Approximated Beta-x is applied '
      WRITE(8,*)  '          B2: Approximated Cw is applied  '
      WRITE(8,*)  '                                          '
      WRITE(8,907)
      WRITE(8,914) CB, FY
C
C     CALCULATE Mp AND Mr
C
C     AISC
C
      JA = JW + JC
      IYAC = IXC + 0.5*IYW
      IYA = IXC + IYW
      HA = WD - 2.* WTF
C
C     PROPOSED MODELS
C
      JM = JW + JC + 0.33333*WBF*(WTF+CTW)**3
      JM = JM - 0.33333*WBF*(WTF**3+CTW**3)
      RHO =  IYAC/IYA
      DD =  WD + CTW
      XXX = 0.87 * (2.*RHO-1.)
      BETAM = XXX * (DD+CBF/2.)
      XX = CA/WA
      CWM = 0.7943 + 1.7924*SQRT(XX)
      CWM = CWM * CIW
C
C     TRAHAIR'S MODELS
C
      BETAXT = BETAXT
      CWT = CWT
C
      IF (ISC .EQ. 1) THEN
      XX1 = (FY - 10.0) * SXC
      ENDIF
      IF (ISC .EQ. 2) THEN
      XX1 = (FY - 16.5) * SXC
      ENDIF
      XX2 = FY * SXT
      IF (XX1 .GE. XX2) MR = XX2
      IF (XX2 .GE. XX1) MR = XX1
      MP = ZX * FY
      IF (ISC .EQ. 1) THEN
      WRITE(8,930)  XX1,  XX2
      ENDIF
      IF (ISC .EQ. 2) THEN
      WRITE(8,934)  XX1,  XX2
      ENDIF
C
```

```
C     CALCULATE Lp AND Lr (EXACT)
C
      WRITE(8,915)
      N = 1
      DO 230 I = 1, N
      AA = CA + WBF * WTF
      LPS = 300. * SQRT(IYAC/AA) / SQRT(FY)
      PP = LPS
  210 XXX = IYS / JS
      B1S(I) = 2.5276 * BETAX / PP * SQRT(XXX)
      B2S(I) = (25.56*CW) / JS / (PP**2)
C     WRITE(8,920) I, B1S(I), B2S(I)
      XXX = 1. + B2S(I) + B1S(I)**2
      XXX = SQRT(XXX) + B1S(I)
      XXS = SQRT(IYS*JS) * XXX
      MCRSS(I) = 56618. * 1.0 / PP * XXS
      RATIO = (MCRSS(I)-MR) / MR
      DM = ABS(MCRSS(I)-MR)
      IF (DM .LE. 0.01) GO TO 220
      PP = PP * (1.+RATIO/4.)
      GO TO 210
  220 LRS = PP
      WRITE(8,917) MP, MR, LPS, LRS
  230 CONTINUE
C
C     CALCULATE Lp AND Lr (AISC)
C
      DO 130 I = 1, N
      AA = CA + WBF * WTF
      LPA = 300. * SQRT(IYAC/AA) / SQRT(FY)
      PP = LPA
  110 XXX = 2.*(IYAC/IYA) - 1.
      XXX = 2.25 * XXX * HA / PP
      B1A(I) = SQRT(IYA/JA) * XXX
      XXX = (1.0 - IYAC/IYA) * (IYAC/JA)
      B2A(I) =  25. * XXX * (HA/PP)**2
C     WRITE(8,920) I, B1A(I), B2A(I)
      XXX = 1. + B2A(I) + B1A(I)**2
      XXX = B1A(I) + SQRT(XXX)
      XXA = SQRT(IYA*JA) * XXX
      MCRAA(I) = 57000. * 1.0 / PP * XXA
      RATIO = (MCRAA(I)-MR) / MR
      DM = ABS(MCRAA(I)-MR)
C     WRITE(8,*) I, PP, MCRAA(I), MR, DM
      IF (DM .LE. 0.01) GO TO 120
      PP = PP * (1.+RATIO/4.)
      GO TO 110
  120 LRA = PP
      WRITE(8,918) MP, MR, LPA, LRA
  130 CONTINUE
C
C     CALCULATE Lp AND Lr (MODEL)
C
      DO 150 I = 1, N
      AA = CA + WBF * WTF
      LPM = 300. * SQRT(IYAC/AA) / SQRT(FY)
      PP = LPM
  140 XXX = IYA/JM
      B1M(I) = 2.5276 * BETAM / PP * SQRT(XXX)
      B2M(I) = (25.56*CWM) / JM / (PP**2)
```

```
      XXX = 1. + B2M(I) + B1M(I)**2
      XXX = SQRT(XXX) + B1M(I)
      XXS = SQRT(IYA*JM)*XXX
      MCRMM(I) = 56000. * 1.0 / PP * XXS
      RATIO = (MCRMM(I)-MR) / MR
      DM = ABS(MCRMM(I)-MR)
      IF (DM .LE. 0.01) GO TO 145
      PP = PP * (1.+RATIO/4.)
      GO TO 140
  145 LRM = PP
      WRITE(8,919) MP, MR, LPM, LRM
  150 CONTINUE
C
C     CALCULATE Lp AND Lr (TRAHAIR)
C
      DO 170 I = 1, N
      AA = CA + WBF * WTF
      LPT = 300. * SQRT(IYAC/AA) / SQRT(FY)
      PP = LPT
  160 XXX = IYA/JM
      B1T(I) = 2.5276 * BETAXT / PP * SQRT(XXX)
      B2T(I) = (25.56*CWT) / JM / (PP**2)
      XXX = 1. + B2T(I) + B1T(I)**2
      XXX = SQRT(XXX) + B1T(I)
      XXS = SQRT(IYA*JM)*XXX
      MCRTT(I) = 56000. * 1.0 / PP * XXS
      RATIO = (MCRTT(I)-MR) / MR
      DM = ABS(MCRTT(I)-MR)
      IF (DM .LE. 0.01) GO TO 165
      PP = PP * (1.+RATIO/4.)
      GO TO 160
  165 LRT = PP
      WRITE(8,921) MP, MR, LPT, LRT
  170 CONTINUE
C
C     ELASTIC CURVE
C
      IF ( SSPTN .EQ. 0 ) GO TO 500
      DO 340 I = 1, SSPTN
      XXX = IYS / JS
      B1S(I) = 2.5276 * BETAX / SSLBS(I) * SQRT(XXX)
      XXX = 2.*(IYAC/IYA) - 1.
      XXX = 2.25 * XXX * HA / SSLBA(I)
      B1A(I) = SQRT(IYA/JA) * XXX
      XXX = IYA/JM
      B1M(I) = 2.5276 * BETAM / SSLBM(I) * SQRT(XXX)
      XXX = IYA/JM
      B1T(I) = 2.5276 * BETAXT / SSLBT(I) * SQRT(XXX)
C
      B2S(I) = (25.56*CW) / JS / (SSLBS(I)**2)
      XXX = (1.0 - IYAC/IYA) * (IYAC/JA)
      B2A(I) =  25. * XXX * (HA/SSLBA(I))**2
      B2M(I) = (25.56*CWM) / JM / (SSLBM(I)**2)
      B2T(I) = (25.56*CWT) / JM / (SSLBT(I)**2)
C
      XXX = 1. + B2S(I) + B1S(I)**2
      XXX = SQRT(XXX) + B1S(I)
      XXX = SQRT(IYS*JS) * XXX
      MCRS(I) = 56618. * CB / SSLBS(I) * XXX
      MCRE(I) = MCRS(I)
```

```
      XXX = 1. + B2A(I) + B1A(I)**2
      XXX = SQRT(XXX) + B1A(I)
      XXX = SQRT(IYA*JA) * XXX
      MCRA(I) = 57000. * CB / SSLBA(I) * XXX
      XXX = 1. + B2M(I) + B1M(I)**2
      XXX = SQRT(XXX) + B1M(I)
      XXX = SQRT(IYA*JM) * XXX
      MCRM(I) = 56000. * CB / SSLBM(I) * XXX
      XXX = 1. + B2T(I) + B1T(I)**2
      XXX = SQRT(XXX) + B1T(I)
      XXX = SQRT(IYA*JM) * XXX
      MCRT(I) = 56000. * CB / SSLBT(I) * XXX
C
C     COMPARISON BETWEEN EXACT, AISC, MODEL
C
      PB1S(I) = 0.
      PB2S(I) = 0.
      PMCRS(I) = 0.
      PB1A(I) = ((B1A(I) / B1S(I)) - 1.) * 100.
      PB2A(I) = ((B2A(I) / B2S(I)) - 1.) * 100.
      PMCRA(I) = ((MCRA(I) / MCRS(I)) - 1.) * 100.
      PB1M(I) = ((B1M(I) / B1S(I)) - 1.) * 100.
      PB2M(I) = ((B2M(I) / B2S(I)) - 1.) * 100.
      PMCRM(I) = ((MCRM(I) / MCRS(I)) - 1.) * 100.
      PB1T(I) = ((B1T(I) / B1S(I)) - 1.) * 100.
      PB2T(I) = ((B2T(I) / B2S(I)) - 1.) * 100.
      PMCRT(I) = ((MCRT(I) / MCRS(I)) - 1.) * 100.
  340 CONTINUE
C
      WRITE(8,922)
      WRITE(8,931)
      WRITE(8,932)
      DO 410 I = 1, SSPTN
      IF (SSLBS(I) .LE. LPS) GO TO 402
      IF ( (SSLBS(I) .GT. LPS) .AND. (SSLBS(I) .LT. LRS) ) GO TO 404
      IF (SSLBS(I) .GE. LRS) GO TO 406
  402 B1S(I) = 0.
      B2S(I) = 0.
      MCRS(I) = MP
      GO TO 406
  404 XX = (MR-MP)/(LRS-LPS) * (SSLBS(I)-LPS) + MP
      MCRS(I) = CB * XX
      IF (MCRS(I) .GE. MP) THEN
      MCRS(I) = MP
      ENDIF
      XX1 = CB * MR
      XX = ABS(MCRS(I)-XX1)
      IF (XX .LE. 1.0) THEN
      GO TO 406
      ENDIF
      B1S(I) = 0.
      B2S(I) = 0.
  406 CONTINUE
      WRITE(8, 925) SSLBS(I), B1S(I), B2S(I), MCRS(I), PB1S(I), PB2S(I),
     * PMCRS(I)
  410 CONTINUE
C
      WRITE(8,933)
      WRITE(8,932)
      DO 420 I = 1, SSPTN
```

```
      IF (SSLBA(I) .LE. LPA) GO TO 412
      IF ( (SSLBA(I) .GT. LPA) .AND. (SSLBA(I) .LT. LRA) ) GO TO 414
      IF (SSLBA(I) .GE. LRA) GO TO 416
  412 B1A(I) = 0.
      B2A(I) = 0.
      PB1A(I) = 0.
      PB2A(I) = 0.
      PMCRA(I) = 0.
      MCRA(I) = MP
      GO TO 416
  414 XX = (MR-MP)/(LRA-LPA) * (SSLBA(I)-LPA) + MP
      MCRA(I) = CB * XX
      IF (MCRA(I) .GE. MP) THEN
      MCRA(I) = MP
      ENDIF
      XX1 = CB * MR
      XX = ABS(MCRA(I)-XX1)
      IF (XX .LE. 1.0) THEN
      GO TO 416
      ENDIF
      B1A(I) = 0.
      B2A(I) = 0.
      PB1A(I) = 0.
      PB2A(I) = 0.
      PMCRA(I) = (MCRA(I)/MCRS(I) - 1.) * 100.
  416 CONTINUE
      WRITE(8, 926) SSLBA(I), B1A(I), B2A(I), MCRA(I), PB1A(I), PB2A(I),
     * PMCRA(I)
  420 CONTINUE
C
      WRITE(8,935)
      WRITE(8,932)
      DO 430 I = 1, SSPTN
      IF (SSLBM(I) .LE. LPM) GO TO 422
      IF ( (SSLBM(I) .GT. LPM) .AND. (SSLBM(I) .LT. LRM) ) GO TO 424
      IF (SSLBM(I) .GE. LRM) GO TO 426
  422 B1M(I) = 0.
      B2M(I) = 0.
      PB1M(I) = 0.
      PB2M(I) = 0.
      PMCRM(I) = 0.
      MCRM(I) = MP
      GO TO 426
  424 XX = (MR-MP)/(LRM-LPM) * (SSLBM(I)-LPM) + MP
      MCRM(I) = CB * XX
      IF (MCRM(I) .GE. MP) THEN
      MCRM(I) = MP
      ENDIF
      XX1 = CB * MR
      XX = ABS(MCRM(I)-XX1)
      IF (XX .LE. 1.0) THEN
      GO TO 426
      ENDIF
      B1M(I) = 0.
      B2M(I) = 0.
      PB1M(I) = 0.
      PB2M(I) = 0.
      PMCRM(I) = (MCRM(I)/MCRS(I) - 1.) * 100.
  426 CONTINUE
      WRITE(8, 926) SSLBM(I), B1M(I), B2M(I), MCRM(I), PB1M(I), PB2M(I),
```

```
     * PMCRM(I)
  430 CONTINUE
C
      WRITE(8,*) '  '
      WRITE(8,*) ' Lb  MCRS, MCRA, MCRM, PMCRM (FT, K-FT)  '
      WRITE(8,*) '  '
  940 FORMAT(F7.2, F10.1, F10.1, F10.1, F10.1)
      DO 600 I = 1, SSPTN
      XX1 = SSLBS(I)/12.
      XX2 = MCRS(I)/12.
      XX3 = MCRA(I)/12.
      XX4 = MCRM(I)/12.
      XX5 = 100. + PMCRM(I)
      WRITE(8,940) XX1, XX2, XX3, XX4, XX5
  600 CONTINUE
C
      WRITE(8,*) '  '
      WRITE(8,*) ' Lb  MCRS, MCRE, LAMBDA, MCRS/Mp '
      WRITE(8,*) '  '
  945 FORMAT(F7.2, F10.1, F10.1, F10.3, F10.3)
      DO 620 I = 1, SSPTN
      XX1 = SSLBS(I)/12.
      XX2 = MCRS(I)/12.
      XX3 = MCRE(I)/12.
      XX4 = MP / MCRE(I)
      XX4 = SQRT(XX4)
      XX5 = MCRS(I) / MP
      WRITE(8,945) XX1, XX2, XX3, XX4, XX5
  620 CONTINUE
C
  500 CONTINUE
      CLOSE (8)
      RETURN
      END
C
```

APPENDIX C

DISPLACEMENTS OF STEEL BEAMS

Displacement results from phase two tests are given here. Loads are in pounds and displacements in inches. Tables show both horizontal and vertical displacements for all 20 tests. Each table is followed by load versus horizontal displacement (H-DISP) and load versus vertical displacement (V-DISP). The specified beam displacements are measured right below the point of the applied load.

Table C-1. Beam W-01 W12x19 L=24'

VOLTAGE	LOAD	VOLTAGE	H-DISP	VOLTAGE	V-DISP
1.6150	256.3	-8.2278	0.0000	-10.4057	0.0000
1.8231	-627.9	-7.4841	0.0720	-8.9112	0.1477
1.9273	-1070.7	-7.3610	0.0840	-8.3718	0.2010
2.0688	-1671.9	-7.0713	0.1120	-7.5795	0.2793
2.1751	-2123.6	-6.8652	0.1320	-6.9744	0.3391
2.2797	-2568.1	-6.6314	0.1546	-6.3890	0.3970
2.3459	-2849.4	-6.4517	0.1715	-6.0193	0.4335
2.3679	-2942.9	-6.3948	0.1775	-5.8983	0.4455
2.4356	-3230.5	-6.2150	0.1950	-5.5237	0.4825
2.4966	-3489.7	-6.0135	0.2145	-5.1810	0.5164
2.4751	-3398.4	5.6926	1.3482	-4.6298	0.5709
2.3926	-3047.8	9.5984	1.7265	-4.5623	0.5775

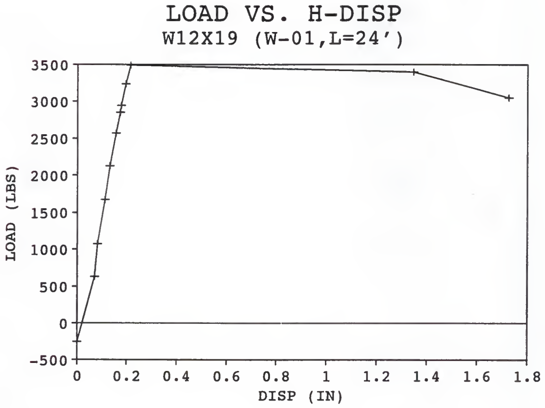

Figure C-1. Beam W-01

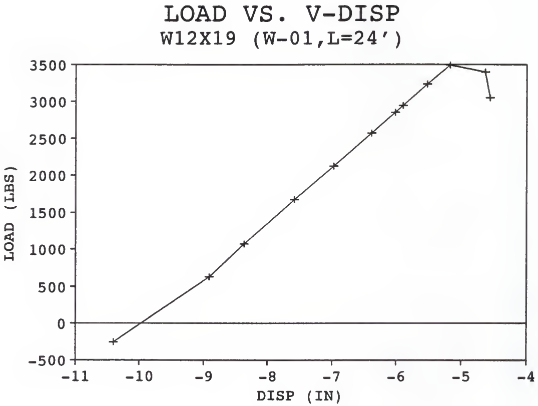

Figure C-2. Beam W-01

Table C-2. Beam WC-01 W12x19 with C6x8.2 L=24'
Set-01

VOLTAGE	LOAD	VOLTAGE	H-DISP	VOLTAGE	V-DISP
1.6128	265.7	-9.7894	0.0000	-10.2538	0.0000
1.9188	-1034.6	-8.4787	0.1311	-8.4385	0.1797
2.3988	-3074.2	-8.4038	0.1386	-6.5419	0.3673
2.8825	-5129.5	-8.3133	0.1476	-4.6578	0.5536
3.3490	-7111.7	-8.0940	0.1695	-2.7799	0.7394
3.8003	-9029.3	-7.9671	0.1822	-0.9163	0.9237
4.2722	-11034.5	-7.7514	0.2038	1.0819	1.1213
4.4723	-11884.7	-5.7353	0.4054	1.9920	1.2114
4.5333	-12143.9	6.4984	1.6288	3.4176	1.3524
4.5187	-12081.9	6.6069	1.6396	3.4249	1.3531

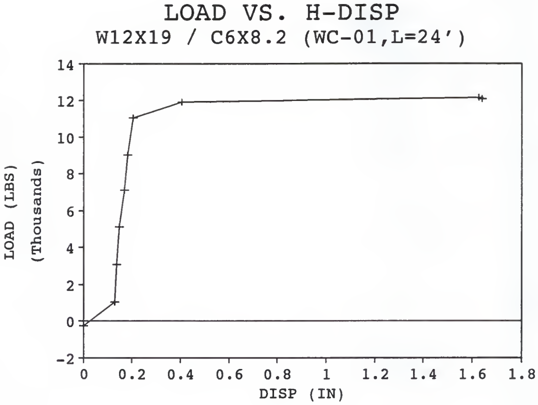

Figure C-3. Beam WC-01

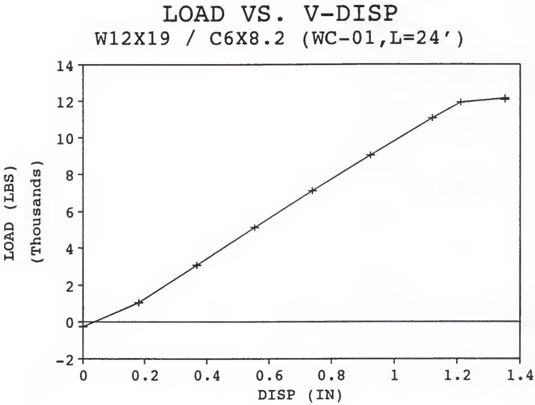

Figure C-4. Beam WC-01

Table C-3. Beam WC-01 W12x19 with C6x8.2 L=24'
Set-02

VOLTAGE	LOAD	VOLTAGE	H-DISP	VOLTAGE	V-DISP
1.6168	248.7	-10.8502	-0.1061	-10.5231	-0.0265
1.9240	-1056.7	-9.3265	0.0463	-7.8263	0.2402
2.3905	-3038.9	-9.5532	0.0236	-6.0193	0.4189
2.8651	-5055.5	-9.4986	0.0291	-4.1924	0.5996
3.3381	-7065.4	-9.2848	0.0505	-2.3445	0.7824
3.8324	-9165.7	-8.9759	0.0813	-0.4141	0.9734
4.2700	-11025.1	-8.3122	0.1477	1.3256	1.1454
4.4065	-11605.1	-7.3108	0.2479	1.8752	1.1998
4.5169	-12074.2	-4.3276	0.5462	2.4220	1.2539
4.5411	-12177.1	-1.0921	0.8697	2.7679	1.2881
4.5596	-12255.7	1.7317	1.1521	3.1459	1.3255
4.5648	-12277.8	5.6010	1.5390	3.7345	1.3837
4.6977	-12842.5	8.6653	1.8455	4.7414	1.4833

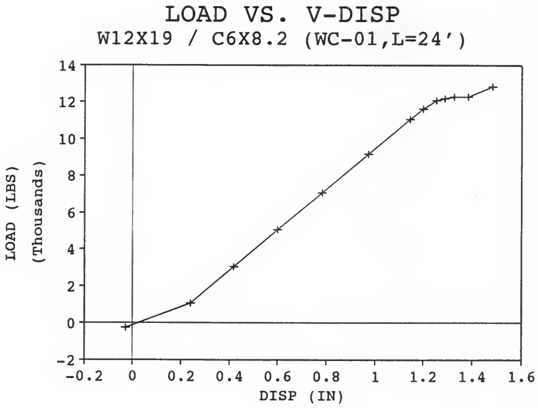

Figure C-6. Beam WC-01

Table C-4. Beam W-02 W12x22 L=18' set-01

VOLTAGE	LOAD	VOLTAGE	H-DISP	VOLTAGE	V-DISP
1.6075	288.2	-10.6915	0.0000	-9.7835	0.0000
2.1928	-2198.8	-9.0967	0.0785	-8.1775	0.0798
2.6209	-4017.9	-8.7143	0.0973	-7.4550	0.1158
2.8950	-5182.6	-8.5320	0.1062	-7.0113	0.1378
3.1287	-6175.6	-8.4034	0.1126	-6.6223	0.1571
3.2284	-6599.2	-8.3495	0.1152	-6.4561	0.1654
3.2770	-6805.7	-8.3251	0.1164	-6.3746	0.1695
3.3227	-6999.9	-8.3048	0.1174	-6.2997	0.1732
3.4612	-7588.4	-8.2334	0.1209	-6.0674	0.1847
3.5586	-8002.3	-8.1715	0.1240	-5.8991	0.1931
3.7063	-8629.9	-8.0683	0.1291	-5.6497	0.2054
3.7982	-9020.4	-8.0019	0.1323	-5.4908	0.2134
3.9179	-9529.0	-7.8933	0.1377	-5.2797	0.2239
4.0646	-10152.3	-7.7068	0.1468	-5.0285	0.2364
4.1463	-10499.5	-7.5902	0.1526	-4.8794	0.2438
3.9264	-9565.1	3.7789	0.7119	-4.5684	0.2592

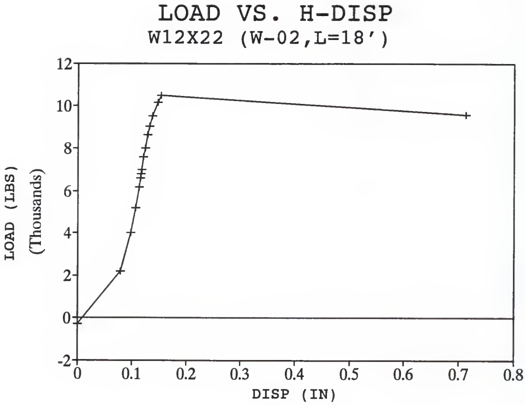

Figure C-7. Beam W-02

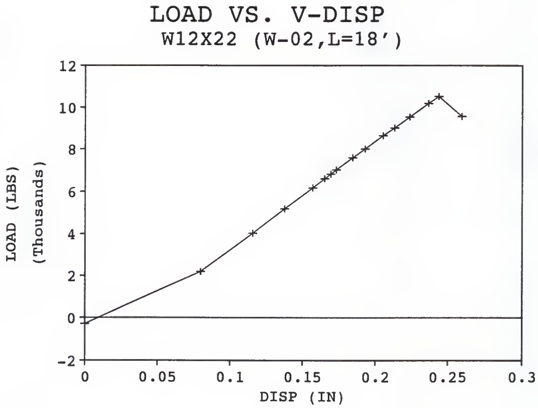

Figure C-8. Beam W-02

Table C-5. Beam W-02 W12x22 L=18' Set-02

VOLTAGE	LOAD	VOLTAGE	H-DISP	VOLTAGE	V-DISP
1.6168	248.7	-10.7922	0.0000	-8.9344	0.0000
2.1958	-2211.6	-9.8323	0.0472	-8.0115	0.0459
2.6496	-4139.8	-7.8997	0.1423	-7.2645	0.0830
3.1622	-6317.9	-7.6667	0.1538	-6.4432	0.1238
3.6083	-8213.5	-7.2597	0.1738	-5.7093	0.1603
3.8430	-9210.7	-6.9236	0.1903	-5.3219	0.1796
4.0438	-10064.0	-6.3941	0.2164	-4.9801	0.1966
3.9947	-9855.3	0.2768	0.5446	-4.7477	0.2081
3.9737	-9766.1	6.8860	0.8698	-4.0947	0.2406

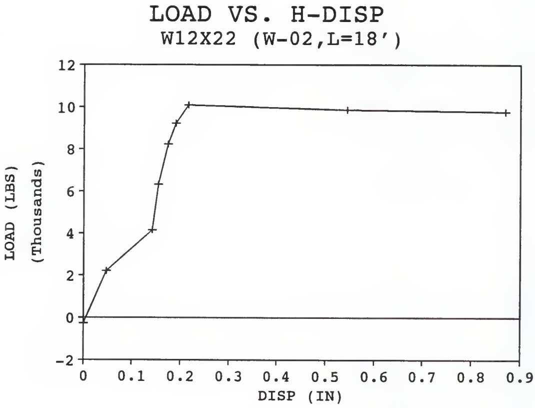

Figure C-9. Beam W-02

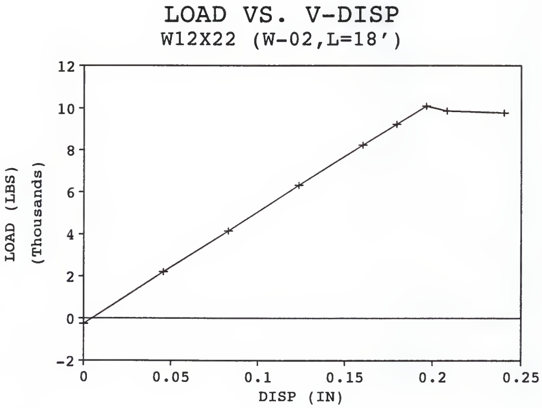

Figure C-10. Beam W-02

Table C-6. Beam WC-02 W12x22 with C6x8.2 L=18'

VOLTAGE	LOAD	VOLTAGE	H-DISP	VOLTAGE	V-DISP
1.7096	-145.7	-11.7465	0.0000	-10.0670	0.0000
2.2048	-2249.8	-11.6668	0.0078	-9.5041	0.0556
2.8614	-5039.8	-9.6610	0.2020	-8.6104	0.1439
4.0682	-10167.6	-9.7586	0.1926	-7.0697	0.2962
5.2045	-14995.9	-9.8562	0.1831	-5.4783	0.4535
6.0069	-18405.4	-9.6472	0.2034	-3.9704	0.6025
6.4469	-20275.0	-9.4597	0.2215	-3.3185	0.6670
6.6660	-21206.0	-9.3330	0.2338	-2.9981	0.6986
6.8758	-22097.5	-9.2313	0.2437	-2.7013	0.7280
7.1527	-23274.1	-9.0670	0.2596	-2.3184	0.7658
7.3327	-24038.9	-8.9215	0.2737	-2.0358	0.7937
7.5561	-24988.2	-8.7091	0.2942	-1.6549	0.8314
7.8473	-26225.5	-8.4529	0.3191	-1.2347	0.8729
8.0489	-27082.1	-8.2149	0.3421	-0.9315	0.9029
8.2935	-28121.5	-7.8932	0.3733	-0.5118	0.9444
8.5460	-29194.4	-6.9320	0.4664	0.0639	1.0013
8.7218	-29941.4	-5.1291	0.6410	0.5169	1.0461
8.8228	-30370.5	-3.0007	0.8471	0.9208	1.0860
8.8395	-30441.5	-1.0612	1.0350	1.2067	1.1142
8.7485	-30054.8	2.8127	1.4102	1.6710	1.1601
8.6464	-29621.0	3.4681	1.4736	1.6917	1.1622

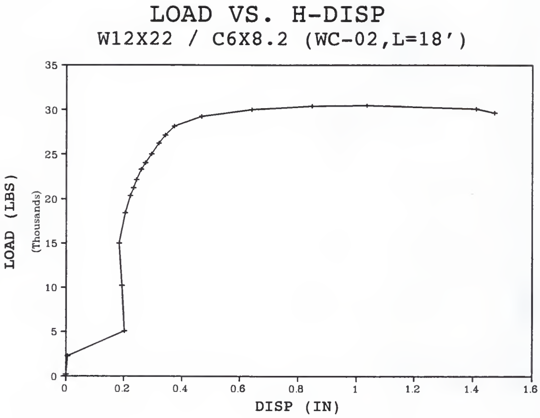

Figure C-11. Beam W-02

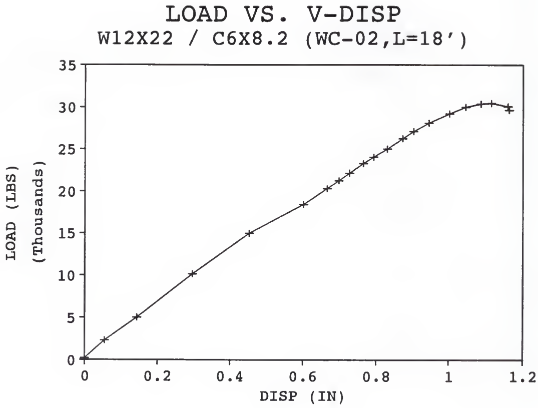

Figure C-12. Beam W-02

Table C-7. Beam W-03 W10x15 L=18'

VOLTAGE	LOAD	VOLTAGE	H-DISP	VOLTAGE	V-DISP
1.5996	321.7	-10.6833	0.0000	-7.1833	0.0003
1.9163	-1024.0	-9.2130	0.1423	-5.3323	0.1833
2.0484	-1585.3	-7.9773	0.2620	-4.8455	0.2314
2.1621	-2068.4	-7.8926	0.2702	-4.4368	0.2718
2.2838	-2585.5	-7.7678	0.2823	-3.9802	0.3169
2.4159	-3146.8	-7.6227	0.2963	-3.4967	0.3647
2.5285	-3625.3	-7.3243	0.3252	-3.0768	0.4062
2.6285	-4050.2	-6.4210	0.4127	-2.6825	0.4452
2.6667	-4212.5	-3.2323	0.7215	-2.3736	0.4757
2.6686	-4220.6	8.5452	1.8622	-0.9153	0.6199
2.6667	-4212.5	8.6013	1.8676	-0.9137	0.6200
2.5200	-3589.2	9.1000	1.9100	-0.9300	0.6400

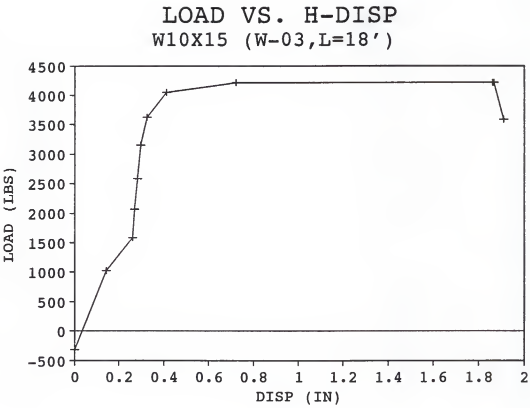

Figure C-13. Beam WC-03

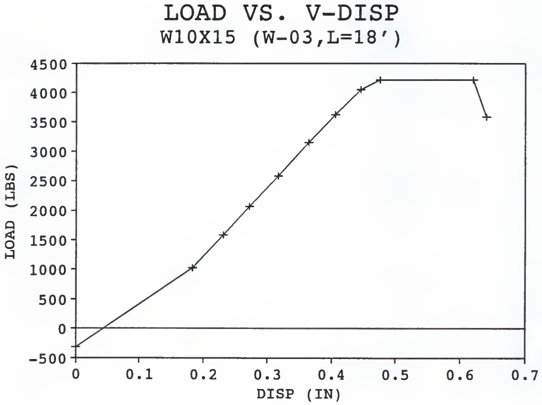

Figure C-14. Beam WC-03

Table C-8. Beam WC-03 W10x15 with C6x8.2 L=18'

VOLTAGE	LOAD	VOLTAGE	H-DISP	VOLTAGE	V-DISP
1.6261	209.1	-9.4457	0.0000	-7.4088	0.0000
2.8789	-5114.2	-11.8150	0.0077	-3.5839	0.3781
4.0436	-10063.1	-11.6283	0.0544	-0.5808	0.6750
4.5420	-12180.9	-11.5616	0.0711	0.6994	0.8015
4.9734	-14013.9	-11.5114	0.0836	1.8630	0.9165
5.2127	-15030.8	-11.4876	0.0896	2.5831	0.9877
5.4493	-16036.1	-11.4660	0.0950	3.4186	1.0703
5.4816	-16173.4	-11.4639	0.0955	3.6022	1.0884
5.6761	-16999.8	-11.4427	0.1008	4.3225	1.1596
5.7128	-17155.7	-11.4108	0.1088	4.5443	1.1815
5.9022	-17960.5	-11.3810	0.1162	5.3297	1.2592
5.8998	-17950.3	-11.3617	0.1210	5.4532	1.2714
5.9646	-18225.7	-11.3503	0.1239	5.7398	1.2997
6.0106	-18421.1	-11.3365	0.1273	6.0277	1.3282
6.0917	-18765.7	-11.3116	0.1336	6.4646	1.3714
6.1493	-19010.5	-11.2811	0.1412	6.9477	1.4191
6.3506	-19865.8	-11.1827	0.1658	8.5927	1.5817
6.3598	-19904.9	-11.1657	0.1700	8.7390	1.5962
6.4722	-20382.5	-11.1497	0.1740	9.1809	1.6398
6.4994	-20498.1	-11.1218	0.1810	9.6808	1.6893
6.5680	-20789.6	-11.0885	0.1893	10.3470	1.7551
6.6038	-20941.7	-11.0545	0.1978	10.8355	1.8034
6.6683	-21215.8	-11.0123	0.2084	11.0305	1.8227
6.7074	-21381.9	-10.9840	0.2155	11.1137	1.8309
6.7486	-21557.0	-10.9568	0.2223	11.1358	1.8331
6.7905	-21735.0	-10.9086	0.2343	11.1807	1.8375
6.8129	-21830.2	-10.8455	0.2501	11.1846	1.8379
6.8340	-21919.9	-10.7857	0.2650		
6.8592	-22026.9	-10.7856	0.2651		
6.9010	-22204.6	-10.7847	0.2653		
6.9383	-22363.0	-10.7836	0.2656		
6.9417	-22377.5	-10.7827	0.2658		
6.9587	-22449.7	-10.7800	0.2665		
6.9903	-22584.0	-10.7704	0.2689		
6.9980	-22616.7	-10.7578	0.2720		
7.0074	-22656.7	-10.7503	0.2739		
7.0232	-22723.8	-10.7486	0.2743		
7.0535	-22852.5	-10.7434	0.2756		
7.0538	-22853.8	-10.7348	0.2778		
7.0730	-22935.4	-10.7311	0.2787		
6.9790	-22536.0	-10.7258	0.2800		
6.9060	-22225.8	-10.7260	0.2800		

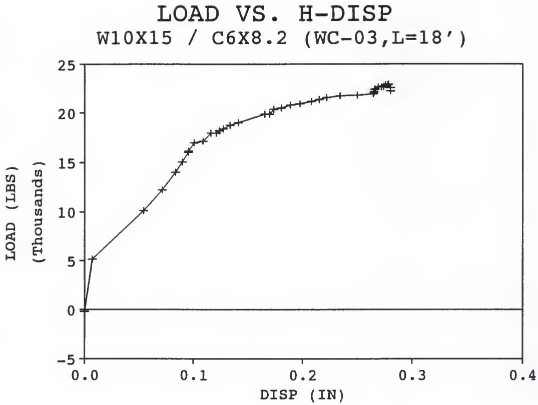

Figure C-15. Beam WC-03

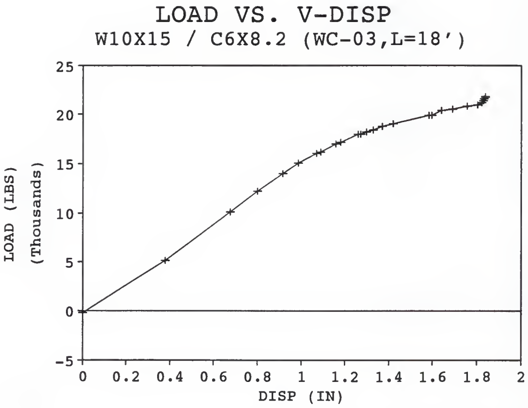

Figure C-16. Beam WC-03

Table C-9. Beam W-04 W12x19 L=18'

VOLTAGE	LOAD	VOLTAGE	H-DISP	VOLTAGE	V-DISP
	0.0		0.0000		0.0000
	1000.0		0.0970		0.1470
	2000.0		0.3050		0.2000
	3000.0		0.3110		0.2360
	4000.0		0.3190		0.2850
	5000.0		0.3210		0.3100
	5500.0		0.3240		0.3340
	6000.0		0.3320		0.3790
	7000.0		0.3360		0.4020
	7500.0		0.3440		0.4260
	8000.0		0.3480		0.4330
	8100.0		0.3620		0.4680
	8200.0		0.3680		0.4780
	8500.0		0.3820		0.4990
	9000.0		0.4080		0.5220
	9500.0		0.4240		0.5320
	9600.0		0.4510		0.5440
	10000.0		1.5320		0.6160
	10000.0		1.5320		0.6160
	9400.0		1.6300		0.6700
	9200.0		1.6700		0.7000

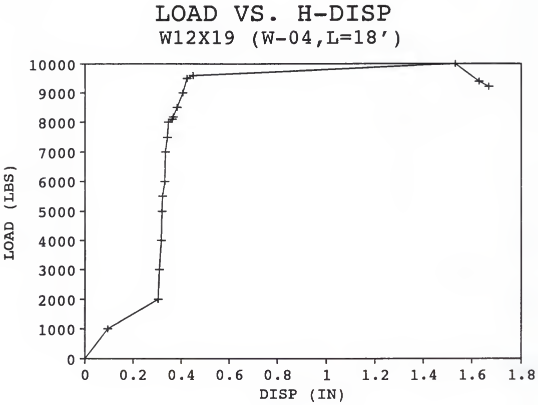

Figure C-17. Beam W-04

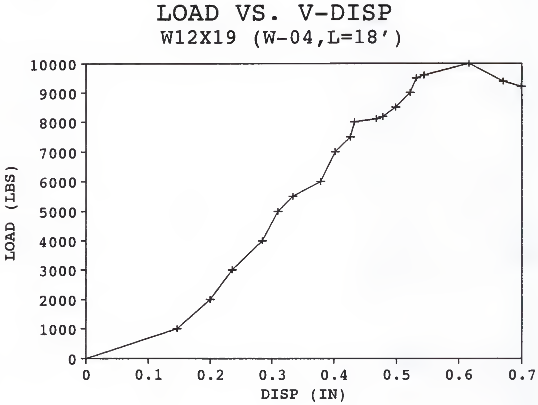

Figure C-18. Beam W-04

Table C-10. Beam WC-04 W12x19 with C6x8.2 L=18′

VOLTAGE	LOAD	VOLTAGE	H-DISP	VOLTAGE	V-DISP
1.6070	290.3	-11.8267	0.0000	-10.8995	0.0000
1.9175	-1029.1	-11.8325	-0.0006	-9.8577	0.1030
2.8712	-5081.4	-11.8328	-0.0006	-8.3323	0.2538
4.0539	-10106.9	-11.8326	-0.0006	-6.6218	0.4228
5.2156	-15043.1	-11.8331	-0.0006	-4.9256	0.5905
6.4428	-20257.6	-11.8330	-0.0006	-3.0538	0.7755
6.6289	-21048.4	-11.8329	-0.0006	-2.7649	0.8041
6.8596	-22028.6	-11.8328	-0.0006	-2.3962	0.8405
6.9740	-22514.7	-11.8329	-0.0006	-2.2043	0.8595
7.3785	-24233.5	-11.8329	-0.0006	-1.5605	0.9231
7.5122	-24801.6	-11.8329	-0.0006	-1.3414	0.9448
7.7417	-25776.8	-11.8330	-0.0006	-0.9514	0.9833
7.7987	-26019.0	-11.8330	-0.0006	-0.8248	0.9958
8.2130	-27779.4	-11.8329	-0.0006	-0.0766	1.0698
8.2616	-27985.9	-11.8329	-0.0006	0.0595	1.0832
8.2940	-28123.6	-11.8328	-0.0006	0.2385	1.1009
8.5243	-29102.2	-11.8330	-0.0006	0.6145	1.1381
8.7405	-30020.8	-11.8328	-0.0006	1.1508	1.1911
8.8225	-30369.2	-11.8331	-0.0006	1.3830	1.2141
8.9213	-30789.1	-11.8331	-0.0006	1.6081	1.2363
9.1250	-31654.6	-11.8333	-0.0007	2.0877	1.2837
9.1909	-31934.6	-11.8334	-0.0007	2.3441	1.3090
9.1968	-31959.7	-11.8331	-0.0006	2.5259	1.3270
9.3839	-32754.7	-11.8334	-0.0007	2.8509	1.3591
9.4585	-33071.7	-11.8333	-0.0007	3.0883	1.3826
9.4396	-32991.4	-11.8333	-0.0007	3.2287	1.3965
9.5705	-33547.6	-11.8333	-0.0007	3.4657	1.4199
9.6575	-33917.3	-11.8332	-0.0007	3.7206	1.4451
9.6980	-34089.4	-11.8332	-0.0007	3.8568	1.4586
9.8122	-34574.6	-11.8332	-0.0007	4.2271	1.4952
9.8915	-34911.6	-11.5996	0.0227	4.4890	1.5211
9.8948	-34925.6	-11.3196	0.0507	4.6300	1.5350
9.8702	-34821.0	-10.9274	0.0899	4.8620	1.5579
10.0373	-35531.1	-10.1763	0.1650	5.2055	1.5919
7.4549	-24558.1	11.8486	2.3675	6.2783	1.6979
7.4448	-24515.2	11.8497	2.3676	6.2754	1.6976

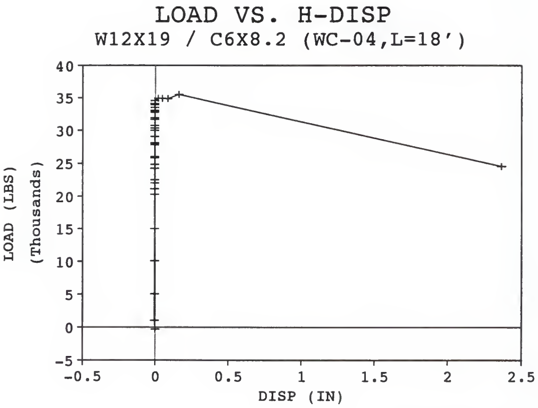

Figure C-19. Beam WC-04

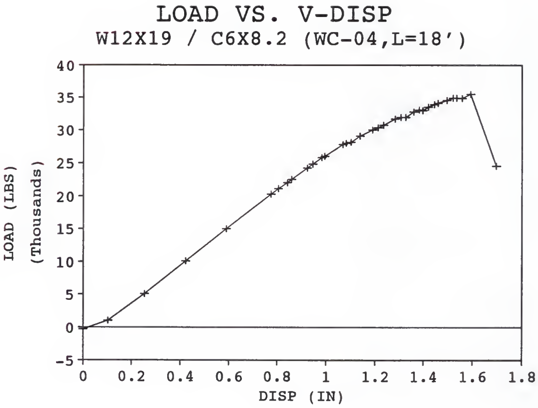

Figure C-20. Beam WC-04

Table C-11. Beam W-05 W12x19 L=12'

VOLTAGE	LOAD	VOLTAGE	H-DISP	VOLTAGE	V-DISP
1.6141	260.1	-8.3047	0.0000	-9.3141	0.0000
1.9367	-1110.6	-8.2578	0.0045	-8.6528	0.0654
2.9370	-5361.0	-8.9637	-0.0638	-7.6455	0.1649
4.0939	-10276.8	-8.7821	-0.0462	-6.6472	0.2635
4.5211	-12092.1	-8.6107	-0.0296	-6.2855	0.2993
4.7648	-13127.6	-8.4660	-0.0156	-6.0774	0.3198
5.0457	-14321.2	-8.2457	0.0057	-5.8368	0.3436
5.2709	-15278.1	-7.6914	0.0594	-5.6201	0.3650
5.2679	-15265.3	-7.6033	0.0679	-5.6051	0.3665
5.3818	-15749.3	-7.0950	0.1172	-5.5081	0.3761
5.1643	-14825.1	-2.4407	0.5679	-5.3853	0.3882
5.1531	-14777.5	-0.4358	0.7621	-5.2004	0.4065
5.1266	-14664.9	1.1746	0.9181	-5.0400	0.4224
5.0589	-14377.2	4.0944	1.2009	-4.7061	0.4554
5.0520	-14347.9	5.1719	1.3052	-4.5474	0.4710
5.0463	-14323.7	5.2019	1.3082	-4.5476	0.4710

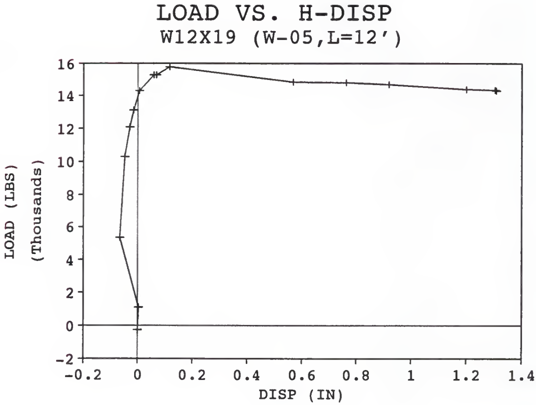

Figure C-21. Beam W-05

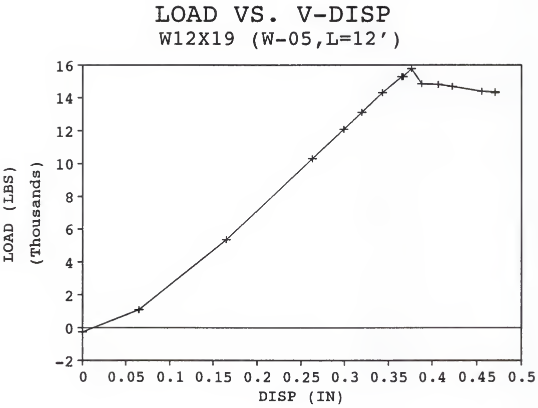

Figure C-22. Beam W-05

Table C-12. Beam WC-05 W12x19 with C6x8.2 L=12'

VOLTAGE	LOAD	VOLTAGE	H-DISP	VOLTAGE	V-DISP
1.6023	310.3	-8.7512	0.0001	-10.4205	0.0001
1.9171	-1027.4	-8.4625	0.0281	-9.7695	0.0652
2.8772	-5106.9	-7.5560	0.1159	-8.9069	0.1514
2.8721	-5085.3	-7.5473	0.1167	-8.9057	0.1516
4.2983	-11145.4	-7.4676	0.1244	-7.8953	0.2526
5.3748	-15719.5	-7.4163	0.1294	-7.2141	0.3207
6.4997	-20499.4	-7.3371	0.1371	-6.5110	0.3910
7.1700	-23347.6	-7.2934	0.1413	-6.0819	0.4339
7.6128	-25229.1	-7.2582	0.1447	-5.7907	0.4631
8.8012	-30278.7	-7.1828	0.1520	-5.0177	0.5404
9.0545	-31355.0	-7.1712	0.1531	-4.8458	0.5575
9.2119	-32023.9	-7.1607	0.1541	-4.7400	0.5681
9.3222	-32492.5	-7.1574	0.1545	-4.6541	0.5767
9.4834	-33177.5	-7.1449	0.1557	-4.5432	0.5878
9.6026	-33684.0	-7.1411	0.1560	-4.4540	0.5967
9.7090	-34136.1	-7.1349	0.1566	-4.3694	0.6052
9.7719	-34403.4	-7.1304	0.1571	-4.3251	0.6096
9.9163	-35016.9	-7.1185	0.1582	-4.2427	0.6179
10.0531	-35598.2	-7.1110	0.1589	-4.1406	0.6281
10.1532	-36023.6	-7.1073	0.1593	-4.0591	0.6362
10.2209	-36311.2	-7.1025	0.1598	-3.9843	0.6437
10.3189	-36727.6	-7.0966	0.1603	-3.9080	0.6513
10.4065	-37099.9	-7.0929	0.1607	-3.8516	0.6570
10.5475	-37699.0	-7.0839	0.1616	-3.7444	0.6677
10.6268	-38035.9	-7.0718	0.1627	-3.6544	0.6767
10.6325	-38060.2	-7.0679	0.1631	-3.6453	0.6776
10.7587	-38596.4	-7.0596	0.1639	-3.5395	0.6882
10.8665	-39054.4	-7.0536	0.1645	-3.4309	0.6990
10.9921	-39588.1	-7.0490	0.1650	-3.3260	0.7095
11.0988	-40041.5	-7.0398	0.1658	-3.2172	0.7204
11.2083	-40506.8	-7.0375	0.1661	-3.1078	0.7313
11.2850	-40832.7	-7.0378	0.1660	-2.9924	0.7429
11.3962	-41305.2	-7.0374	0.1661	-2.8847	0.7537
11.5071	-41776.4	-7.0378	0.1660	-2.7813	0.7640
11.6071	-42201.3	-7.0374	0.1661	-2.6746	0.7747
11.6923	-42563.4	-7.0377	0.1660	-2.5347	0.7887
11.7907	-42981.5	-7.0379	0.1660	-2.4368	0.7984
11.8941	-43420.8	-7.0381	0.1660	-2.3256	0.8096
11.9852	-43807.9	-7.0378	0.1660	-2.2166	0.8205
12.0510	-44087.5	-7.0336	0.1664	-2.0937	0.8328
12.2890	-45098.8	-7.0147	0.1683	-1.8398	0.8581
12.3980	-45562.0	-7.0149	0.1683	-1.7306	0.8691
12.4910	-45957.1	-7.0144	0.1683	-1.6157	0.8806
12.5640	-46267.3	-7.0155	0.1682	-1.4447	0.8977
12.7710	-47146.9	-7.0154	0.1682	-1.2838	0.9137

Continued

12.8530	-47495.3	-7.0158	0.1682	-1.1729	0.9248
12.9340	-47839.5	-7.0155	0.1682	-1.0572	0.9364
12.9980	-48111.5	-7.0157	0.1682	-0.9205	0.9501
13.1100	-48587.4	-7.0158	0.1682	-0.7347	0.9687
13.2860	-49335.2	-7.0163	0.1681	-0.5734	0.9848
13.3450	-49585.9	-7.0155	0.1682	-0.4590	0.9962
13.3970	-49806.9	-7.0161	0.1681	-0.3286	1.0093
13.5580	-50491.0	-7.0157	0.1682	-0.0991	1.0322
13.3000	-49394.7	-7.0143	0.1683	0.8839	1.1305
13.3030	-49407.4	-7.0034	0.1694	1.3534	1.1775
13.3050	-49415.9	-6.9885	0.1708	1.6464	1.2068
13.3100	-49437.2	-6.9556	0.1740	2.2054	1.2627
13.3190	-49475.4	-6.9132	0.1781	2.4511	1.2872
13.3190	-49475.4	-6.9116	0.1783	2.5835	1.3005
13.3190	-49475.4	-6.8910	0.1803	2.8202	1.3241
13.3190	-49475.4	-6.8845	0.1809	2.9867	1.3408
13.3190	-49475.4	-6.8573	0.1835	3.3361	1.3757
13.3190	-49475.4	-6.8549	0.1838	3.3574	1.3779
13.3200	-49479.7	-6.8503	0.1842	3.4046	1.3826

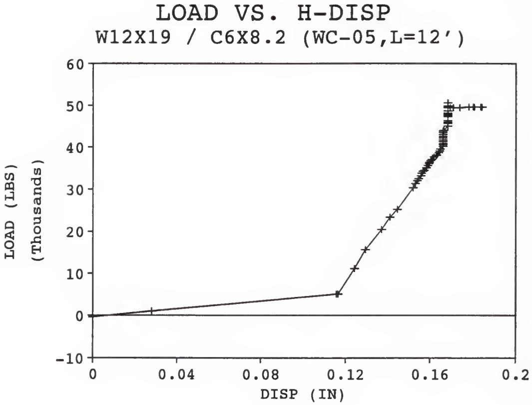

Figure C-23. Beam WC-05

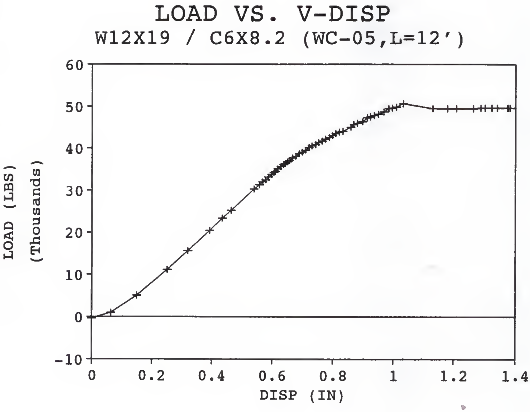

Figure C-24. Beam WC-05

Table C-13. Beam W-06 W10x15 L=12'

VOLTAGE	LOAD	VOLTAGE	H-DISP	VOLTAGE	V-DISP
1.6753	0.1	-8.3285	0.0000	-10.9978	0.0000
1.9229	-1052.0	-7.6531	0.0676	-10.9145	0.0082
2.6320	-4065.1	-6.5165	0.1812	-9.7218	0.1261
3.1119	-6104.2	-6.1100	0.2219	-8.9855	0.1989
3.5576	-7998.0	-4.9338	0.3395	-8.3129	0.2654
3.7805	-8945.2	-2.1021	0.6227	-7.8494	0.3112
3.7850	-8964.3	-1.2001	0.7129	-7.7652	0.3195
3.8128	-9082.4	1.1526	0.9481	-7.4996	0.3458
3.8050	-9049.3	3.7436	1.2072	-7.1878	0.3766
3.7896	-8983.8	6.5423	1.4871	-6.7455	0.4203
3.7766	-8928.6	7.3499	1.5679	-6.6111	0.4336
3.7719	-8908.6	7.3867	1.5715	-6.6101	0.4337
3.7692	-8897.2	7.4002	1.5729	-6.6082	0.4339

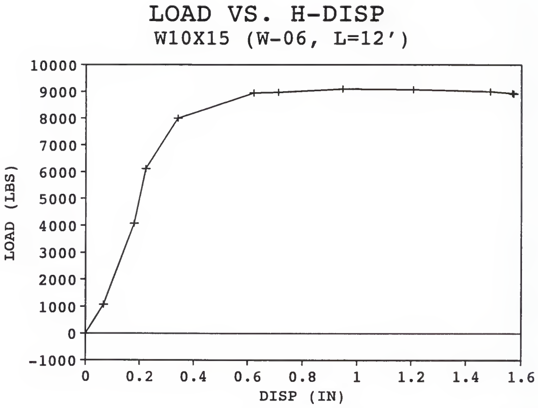

Figure C-25. Beam W-06

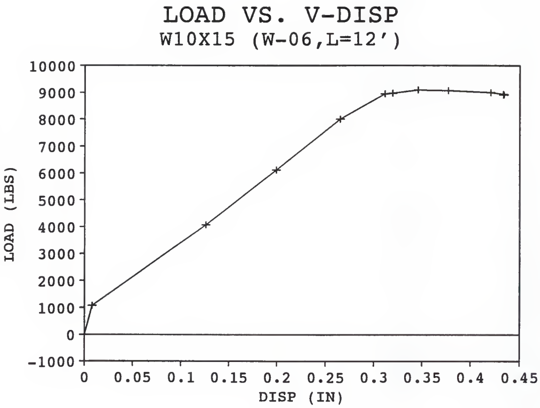

Figure C-26. Beam W-06

Table C-14. Beam WC-06 W10x15 with C6x8.2 L=12'

VOLTAGE	LOAD	VOLTAGE	H-DISP	VOLTAGE	V-DISP
1.6051	298.4	-10.8795	0.0000	-10.5576	0.0000
1.9237	-1055.4	-10.6363	0.0243	-9.2860	0.1231
2.8585	-5027.5	-9.9162	0.0964	-8.0299	0.2448
4.0461	-10073.7	-9.9019	0.0978	-6.7238	0.3713
5.2947	-15379.2	-9.8989	0.0981	-5.4174	0.4978
5.6912	-17064.0	-9.8936	0.0986	-5.0025	0.5380
6.1513	-19019.0	-9.8631	0.1017	-4.4924	0.5874
6.3985	-20069.4	-9.8506	0.1029	-4.1668	0.6189
6.6794	-21263.0	-9.8191	0.1061	-3.8106	0.6534
6.9262	-22311.6	-9.7879	0.1092	-3.4476	0.6886
7.1256	-23158.9	-9.7535	0.1126	-3.1062	0.7216
7.3429	-24082.2	-9.7199	0.1160	-2.6890	0.7620
7.5446	-24939.3	-9.6836	0.1196	-2.2801	0.8016
7.7948	-26002.4	-9.5922	0.1288	-1.6427	0.8634
8.0155	-26940.2	-9.5434	0.1336	-1.0314	0.9226
8.2611	-27983.8	-9.4649	0.1415	-0.1893	1.0041
8.5013	-29004.4	-9.3935	0.1486	0.6602	1.0864
8.7139	-29907.8	-9.3674	0.1512	1.6724	1.1845
8.6904	-29807.9	-9.3629	0.1517	1.8372	1.2004
8.7849	-30209.5	-9.3459	0.1534	2.1634	1.2320
8.8874	-30645.0	-9.3302	0.1550	2.4910	1.2637
8.9137	-30756.8	-9.3059	0.1574	3.0766	1.3205
9.0608	-31381.8	-9.2737	0.1606	3.7527	1.3859
9.0481	-31327.8	-9.2389	0.1641	4.3234	1.4412
9.1161	-31616.8	-9.2115	0.1668	4.6267	1.4706
9.1595	-31801.2	-9.1624	0.1717	5.4904	1.5542
9.1463	-31745.1	-9.1519	0.1728	5.8175	1.5859
9.2149	-32036.6	-9.1260	0.1754	6.1442	1.6176
9.2340	-32117.8	-9.1268	0.1753	6.5218	1.6541
9.2776	-32303.0	-9.1282	0.1752	6.8837	1.6892
9.2295	-32098.6	-9.1296	0.1750	7.1193	1.7120
9.2955	-32379.1	-9.1318	0.1748	7.5026	1.7453
9.2539	-32202.3	-9.1324	0.1747	7.6697	1.7653
9.2585	-32221.9	-9.1325	0.1747	7.7782	1.7758
9.3016	-32405.0	-9.1303	0.1749	7.9857	1.7959
9.3739	-32712.2	-9.1298	0.1750	8.2289	1.8195
9.3695	-32693.5	-9.1232	0.1757	8.4245	1.8384
9.3668	-32682.0	-9.1128	0.1767	8.6610	1.8613
9.3945	-32799.7	-9.1040	0.1776	8.8856	1.8831
9.3685	-32689.3	-8.4409	0.2439	9.0239	1.8965
9.4279	-32941.7	-8.4383	0.2441	9.2294	1.9164
9.2214	-32064.2	-8.4365	0.2443	9.2960	1.9228

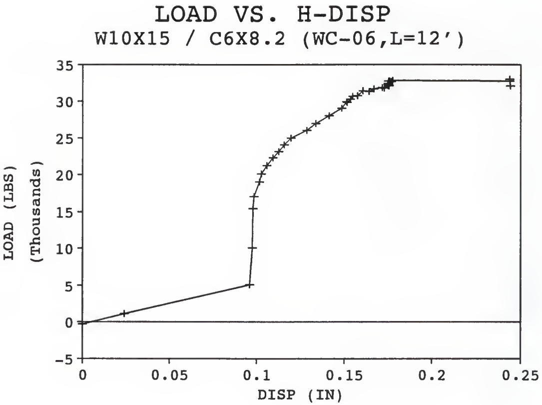

Figure C-27. Beam WC-06

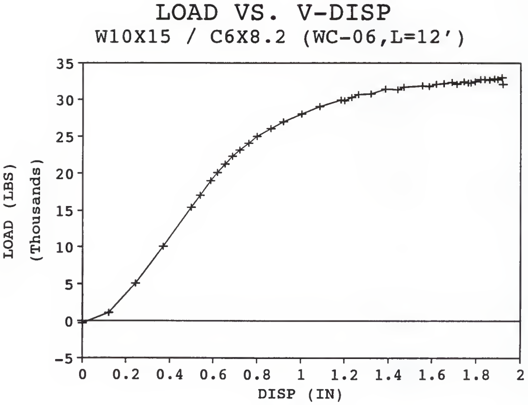

Figure C-28. Beam WC-06

Table C-15. Beam W-07 M8x6.5 L=12'

VOLTAGE	LOAD	VOLTAGE	H-DISP	VOLTAGE	V-DISP
1.6856	-43.7	-9.2408	-0.0001	-10.4248	-0.0002
1.6859	-45.0	-9.2379	0.0002	-10.4267	-0.0001
1.6861	-45.8	-9.2392	0.0001	-10.4278	-0.0002
1.7020	-113.4	-9.2415	0.0002	-10.3644	0.0060
1.7022	-114.2	-9.2507	0.0011	-10.3566	0.0067
1.7417	-282.1	-9.2159	0.0024	-10.1417	0.0276
1.7468	-303.7	-9.3308	0.0091	-10.0587	0.0356
1.7972	-517.9	-9.2689	0.0029	-9.7948	0.0612
1.7969	-516.6	-9.2671	0.0027	-9.7925	0.0614
1.8358	-681.9	-8.6140	0.0626	-9.5824	0.0817
1.8634	-799.2	-8.5278	0.0712	-9.4472	0.0948
1.8943	-930.5	-8.4128	0.0827	-9.2868	0.1104
1.9231	-1052.9	-8.3321	0.0908	-9.1482	0.1238
1.9286	-1076.2	-8.1798	0.1065	-9.1367	0.1249
1.9448	-1145.1	-8.1108	0.1129	-9.0534	0.1330
1.9737	-1267.9	-7.9989	0.1241	-8.9037	0.1475
2.0017	-1386.8	-7.9187	0.1321	-8.7543	0.1619
2.0167	-1450.6	-7.8486	0.1391	-8.6682	0.1703
2.0303	-1508.4	-7.7718	0.1468	-8.6027	0.1766
2.0594	-1632.0	-7.5815	0.1659	-8.4502	0.1914
2.0866	-1747.6	-7.2568	0.1983	-8.3053	0.2054
2.1114	-1853.0	-6.4235	0.2817	-8.1643	0.2191
2.1223	-1899.3	-5.1542	0.4086	-8.0811	0.2271
1.9575	-1199.0	6.3883	1.5628	-7.9626	0.2386
1.9691	-1248.3	6.9119	1.6152	-7.7548	0.2587
1.9689	-1247.5	6.9130	1.6153	-7.7580	0.2584
1.9690	-1247.9	6.9133	1.6153	-7.7566	0.2586
1.9671	-1239.8	9.2309	1.8471	-7.3446	0.2985
1.9649	-1230.5	9.9957	1.9236	-7.1967	0.3128
1.9643	-1227.9	10.5934	1.9833	-7.0185	0.3300
1.9641	-1227.1	10.7358	1.9976	-6.8774	0.3437
1.9638	-1225.8	10.9089	2.0149	-6.4812	0.3821
1.9638	-1225.8	11.0252	2.0265	-6.1375	0.4154
1.9635	-1224.5	11.0259	2.0265	-6.1376	0.4154

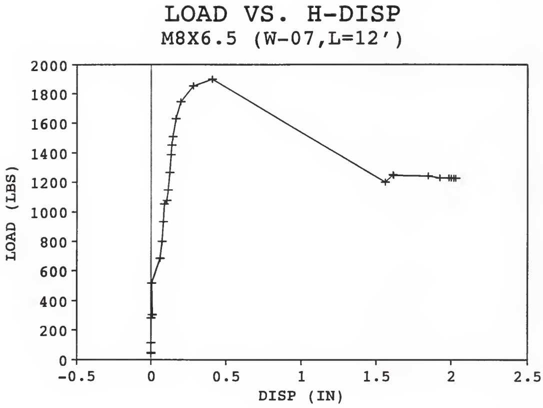

Figure C-29. Beam W-07

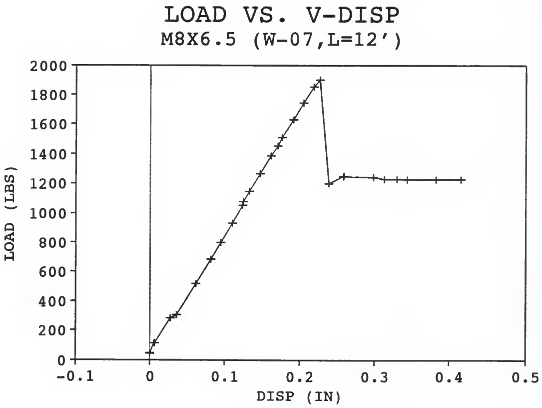

Figure C-30. Beam W-07

Table C-16. Beam WC-07 M8x6.5 with C4x5.4 L=12'

VOLTAGE	LOAD	VOLTAGE	H-DISP	VOLTAGE	V-DISP
1.6168	248.7	-10.0730	0.0000	-9.9448	0.0000
1.8046	-549.3	-9.2878	0.0761	-9.5270	0.0419
1.9124	-1007.4	-9.0065	0.1034	-9.2003	0.0745
1.9178	-1030.3	-9.0052	0.1035	-9.1837	0.0762
2.1565	-2044.6	-8.7312	0.1300	-8.3678	0.1578
2.4135	-3136.6	-8.5096	0.1515	-7.4873	0.2458
2.6275	-4045.9	-8.3471	0.1672	-6.6313	0.3314
2.8527	-5002.8	-8.2165	0.1799	-5.5860	0.4360
2.9929	-5598.6	-8.1222	0.1890	-4.8235	0.5122
3.0367	-5784.7	-8.0800	0.1931	-4.5184	0.5427
3.0757	-5950.4	-8.0568	0.1953	-4.2022	0.5743
3.1207	-6141.6	-8.0281	0.1981	-3.9432	0.6002
3.1430	-6236.4	-8.0102	0.1999	-3.7957	0.6150
3.1579	-6299.7	-8.0017	0.2007	-3.6449	0.6301
3.1760	-6376.6	-7.9820	0.2026	-3.4815	0.6464
3.2131	-6534.2	-7.9466	0.2060	-3.2453	0.6700
3.2435	-6663.4	-7.9392	0.2067	-3.0713	0.6874
3.2576	-6723.3	-7.9240	0.2082	-2.9182	0.7027
3.2741	-6793.4	-7.9128	0.2093	-2.7684	0.7177
3.2897	-6859.7	-7.8920	0.2113	-2.6139	0.7332
3.3054	-6926.4	-7.8872	0.2118	-2.4541	0.7492
3.3187	-6982.9	-7.8833	0.2121	-2.2442	0.7701
3.3324	-7041.1	-7.8738	0.2131	-2.0720	0.7874
3.3783	-7236.2	-7.8525	0.2151	-1.8237	0.8122
3.3982	-7320.7	-7.8375	0.2166	-1.6580	0.8288
3.4045	-7347.5	-7.8248	0.2178	-1.4831	0.8463
3.4173	-7401.9	-7.8131	0.2189	-1.3193	0.8626
3.4282	-7448.2	-7.8020	0.2200	-1.1519	0.8794
3.4381	-7490.3	-7.7887	0.2213	-0.9435	0.9002
3.4791	-7664.5	-7.7670	0.2234	-0.6477	0.9298
3.5249	-7859.1	-7.7194	0.2280	0.0248	0.9970
3.5301	-7881.2	-7.7134	0.2286	0.1921	1.0138
3.5372	-7911.4	-7.7069	0.2292	0.3957	1.0341
3.5610	-8012.5	-7.6940	0.2305	0.6238	1.0569
3.5917	-8142.9	-7.6731	0.2325	0.8475	1.0793
3.5933	-8149.7	-7.6658	0.2332	1.1895	1.1135
3.5989	-8173.5	-7.6568	0.2341	1.3831	1.1329
3.6113	-8226.2	-7.6458	0.2351	1.5817	1.1527
3.6259	-8288.3	-7.6421	0.2355	1.7878	1.1733
3.6553	-8413.2	-7.6227	0.2374	2.0136	1.1959
3.6591	-8429.3	-7.6209	0.2376	2.1867	1.2132
3.6677	-8465.9	-7.6062	0.2390	2.6427	1.2588
3.6997	-8601.8	-7.5881	0.2407	2.8994	1.2845
3.7010	-8607.4	-7.5821	0.2413	3.0810	1.3027
3.7054	-8626.1	-7.5606	0.2434	3.6071	1.3553

Continued

3.7087	-8640.1	-7.5512	0.2443	3.8218	1.3767
3.7423	-8782.9	-7.5325	0.2461	4.1214	1.4067
3.7716	-8907.4	-7.4967	0.2496	4.8491	1.4795
3.7863	-8969.8	-7.4635	0.2528	5.5855	1.5531
3.8201	-9113.4	-7.4286	0.2562	6.3165	1.6262
3.8389	-9193.3	-7.3934	0.2596	6.8732	1.6819
3.8462	-9224.3	-7.3555	0.2633	7.4162	1.7362
3.8658	-9307.6	-7.3057	0.2681	7.9983	1.7944
3.8712	-9330.6	-7.2619	0.2723	8.5630	1.8509
3.8786	-9362.0	-7.2067	0.2777	9.1404	1.9086
3.8979	-9444.0	-7.1768	0.2806	9.5146	1.9460
3.9018	-9460.6	-7.1300	0.2851	10.0605	2.0006
3.9205	-9540.0	-7.0520	0.2927	10.6318	2.0577
3.9482	-9657.7	-6.8969	0.3077	11.5019	2.1448
3.9574	-9696.8	-6.7850	0.3185	12.4402	2.2386
3.9709	-9754.2	-6.5952	0.3369	13.3677	2.3313
3.9764	-9777.6	-6.3836	0.3574	14.3229	2.4269
3.9943	-9853.6	-6.2735	0.3681	14.6982	2.4644
3.9686	-9744.4	-6.2586	0.3695	14.9925	2.4938
3.9823	-9802.6	-6.2045	0.3747	15.2882	2.5234
4.0047	-9897.8	-6.1011	0.3848	15.6642	2.5610
4.0144	-9939.0	-5.9786	0.3966	16.0294	2.5975
4.0089	-9915.7	-5.7569	0.4181	16.2592	2.6205
3.9948	-9855.8	-5.7314	0.4206	16.3372	2.6283
3.9756	-9774.2	-5.7306	0.4206	16.3417	2.6287
3.9673	-9738.9	-5.7302	0.4207	16.3440	2.6290
3.9618	-9715.5	-5.7306	0.4206	16.3459	2.6292
3.9578	-9698.5	-5.7308	0.4206	16.3467	2.6292
3.9546	-9684.9	-5.7305	0.4206	16.3469	2.6293
3.9519	-9673.5	-5.7304	0.4207	16.3474	2.6293

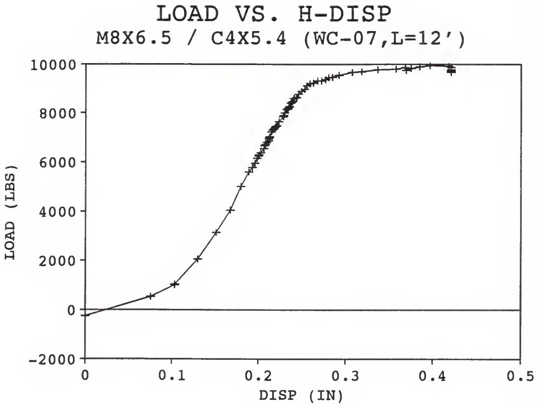

Figure C-31. Beam WC-07

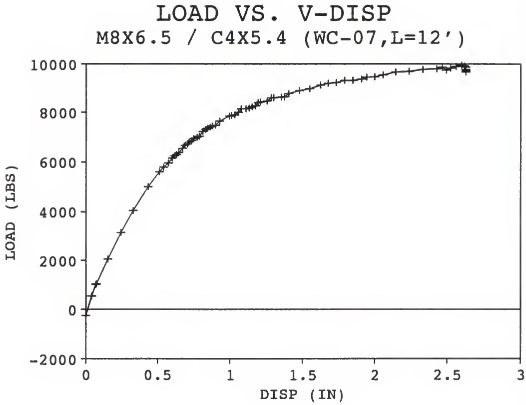

Figure C-32. Beam WC-07

Table C-17. Beam W-08 M8x6.5 L=12'

VOLTAGE	LOAD	VOLTAGE	H-DISP	VOLTAGE	V-DISP
1.6131	264.4	-11.0324	0.0000	-10.7860	0.0002
1.6308	189.2	-11.0274	0.0005	-10.5823	0.0199
1.6643	46.8	-10.9870	0.0045	-10.3305	0.0443
1.7016	-111.7	-11.2285	-0.0194	-10.0751	0.0690
1.7031	-118.0	-11.7971	-0.0757	-9.7774	0.0978
1.7034	-119.3	-11.7971	-0.0757	-9.7594	0.0996
1.7078	-138.0	-11.7973	-0.0757	-9.7467	0.1008
1.7449	-295.7	-11.7954	-0.0755	-9.5590	0.1190
1.7484	-310.5	-11.7952	-0.0755	-9.5420	0.1206
1.7533	-331.4	-11.7971	-0.0757	-9.4709	0.1275
1.7913	-492.8	-11.7893	-0.0749	-9.3102	0.1431
1.8231	-627.9	-11.7650	-0.0725	-9.1403	0.1595
1.8459	-724.8	-11.7578	-0.0718	-9.0103	0.1721
1.8948	-932.6	-11.7557	-0.0716	-8.7532	0.1970
1.9165	-1024.8	-11.7407	-0.0701	-8.6348	0.2085
1.9258	-1064.3	-11.7486	-0.0709	-8.5694	0.2148
1.9430	-1137.4	-11.7930	-0.0752	-8.4792	0.2236
1.9789	-1290.0	-11.6536	-0.0615	-8.2717	0.2437
2.0164	-1449.3	-11.1370	-0.0104	-8.0322	0.2669
2.0321	-1516.0	-10.2630	0.0761	-7.8653	0.2830
1.8562	-768.6	8.9122	1.9728	-7.0420	0.3628

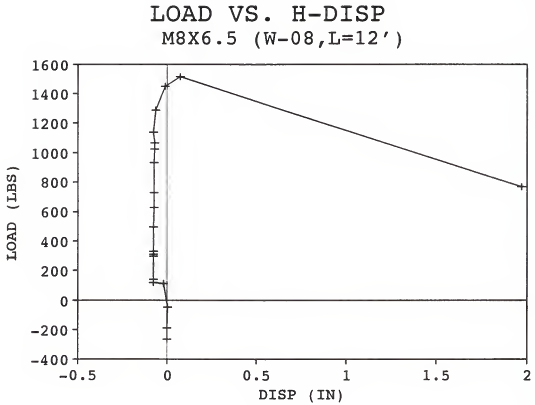

Figure C-33. Beam W-08

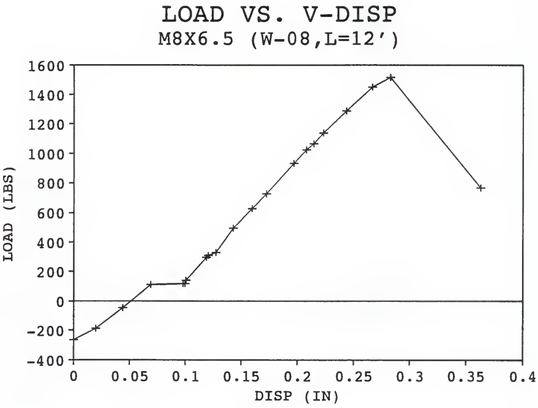

Figure C-34. Beam W-08

Table C-18. Beam WC-08 M8x6.5 with C6x8.2 L=12'

VOLTAGE	LOAD	VOLTAGE	H-DISP	VOLTAGE	V-DISP
1.7006	-107.4	-10.7340	0.0002	-10.8666	0.0000
1.7474	-306.3	-10.8857	-0.0145	-10.6891	0.0178
1.7578	-350.5	-10.7493	-0.0014	-10.6280	0.0239
1.8023	-539.6	-11.1279	-0.0380	-10.5264	0.0340
1.8486	-736.3	-10.0545	0.0660	-10.2918	0.0575
2.0993	-1801.5	-9.6686	0.1033	-9.4443	0.1422
2.2581	-2476.3	-9.4942	0.1202	-8.8052	0.2061
2.3952	-3058.9	-9.3238	0.1367	-8.1691	0.2698
2.5006	-3506.7	-9.2425	0.1446	-7.6717	0.3195
2.5995	-3927.0	-9.1767	0.1510	-7.1479	0.3719
2.6933	-4325.5	-9.1366	0.1549	-6.6184	0.4248
2.7387	-4518.4	-9.1300	0.1555	-6.3590	0.4508
2.7816	-4700.7	-9.1249	0.1560	-6.1049	0.4762
2.7929	-4748.7	-9.1187	0.1566	-5.9775	0.4889
2.8375	-4938.2	-9.1061	0.1578	-5.7342	0.5132
2.8544	-5010.1	-9.1021	0.1582	-5.5075	0.5359
2.8919	-5169.4	-9.0968	0.1587	-5.3521	0.5515
2.9053	-5226.3	-9.0871	0.1597	-5.1440	0.5723
2.9460	-5399.3	-9.0825	0.1601	-4.9481	0.5919
2.9597	-5457.5	-9.0759	0.1608	-4.8066	0.6060
2.9697	-5500.0	-9.0745	0.1609	-4.6725	0.6194
2.9860	-5569.2	-9.0711	0.1612	-4.5104	0.6356
3.0302	-5757.1	-9.0578	0.1625	-4.2606	0.6606
3.0376	-5788.5	-9.0574	0.1625	-4.1200	0.6747
3.0790	-5964.4	-9.0508	0.1632	-3.8422	0.7024
3.0807	-5971.6	-9.0442	0.1638	-3.6915	0.7175
3.1229	-6150.9	-9.0368	0.1645	-3.4196	0.7447
3.1288	-6176.0	-9.0331	0.1649	-3.2585	0.7608
3.1354	-6204.1	-9.0310	0.1651	-3.0536	0.7813
3.1653	-6331.1	-9.0240	0.1658	-2.8073	0.8059
3.2057	-6502.8	-9.0180	0.1664	-2.5139	0.8353
3.2398	-6647.7	-9.0121	0.1669	-2.0768	0.8790
3.2543	-6709.3	-9.0027	0.1678	-1.6983	0.9168
3.2657	-6757.7	-8.9935	0.1687	-1.5368	0.9330
3.2924	-6871.2	-8.9913	0.1689	-1.2734	0.9593
3.2933	-6875.0	-8.9888	0.1692	-1.1346	0.9732
3.3045	-6922.6	-8.9850	0.1696	-0.7698	1.0097
3.3383	-7066.2	-8.9786	0.1702	-0.5648	1.0302
3.3648	-7178.8	-8.9730	0.1707	-0.1210	1.0746
3.3828	-7255.3	-8.9648	0.1715	0.3017	1.1168
3.4072	-7359.0	-8.9605	0.1719	0.9058	1.1772
3.4338	-7472.0	-8.9556	0.1724	1.5035	1.2370
3.4383	-7491.1	-8.9408	0.1738	1.9486	1.2815
3.4423	-7508.1	-8.9439	0.1735	2.1450	1.3012
3.4665	-7610.9	-8.9426	0.1737	2.4625	1.3329

Continued

3.4750	-7647.1	-8.9402	0.1739	2.9563	1.3823
3.4811	-7673.0	-8.9404	0.1739	3.2837	1.4150
3.5037	-7769.0	-8.9341	0.1745	3.7608	1.4627
3.4907	-7713.8	-8.9305	0.1748	3.9401	1.4807
3.5045	-7772.4	-8.9224	0.1756	4.2706	1.5137
3.5271	-7868.4	-8.9155	0.1763	4.6134	1.5480
3.5385	-7916.9	-8.9052	0.1773	5.1190	1.5986
3.5434	-7937.7	-8.9033	0.1775	5.6295	1.6496
3.5515	-7972.1	-8.8886	0.1789	6.1341	1.6997
3.5602	-8009.1	-8.8873	0.1790	6.4538	1.7320
3.5608	-8011.6	-8.8704	0.1807	7.1197	1.7986
3.5846	-8112.8	-8.8575	0.1819	7.4495	1.8316
3.5911	-8140.4	-8.8156	0.1860	8.6270	1.9494
3.5972	-8166.3	-8.8007	0.1874	8.9707	1.9837
3.6037	-8193.9	-8.7924	0.1882	9.3107	2.0177
3.6194	-8260.6	-8.7635	0.1910	9.9153	2.0782
3.6308	-8309.1	-8.7344	0.1938	10.4563	2.1323
3.6573	-8421.7	-8.6639	0.2007	11.0238	2.1890
3.6808	-8521.5	-8.5809	0.2087	12.3827	2.3249
3.6821	-8527.1	-8.5227	0.2143	13.2646	2.4131
3.6936	-8575.9	-8.4900	0.2175	13.6220	2.4489
3.7099	-8645.2	-8.4010	0.2261	14.5304	2.5397
3.7447	-8793.1	-7.9279	0.2719	17.2854	2.8152
3.7617	-8865.3	-7.5725	0.3064	19.1283	2.9995
3.7623	-8867.8	-7.0523	0.3567	21.0057	3.1872
3.7697	-8899.3	-6.9183	0.3697	21.3822	3.2249
3.7741	-8918.0	-6.7883	0.3823	21.7552	3.2622
3.7866	-8971.1	-6.6411	0.3966	22.1190	3.2986
3.7965	-9013.2	-6.4792	0.4122	22.4872	3.3354
3.7859	-8968.1	-5.8515	0.4730	23.7724	3.4639
3.7651	-8879.7	-5.6837	0.4893	24.1825	3.5049
3.7514	-8821.5	-5.6824	0.4894	24.1907	3.5057
3.7449	-8793.9	-5.6801	0.4896	24.1937	3.5034
3.7378	-8763.7	-5.6754	0.4901	24.1976	3.5064

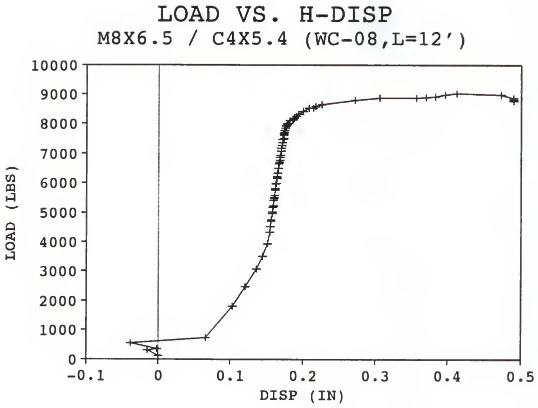

Figure C-35. Beam WC-08

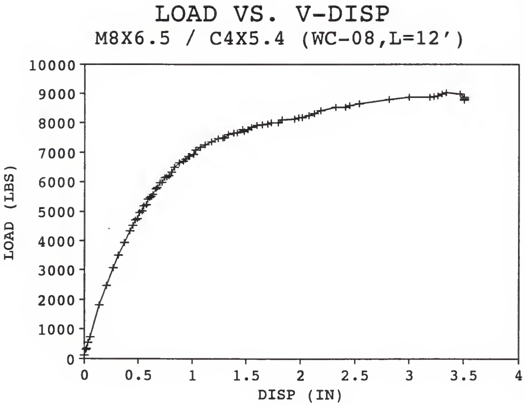

Figure C-36. Beam WC-08

Table C-19. Beam WC-1A W12x19 with C6x8.2 L=24'

VOLTAGE	LOAD	VOLTAGE	H-DISP	VOLTAGE	V-DISP
1.6844	-38.6	-9.5022	0.0000	-9.6860	0.0000
1.8105	-574.4	-10.0238	-0.0516	-8.9657	0.0720
1.9568	-1196.0	-11.8077	-0.2280	-8.4307	0.1255
2.8703	-5077.6	-11.4343	-0.1911	-4.7595	0.4926
3.3385	-7067.1	-11.1605	-0.1640	-2.8609	0.6825
3.8254	-9136.0	-10.8989	-0.1381	-0.9218	0.8764
4.0573	-10121.3	-10.7668	-0.1251	-0.0006	0.9685
4.1744	-10618.9	-10.7466	-0.1231	0.3701	1.0056
4.2472	-10928.2	-10.7612	-0.1245	0.5780	1.0264
4.2835	-11082.5	-10.7700	-0.1254	0.6843	1.0370
4.3206	-11240.1	-10.7815	-0.1265	0.7831	1.0469
4.3583	-11400.3	-10.8113	-0.1295	0.8857	1.0571
4.4017	-11584.7	-10.8465	-0.1330	1.0378	1.0723
4.4724	-11885.1	-10.8981	-0.1381	1.1912	1.0877
4.5098	-12044.1	-10.9272	-0.1409	1.2917	1.0977
4.5439	-12189.0	-10.9522	-0.1434	1.4086	1.1094
4.6185	-12505.9	-11.0136	-0.1495	1.5914	1.1277
4.6215	-12518.7	-11.0137	-0.1495	1.5921	1.1278
4.6511	-12644.5	-11.0291	-0.1510	1.6684	1.1354
4.6834	-12781.7	-11.0561	-0.1537	1.7547	1.1440
4.7242	-12955.1	-11.0901	-0.1571	1.8944	1.1580
4.7903	-13235.9	-11.1320	-0.1612	2.0366	1.1722
4.8632	-13545.7	-11.1823	-0.1662	2.2302	1.1916
4.8998	-13701.2	-11.2081	-0.1687	2.3290	1.2015
4.9553	-13937.0	-11.2510	-0.1730	2.5158	1.2201
5.0101	-14169.9	-11.2793	-0.1758	2.6267	1.2312
5.0427	-14308.4	-11.2969	-0.1775	2.7198	1.2405
5.0764	-14451.6	-11.3182	-0.1796	2.8165	1.2502
5.1086	-14588.4	-11.3310	-0.1804	2.9151	1.2601
5.1437	-14737.6	-11.3403	-0.1818	3.0163	1.2702
5.1733	-14863.3	-11.3188	-0.1797	3.1346	1.2820
5.2351	-15125.9	-11.1071	-0.1587	3.3082	1.2994
5.2668	-15260.6	-11.1215	-0.1602	3.4017	1.3087
5.2999	-15401.3	-11.1414	-0.1621	3.5061	1.3192
5.3536	-15629.5	-11.1788	-0.1658	3.6983	1.3384
5.4045	-15845.7	-11.1920	-0.1671	3.8164	1.3502
5.4358	-15978.7	-11.0012	-0.1483	3.9595	1.3645
5.4815	-16172.9	-10.9882	-0.1470	4.1228	1.3808
5.5371	-16409.2	-10.9942	-0.1476	4.2545	1.3940
5.5668	-16535.4	-10.8646	-0.1348	4.3631	1.4049
5.6265	-16789.0	-10.8004	-0.1284	4.5685	1.4254
5.6570	-16918.6	-10.6254	-0.1111	4.6709	1.4356
5.7132	-17157.4	-10.5618	-0.1048	4.8762	1.4562
5.7729	-17411.1	-9.9380	-0.0431	5.1034	1.4789
5.7655	-17379.7	-9.9218	-0.0415	5.1230	1.4809

Continued

5.8138	-17584.9	-9.9140	-0.0407	5.2915	1.4977
5.8523	-17748.5	-9.2847	0.0215	5.4342	1.5120
5.9118	-18001.3	-8.9091	0.0587	5.7085	1.5394
5.9259	-18061.2	-8.5865	0.0906	5.7620	1.5448
5.9173	-18024.7	-8.5761	0.0916	5.7620	1.5448
5.9721	-18257.5	-8.1806	0.1307	5.9617	1.5647
5.9941	-18351.0	-7.2922	0.2186	6.1324	1.5818
6.0264	-18488.3	-4.2984	0.5147	9.4703	1.9156
6.1098	-18842.7	-3.1138	0.6319	10.1534	1.9839
6.1519	-19021.5	-2.1201	0.7302	10.4883	2.0174
6.1896	-19181.7	-1.0169	0.8393	10.8561	2.0542
6.1922	-19192.8	-0.2831	0.9119	11.0689	2.0755
6.2173	-19299.4	0.8927	1.0282	11.3836	2.1069
6.2329	-19365.7	2.2682	1.1642	11.7464	2.1432
6.2335	-19368.3	3.3320	1.2695	12.0583	2.1744
6.2329	-19365.7	4.5604	1.3910	12.3012	2.1987
6.2325	-19364.0	5.9999	1.5334	12.6558	2.2341
6.2328	-19365.3	7.4269	1.6745	13.0207	2.2706
6.2106	-19271.0	8.5889	1.7894	13.3174	2.3003
6.1891	-19179.6	9.9524	1.9243	13.5789	2.3264
6.1739	-19115.0	11.0226	2.0302	13.8640	2.3550
6.1481	-19005.4	11.2780	2.0554	13.8762	2.3562
6.1338	-18944.6	11.3216	2.0597	13.8546	2.3540
6.1237	-18901.7	11.3514	2.0627	13.8398	2.3525
6.1154	-18866.4	11.3746	2.0650	13.8279	2.3513
6.1123	-18853.3	11.3861	2.0661	13.8248	2.3510
6.1095	-18841.4	11.3941	2.0669	13.8214	2.3507
6.1067	-18829.5	11.4038	2.0679	13.8180	2.3504
6.1037	-18816.7	11.4103	2.0685	13.8146	2.3500
6.1019	-18809.1	11.4131	2.0688	13.8123	2.3498
6.1005	-18803.1	11.4181	2.0693	13.8106	2.3496
6.0984	-18794.2	11.4336	2.0708	13.8108	2.3496

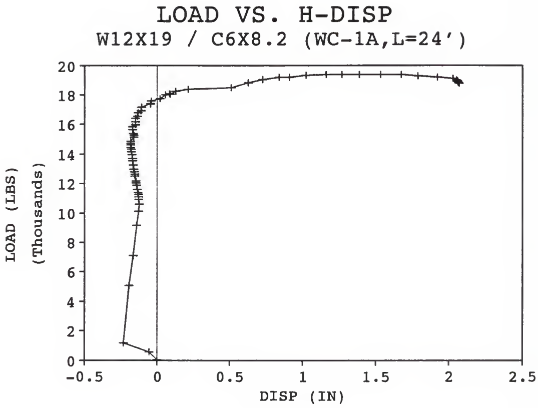

Figure C-37. Beam WC-1A

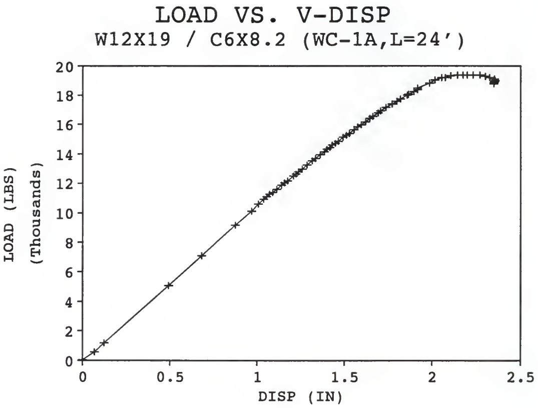

Figure C-38. Beam WC-1A

Table C-20. Beam WC-2A W12x22 with C6x8.2 L=18'

VOLTAGE	LOAD	VOLTAGE	H-DISP	VOLTAGE	V-DISP
1.6771	-7.6	-7.8599	0.0000	-10.0859	0.0000
1.9118	-1004.8	-7.4278	0.0419	-9.8103	0.0275
2.9323	-5341.1	-5.8568	0.1941	-8.2587	0.1827
4.0928	-10272.2	-5.2482	0.2531	-6.6305	0.3455
5.2537	-15205.0	-4.8010	0.2964	-5.0091	0.5076
6.4834	-20430.1	-4.3558	0.3396	-3.3830	0.6702
7.5774	-25078.7	-3.8638	0.3873	-1.9028	0.8183
7.8826	-26375.5	-3.7033	0.4028	-1.4784	0.8607
8.0564	-27114.0	-3.6123	0.4116	-1.2618	0.8824
8.1550	-27533.0	-3.5497	0.4177	-1.1234	0.8962
8.2507	-27939.6	-3.4897	0.4237	-0.9986	0.9087
8.3353	-28299.1	-3.4389	0.4284	-0.8664	0.9219
8.4412	-28749.1	-3.3645	0.4356	-0.7384	0.9347
8.5326	-29137.4	-3.2926	0.4426	-0.6081	0.9477
8.5517	-29218.6	-3.2754	0.4443	-0.5601	0.9525
8.6415	-29600.2	-3.2119	0.4504	-0.4281	0.9657
8.7725	-30156.8	-3.1084	0.4605	-0.2310	0.9854
8.8091	-30312.3	-3.0691	0.4643	-0.2112	0.9874
8.9164	-30768.2	-2.9804	0.4729	0.0023	1.0088
8.9814	-31044.4	-2.9089	0.4798	0.0424	1.0128
9.0583	-31371.2	-2.8344	0.4870	0.1621	1.0247
9.1603	-31804.6	-2.7286	0.4973	0.3673	1.0453
9.2462	-32169.6	-2.6382	0.5060	0.4907	1.0576
9.3028	-32410.1	-2.5652	0.5131	0.5673	1.0653
9.3926	-32791.7	-2.4782	0.5215	0.7073	1.0793
9.4670	-33107.8	-2.3784	0.5312	0.8488	1.0934
9.5306	-33378.0	-2.2844	0.5403	0.9885	1.1074
9.6311	-33805.1	-2.1527	0.5531	1.2023	1.1288
9.6653	-33950.4	-2.0800	0.5601	1.2614	1.1347
9.8179	-34598.8	-1.8675	0.5807	1.5397	1.1625
9.8645	-34796.8	-1.7505	0.5920	1.6784	1.1764
9.9198	-35031.8	-1.6325	0.6035	1.8226	1.1908
9.9395	-35115.5	-1.5731	0.6092	1.9468	1.2032
10.0330	-35512.8	-1.4367	0.6224	2.0811	1.2166
10.1104	-35841.7	-1.2775	0.6379	2.2809	1.2366
10.1468	-35996.4	-1.1611	0.6492	2.3629	1.2448
10.1617	-36059.7	-1.1082	0.6543	2.4612	1.2547
10.2281	-36341.8	-0.9904	0.6657	2.5776	1.2663
10.2823	-36572.1	-0.8264	0.6816	2.7668	1.2852
10.3852	-37009.3	-0.6122	0.7023	2.9579	1.3043
10.4366	-37227.8	-0.4150	0.7215	3.1859	1.3271
10.5229	-37594.5	-0.2024	0.7421	3.3585	1.3444
10.5326	-37635.7	-0.0618	0.7557	3.4922	1.3578
10.6574	-38166.0	0.2885	0.7896	3.7577	1.3843
10.7046	-38366.5	0.5583	0.8158	3.9052	1.3991

Continued

10.7442	-38534.8	0.7815	0.8374	4.0473	1.4133
10.7673	-38632.9	1.0276	0.8612	4.1838	1.4269
10.8317	-38906.6	1.3967	0.8970	4.4068	1.4492
10.8773	-39100.3	1.7851	0.9346	4.5797	1.4665
10.8925	-39164.9	2.0189	0.9573	4.7059	1.4791
10.9302	-39325.1	2.3794	0.9922	4.8543	1.4940
10.9525	-39419.9	2.7900	1.0320	4.9972	1.5083
10.9334	-39338.7	3.5735	1.1079	5.1676	1.5253
10.7409	-38520.8	5.8300	1.3266	5.4948	1.5580
10.4057	-37096.5	8.3751	1.5732	5.7908	1.5876
9.9943	-35348.4	10.6600	1.7946	6.1782	1.6264
9.7362	-34251.7	10.8779	1.8157	6.3108	1.6396
9.6291	-33796.6	10.9264	1.8204	6.3591	1.6444
9.5891	-33626.6	10.9270	1.8205	6.3593	1.6445
9.5565	-33488.1	10.9257	1.8204	6.3597	1.6445
9.5179	-33324.1	10.9245	1.8202	6.3597	1.6445
9.4962	-33231.9	10.9254	1.8203	6.3596	1.6445
9.4819	-33171.1	10.9244	1.8202	6.3601	1.6445
9.4711	-33125.2	10.9246	1.8202	6.3602	1.6446
9.4613	-33083.6	10.9243	1.8202	6.3602	1.6446

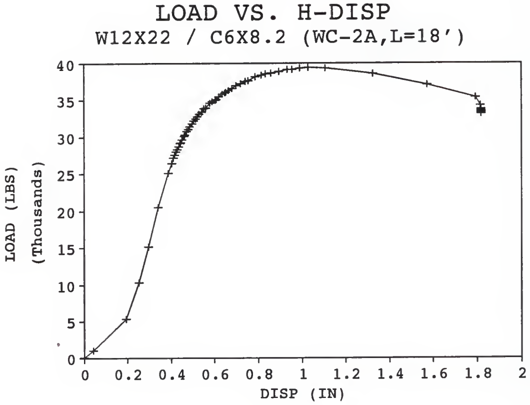

Figure C-39. Beam WC-2A

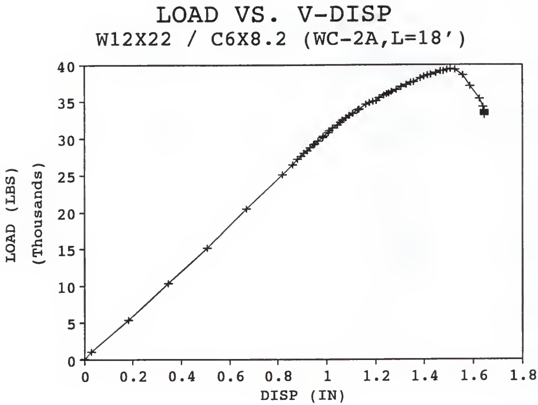

Figure C-40. Beam WC-2A

REFERENCES

American Institute of Steel Construction (1986), Manual of Steel Construction, Load and Resistance Factor Design, First Edition, AISC, Chicago, Illinois.

Anderson, J. M. and Trahair, N. S. (1972), "Stability of Monosymmetric Beams and Cantilever," Journal of the Structural Division, ASCE, Vol. 98, No. ST1, pp. 269-286.

Barsoum, R. S. and Gallagher, R. H. (1970), "Finite Element Analysis of Torsional and Flexural-Torsional Stability Problems,"International Journal of Numerical Methods, Vol. 2, pp. 335-352.

Bleich, F. (1952), Buckling Strength of Metal Structures, McGraw-Hill, New York, Chap. 4.

Chen, W. F. and Lui, E. M. (1988), Structural Stability, Elsevier Science Publishing Company, New York, pp. 307-380.

Clark, J. W. and Hill, H. N. (1960), "Lateral Buckling of Beams,"Journal of the Structural Division, ASCE, Vol. 86, No. ST7, pp. 175-196.

Fukumoto, Y. and Itoh, Y. (1981), "Statistical Study of Experiments on Welded Beams," Journal of the Structural Division, ASCE, Vol. 107, No. ST1, pp. 89-104.

Galambos, T. V. (1963), "Inelastic Lateral Torsional Buckling of Beams," Journal of the Structural Division, ASCE, Vol. 89, No. ST5, pp. 217-242.

Galambos, T. V. (1968), Structural Members and Frames, Prentice-Hall, Englewood Cliffs, New Jersey, pp. 80-158.

Galambos, T. V. (1988), Guide to Stability Design Criteria for Metal Structures, Wiley, New York, pp. 155-188.

Goodier, J. N. (1942). "Flexural-Torsional Buckling of Bars of Open Section," Bulletin No. 28, Cornell University Engineering Experiment Station, pp. 3-16.

Hancock, G. J. (1978), "Local Distortional and Lateral Buckling of I-Beams," Journal of the Structural Division, ASCE, Vol. 104, No. ST11, pp. 1787-1800.

Hartmann, A. J. (1967), "Elastic Lateral Buckling of I-Beams," Journal of the Structural Division, ASCE, Vol. 93, No. ST4, pp. 11-28.

Hechtman, R. A. and Hattrup, J. M. (1955), "Lateral Buckling of Rolled Steel Beams," Journal of the Engineering Mechanics Division, ASCE, Vol. 81, No. 797, pp. 797-830.

Hechtman, R. A., Hattrup, J. S., and Tiedemann, J. L. (1955), "Lateral Buckling of Rolled Steel Beams," Journal of the Structural Division, ASCE, Vol. 81, No. 797, pp. 1-33.

Heins, C. P. (1975), Bending and Torsional Design in Structural Members, Lexington Books, Lexington, Massachusetts, pp. 35-80.

Hill, N. H. (1942), "The Lateral Instability of Unsymmetrical I-Beams," Journal of the Aeronautical Sciences, pp. 175-180.

Johnston, B. G. (1976), Guide to Stability Design Criteria for Metal Structures (SSRC), Wiley, New York, pp. 95-115.

Kirby, P. A. and Nethercot, D. A. (1979), Design for Structural Stability, John Wiley and Sons, New York, pp. 63-100.

Kitipornchai, S. and Trahair, N. S. (1970), "Elastic Stability of Tapered I-Beams," Journal of the Structural Division, ASCE, Vol. 98, No. ST3, pp. 713-728.

Kitipornchai, S. and Trahair, N. S. (1975), "Elastic Stability of Tapered Monosymmetric Beams," Journal of the Structural Division, ASCE, Vol. 101, No. ST8, pp. 1661-1678.

Kitipornchai, S. and Trahair, N. S. (1980), "Buckling Properties of Monosymmetric I-Beams," Journal of the Structural Division, ASCE, Vol. 106, No. ST5, pp. 941-957.

Kubo, M. and Fukumoto, Y. (1988), "Lateral Torsional Buckling of Thin-Walled I-Beams," Journal of the Structural Division, ASCE, Vol. 114, No. ST 4, pp. 841-855.

Lee, G. C. (1960), "A Survey of Literature on the Lateral Instability of Beams," Welding Research Council Bulletin Series No. 63, pp. 50-59.

Morrison Molded Fiber Glass Company (1989), The EXTREN Fiberglass Design Manual, Bristol, Virginia, Sec. 1-7.

Neal, B. G. (1950), "The Lateral Instability of Yielded Mild Steel Beams of Rectangular Cross Section," Philosophical Transactions of the Royal Society, Vol. A242, London, pp. 100-130.

Nethercot, D. A. (1983), " Elastic Lateral Buckling of Beams," in Beams and Beam-Columns - Stability in Strength, Applied Science Publishers, Barking, Essex, England.

Nethercot, D. A. and Rockey, K. C. (1971), "A Unified Approach to the Elastic Lateral Buckling of Beams," The Structural Engineer, Volume 49, No. 7, London, British, pp. 321-330.

O'Connor, C. O. (1964), "The Buckling of A Monosymmetric Beam Loaded in the Plane of Symmetry," Australia Journal of Applied Science, pp. 191-203.

Pi, Yong L., Trahair, N. S., and Rajasekaran, S. (1992), "Energy Equation for Beam Lateral Buckling," Journal of the Structural Division, ASCE, Vol. 118, No. 6, pp. 1462-1477.

Pi, Yong L. and Trahair, N. S. (1992), "Prebuckling Deflections and Lateral Buckling I-Theory," Journal of the Structural Division, ASCE, Vol. 118, No. 11, pp. 2949-2965.

Pi, Yong L. and Trahair, N. S. (1992), "Prebuckling Deflections and Lateral Buckling I-Applications," Journal of the Structural Division, ASCE, Vol. 118, No. 11, pp. 2967-2985.

Powell, G., and Klingner, R. (1970), " Elastic Lateral Buckling of Steel Beams," Journal of the Structural Division, ASCE, Vol. 96, No. ST9, pp. 1919-1932.

Salvadori, M. G. (1955), " Lateral Buckling of I-Beams," Transactions, ASCE, Vol. 120, pp. 1165-1167.

Timoshenko, S. P. and Gere, J. M. (1961), Theory of Elastic Stability, McGraw-Hill, New York, Chap. 6.

Trahair, N. S. (1969),"Elastic Stability of Continuous Beams," Journal of the Structural Division, ASCE, Vol. 95, No. ST6, pp. 1295-1312.

Trahair, N. S. (1977), The Behaviour and Design of Steel Structures, Chapman & Hall, London.

Trahair, N. S. (1983), "Inelastic Lateral Buckling of Beams," Beams and Beam-Columns Stability and Strength, Applied Science Publishers, Barking, Essex, England.

Trahair, N. S. and Kitipornchai, S. (1972), "Buckling of Inelastic I-Beams Under Uniform Moment," Journal of the Structural Division, ASCE, Vol. 98, No. ST11, pp. 217-244.

Vinnakota, S. (1977), "Finite Difference Methods for Plastic Beam-Columns," in Theory of Beam-Columns, Volume 2, W. F. Chen and T. Atsuta, McGraw-Hill, New York.

Vinnakota, S. (1979), "Inelastic Stability of Laterally Unsupported Beams," Computers and Structures, Vol. 7, No. 3, pp. 15-27.

Vlasov, V. Z. (1961), Thin-Walled Elastic Beams, 2nd edition, Israel Program for Scientific Translations, Jerusalem.

Wang, C. M. and Kitipornchai, S. (1989), "New Set of Buckling Parameters For Monosymmetric Beam-Columns / Tie-Beams," Journal of the Structural Division, ASCE, Vol. 115, No. ST 6, pp. 1497-1513.

Winter, George (1941), "Lateral Stability of Unsymmetrical I-Beams and Trusses in Bending," Journal of the Structural Division, ASCE, Vol. 67, pp. 1851-1864.

Yarimci, E., Yura, J. A., and Lu, L. W. (1967), "Techniques for Testing Structures Permitted to Sway," Experimental Mechanics, pp. 321-331.

BIOGRAPHICAL SKETCH

Dung Myau Lue, better known to people as Tony, was born on February 12, 1955, in Taiwan, the Republic of China.

He received his Bachelor of Science in civil engineering from National Chung Hsing University (Taiwan) in July 1979. Soon after graduation, he had the obligation to fulfill three-months of compulsory military training. After finishing his military service, he worked for Wu-Zhou Ready-Mix Concrete Company (Taiwan) for almost two years.

He was admitted to the master's program at North Carolina State University in August 1981 and graduated with the degree of Master of Science in May 1983. He then entered the graduate program in civil engineering at the University of Florida and graduated with the degree of Engineer in December 1985.

Thereafter he worked as a structural engineer for Entech, Inc. (Atlanta, Georgia) and the Bridge Engineering Software Transfer Center at the University of Maryland (College Park, Maryland) for five years.

He returned to Gainesville for the doctoral program in civil engineering at the University of Florida in August 1990, and expects to complete his Ph.D. in December 1993.

He is a member of Tau Beta Pi Engineering Honor Society and the Chinese Society of Civil Engineers.

I certify that I have read this study and that in my opinion it conforms to acceptable standards of scholarly presentation and is fully adequate, in scope and quality, as a dissertation for the degree of Doctor of Philosophy.

Duane S. Ellifritt

Duane S. Ellifritt, Chairman
Professor of Civil Engineering

I certify that I have read this study and that in my opinion it conforms to acceptable standards of scholarly presentation and is fully adequate, in scope and quality, as a dissertation for the degree of Doctor of Philosophy.

Ronald A. Cook

Ronald A. Cook, Cochairman
Assistant Professor of Civil Engineering

I certify that I have read this study and that in my opinion it conforms to acceptable standards of scholarly presentation and is fully adequate, in scope and quality, as a dissertation for the degree of Doctor of Philosophy.

Mang Tia

Mang Tia
Professor of Civil Engineering

I certify that I have read this study and that in my opinion it conforms to acceptable standards of scholarly presentation and is fully adequate, in scope and quality, as a dissertation for the degree of Doctor of Philosophy.

Ibrahim K. Ebcioglu

Ibrahim K. Ebcioglu
Professor of Aerospace Engineering, Mechanics, and Engineering Science

I certify that I have read this study and that in my opinion it conforms to acceptable standards of scholarly presentation and is fully adequate, in scope and quality, as a dissertation for the degree of Doctor of Philosophy.

Myron Chang

Myron Chang
Associate Professor of Statistics

This dissertation was submitted to the Graduate Faculty of the College of Engineering and to the Graduate School and was accepted as partial fulfillment of the requirements for the degree of Doctor of Philosophy.

December 1993

Winfred M. Phillips
Dean, College of Engineering

Karen A. Holbrook
Dean, Graduate School